DESIGN OF WHEELCHAIR SEATING SYSTEMS FOR USERS WITH HIGH-TONE EXTENSOR THRUST

A Thesis
Presented to
The Academic Faculty

By

James Patrick Kitchen

In Partial Fulfillment
of the Requirements for the Degree
Master of Science in Mechanical Engineering

Georgia Institute of Technology

August 2006

DESIGN OF WHEELCHAIR SEATING SYSTEMS FOR USERS WITH HIGH-TONE EXTENSOR THRUST

Approved by:

Dr. William Singhose, Advisor
School of Mechanical Engineering
Georgia Institute of Technology

Dr. Stephen Sprigle , Committee Member
School of Applied Physiology
Georgia Institute of Technology

Dr. Raymond Vito, Committee Member
School of Mechanical Engineering
Georgia Institute of Technology

Date Approved: May 12th, 2006

ACKNOWLEDGEMENTS

I would like to thank my advisor, Dr. William Singhose, for his leadership in this project. I also want to thank Dr. Stephen Sprigle for teaching me a great deal about the biomechanics of the human body, which was invaluable for this project. Vlad Patrangenaru also played a large role in this thesis with his help in modeling and the hinge-back seating design.

I need to thank those at CATEA for their help on the designs as well as being test subjects. Vibhor Agrawal, Jon Jowers, Linghua Kong, Chris Maurer, Adrienne Davis, and Clint Cope deserve special mention in this regard.

I also want to thank my wife, Necia, and our two children, Madeline and Nathan, for putting up with my late nights on campus writing this thesis. Finally, I need to thank my Father in Heaven for his constant support and guidance throughout my life.

TABLE OF CONTENTS

ACKNOWLEDGEMENTS ..... **iii**

LIST OF TABLES ..... **viii**

LIST OF FIGURES ..... **ix**

SUMMARY ..... **xiii**

1. INTRODUCTION **1**

1.1 Extensor Thrusts 1

1.2 Dynamic Seating Systems 5

1.2.1 Existing Concepts 5

1.2.2 Dynamic Seating Survey 10

1.3 Pressure Ulcers 12

1.4 Research Goals and Thesis Outline 15

2. SINGLE HINGED-BACK SEATING SYSTEM **17**

2.1 Similar Studies 17

2.2 Hinged-Back Seat Components 18

2.2.1 Mounting Platform 19

2.2.2 Adjustable Frame 20

2.2.3 Dynamic Hinged Seatback 21

2.2.4 Seatback Rigidizer 23

2.3 Methods for Sensing and Differentiating Thrusts 25

2.3.1 Options for Sensing Methods 26

2.3.2 Active Breakaway 27

2.3.2.1 Data Collection Setup 28

2.3.2.2 Control Setup 29

2.3.3 Passive Breakaway....32
2.4 Experimental Data....37
2.4.1 Dynamic Seating Forces....37
2.4.2 Active Breakaway Data....39
2.4.3 Passive Breakaway Data....45
2.4.4 Summary....46
3. DEVELOPMENT OF ADVANCED DYNAMIC SEATING SYSTEM....47
3.1 Guiding Principles....47
3.2 Variable Stiffness Seating System....49
3.2.1 Roller Seat Back Design....52
3.2.2 Tilt-Away Seat Bottom Design....57
3.2.3 Two Degree of Freedom Footrest....59
3.2.3.1 2 DOF Design....60
3.2.3.2 Electromagnet Breakaway....62
3.2.3.3 Permanent Magnet Breakaway....65
3.3 Alternate Designs....68
3.3.1 Seat Lifting Concept....69
3.3.2 Double Roller Variable Stiffness Concept....72
3.4 Experimental Data....73
3.4.1 Seat Back Stiffness....74
3.4.2 Motor Speeds....78
3.4.3 Thrust Interaction Forces....82
3.4.3.1 Methodology....82
3.4.3.2 Seat Back Forces....84
3.4.3.3 Seat Bottom Forces....90

3.4.3.4 Seat Belt Forces 95
3.4.3.5 Combined Force 97
3.5 Conclusion 99
4. LOAD DISTRIBUTION IN STANDARD CONFIGURATIONS 102
4.1 Levo Wheelchair 105
4.2 Tilt Mechanism 106
4.2.1 Tilting Ramp 107
4.2.2 Overhead Winch Design 108
4.3 Wheelchair Mountings 112
4.4 Methodology 116
4.5 Modeling 120
4.6 Results 123
4.6.1 Tilt Results 124
4.6.2 Recline Results 127
4.6.3 Stand Results 130
4.6.4 Comparison of Methods 134
4.7 Conclusion 139
5. CONCLUSION 141
5.1 Hinged-Back Dynamic Seat 141
5.2 Development of Advanced Dynamic Seating System 142
5.3 Pressure Relief Comparison 143
5.4 Future Work 144
5.4.1 Dynamic Seating Systems 144
5.4.2 Pressure Relief Study 147
APPENDIX A: DSS SURVERY REPORT 148

APPENDIX B: UNDERGRAD DESIGN CALCULATION.....162

APPENDIX C: THRUST INTERACTION FORCE DATA 163

APPENDIX D: THRUST INTERACTION FORCE METHODOLOGY 174

APPENDIX E: DATA FROM PRESSURE RELIEF STUDY.....179

REFERENCES.....183

LIST OF TABLES

Page

Table 1: Advanced Dynamic Seating Components 51

Table 2: Seat Back Materials Used 75

Table 3: Wheelchair Test Configurations 83

Table 4: Significant Differences in Seat Back Normal Forces 86

Table 5: Correlations Between Seat Back Data 89

Table 6: Significant Differences Between Seat Bottom Normal Forces 91

Table 7: Correlations Between Seat Bottom Data 94

Table 8: Significant Differences Between Seatbelt Tension Forces 97

Table 9: Significant Differences Between Combined Interaction Forces 99

Table 10: Combined Force Summary Comparison 99

Table 11: Angles for Data Collection 117

Table 12: Mat Reading for Creep Study 119

Table 13: Body Segment Parameters in Person Model 122

Table 14: Legend for Pressure Relief Data 124

Table 15: Knee Preload Forces 131

Table 16: Polynomial Fit Lines for Tilt 135

Table 17: Polynomial Fit Lines for Recline 136

Table 18: Polynomial Fit Lines for Stand 137

Table 19: Seat Bottom Reduction Comparison 144

LIST OF FIGURES

Page

Figure 1: Progression of an Unconstrained Extensor Thrust in a Fixed Chair 2

Figure 2: Dynamic Backrest from Miller's Adaptive.....6

Figure 3: Dynamic Footrest from Miller's Adaptive 6

Figure 4: Aktivline Dynamic Seating System by InterCo Gmbh 7

Figure 5: Traveling Seat Concept (US Patent 6,488,332), 2002 8

Figure 6: Ergonomically Designed Seat Concept (US Patent 5,904,398), 1999 8

Figure 7: Headrest with Pivotal Support Concept (US Patent 5,791,735), 1998.....9

Figure 8: Stage Four Pressure Ulcer 13

Figure 9: Dynamic Hinged-back Seat Prototype 18

Figure 10: Dynamic Hinged-back Seating Components 19

Figure 11: Mobile Mounting Platform.....20

Figure 12: Diagram of Adjustable Components 21

Figure 13: Hinged Seatback in upright and bent configurations 22

Figure 14: Carabiner (www.omegapac.com).....23

Figure 15: Action Sequence of Seatback Rigidizer 25

Figure 16: Strain Gauges on Flexible Seat Back 28

Figure 17: Motion Capture and Tracking 30

Figure 18: Labview Control Schematic 31

Figure 19: Labview Interface for Control Algorithm 31

Figure 20: Spring Preload and Ideal Breakaway Curves 34

Figure 21: Motion of Footrest During Plantar Flexion 35

Figure 22: Interaction Between Shaft and Spring Detent 36

Figure 23: Footrest Prototype with Passive Breakaway 36
Figure 24: Strain Gauge Profiles and Trends vs. Maximum Seatback Deflection 38
Figure 25: Foot Force Profile and Trends vs. Maximum Seatback Deflection 38
Figure 26: Force Threshold Activation Profile 40
Figure 27: Horizontal Velocity During Force Threshold Breakaway 41
Figure 28: Strain Voltage and Gradient for Threshold = 0.03 42
Figure 29: Strain Voltage and Gradient for Threshold = 0.062 43
Figure 30: Vibration Spikes under No-Load Condition 44
Figure 31: Passive Sensor Breakaway Force Curve 45
Figure 32: Variable Stiffness Concept with Moving Flexure Point 50
Figure 33: Rigidizer Tilt-Away Concept with Fixed Flexure Point 51
Figure 34: Full-body Motion of Variable Stiffness Prototype 52
Figure 35: Diagram of Double Rail Design 53
Figure 36: Rigid and Dynamic Configurations of Double Rail Design 54
Figure 37: Side View of Improve Double Rail Design 54
Figure 38: Back View of Improved Double Rail Design 55
Figure 39: View of Offset Roller on Seat Back 57
Figure 40: Overhead view of Tilt-Away Mechanism 58
Figure 41: Motion of Tilt-Away Mechanism 59
Figure 42: Motion of the Improved Footrest 60
Figure 43: Improved Footrest Prototype 61
Figure 44: Electromagnet with Permanent Magnet Array 63
Figure 45: Force Profiles of Electromagnet 64
Figure 46: Footrest Motion during Electromagnet Breakaway 65
Figure 47: Footrest with Permanent Magnet 66

Figure 48: Force Reading During Breakaway with No Spacing 67
Figure 49: Peak Normal Force During Footrest Breakaway 68
Figure 50: Motion Profile of Four-Bar Concept 70
Figure 51: Four-Bar Prototype with Component Diagram 71
Figure 52: Four-Bar Prototype in Actuated Position 71
Figure 53: Schematic of Non-Parallel Support Rods 73
Figure 54: Force-Deflection Curves of Seat Back 74
Figure 55: Material Thickness-Deflection Curves of Seat Back 75
Figure 56: Effect of Offset Roller on Seat Back Corner Deflection 77
Figure 57: Effect of Offset Roller on Seat Back Center Deflection 78
Figure 58: Roller Speed vs. Load on Seat Back 80
Figure 59: Rigidizer Speed vs. Load on Seat Bottom 81
Figure 60: Seat Back Normal Force in Full Extension 85
Figure 61: Seat Back Contact Area in Full Extension 87
Figure 62: Seat Back Vertical Center of Pressure in Full Extension 87
Figure 63: Seat Back Peak Pressure Index in Full Extension 89
Figure 64: Seat Bottom Normal Force in Full Extension 90
Figure 65: Seat Bottom Contact Area in Full Extension 92
Figure 66: Seat Bottom Horizontal Center of Pressure in Full Extension 93
Figure 67: Seat Bottom Peak Pressure Index in Full Extension 94
Figure 68: Seatbelt Preload Forces 95
Figure 69: Seatbelt Tension Force in Full Extension 96
Figure 70: Combined Seat, Back, and Seatbelt Force in Full Extension 98
Figure 71: Schematic of Tilt, Recline, and Stand Positions 103
Figure 72: Levo Combi Wheelchair 104

Figure 73: Levo Combi Wheelchair Positions 106
Figure 74: Schematic of Tilting Ramp Platform 107
Figure 75: Overhead Winch Tilt Mechanism 108
Figure 76: Schematic of Overhead Winch Mechanism 109
Figure 77: Overhead Winch with Separator Block 110
Figure 78: Removable Ramp for Tilt Platform 111
Figure 79: Wheel Block and Front Caster Tie-down 112
Figure 80: 15 degree Tilting Block 113
Figure 81: Subject in Chair with Platform tilted to 35 degrees 114
Figure 82: Anti-tip Block During Recline 115
Figure 83: Levo Wheelchair in Recline Position on Tilt Platform 115
Figure 84: Levo Wheelchair in Standing Configuration 116
Figure 85: Simulated Tilt Configuration using Working Model 2D 120
Figure 86: Experimental and Simulated Forces in Tilt 125
Figure 87: Sum of Forces in Tilt 127
Figure 88: Experimental and Simulated Forces in Recline 128
Figure 89: Sum of Forces in Recline 129
Figure 90: Experimental and Simulated Force in Stand 130
Figure 91: Sum of Forces in Stand 133
Figure 92: Best Fit for Tilt Results 135
Figure 93: Best Fit for Recline Results 136
Figure 94: Best Fit for Stand Results 137
Figure 95: Comparison of Pressure Relief at Seat Bottom 139
Figure 96: Mat Placement for Dynamic Seat Data Collection 174
Figure 97: Dynamic Seat Motor Power and Control 176

SUMMARY

High-tone extensor thrust is common to those with cerebral palsy and spinal cord injuries. It is a muscle-control phenomenon that causes the body to straighten spastically. To prevent users from sliding out of wheelchairs and injuring themselves, they are restrained with belts and harnesses. While this solves one problem, it causes others, namely, high forces on the wheelchair frame and discomfort for the user. One goal of this thesis is to design a dynamic seating system that moves with respect to the wheelchair frame, allowing the seat to move with the user during an extensor thrust. This should reduce the forces felt by the user during an extensor thrust.

One unique challenge to the problem is that the seat needs to remain rigid during normal functional activities of the user and only become dynamic when an involuntary thrust is detected. A second goal of this thesis is to design a control scheme that is able to differentiate between these two types of motion and control the seating system appropriately. These design goals are initially investigated with a hinged seat back system. It is instrumented with sensors and linked to a computer to allow for the detection of thrusts and to actively control seating components. After this initial evaluation, a full seating system is designed and built to allow for a full-body extensor thrust, involving the seat back, seat bottom, and leg rest of the wheelchair. This system is analyzed for effectiveness of reducing forces on the body during an extensor thrust.

In addition to the challenge of extensor thrusts, another serious problem for this segment of the population is pressure ulcers. These are caused by prolonged pressure on the skin from weight-bearing bony prominences. Normal users shift their weight often

and reduce the chance of skin breakdown. Those with spinal cord injuries cannot feel the discomfort and have a challenge in repositioning themselves often. Thus, they are at high risk for pressure ulcers. Various seating system configurations are known to help with pressure relief. The three standard configurations for a chair are tilt, recline, and standing. While each effectively reduces and/or shifts the weight of the person, a formal study comparing the effectiveness of the three methods against each other with the same chair has never been done. The final goal of this thesis is to measure and compare the effectiveness of these three methods for their ability to relieve pressure on the seat bottom. To accomplish this, a powered wheelchair with built-in capabilities for recline and standing is mounted to a tilting mechanism. Test subjects are used to experimentally compare the effectiveness of each method for pressure reduction using pressure mats on all weight-bearing surfaces. In addition, a two-dimensional model is developed and validated with the experimental results.

CHAPTER 1

INTRODUCTION

Medical, technological, and societal advances have increased the quality of life dramatically for wheelchair users. As those with disabilities live longer and continue to strive for greater personal freedom, increasing demands must be placed on their wheelchair. Research in this area is thus focused on long-term usage, along with the prevention of secondary disability [1]. Wheelchairs must be able to provide more functionality and reduce the user's dependence on a caregiver. The types of functionality depend on the specific challenges of the population for whom the wheelchair is designed.

One segment of the wheelchair population where needs are greatest is those who experience high-tone extensor thrusts. Challenges facing this group include frequent breakage of chair components, the constant need to be repositioned properly in the wheelchair, and a high risk for the development of pressure sores. The work in the thesis seeks to design wheelchair seating systems that address these challenges in the functionality of the wheelchair, and by so doing, improve the comfort and quality of life of those affected by high-tone extensor thrust.

1.1 Extensor Thrusts

Extensor thrusts are a symptom of muscle control problems. The condition causes the major muscles in the body to contract simultaneously. As the extensor muscles are generally stronger than the flexor muscles, the person tends to straighten out as shown in Figure 1. For wheelchair users, this leads to the user sliding or falling out of the chair. The most common remedy is to highly constrain the user with belts or other restraints.

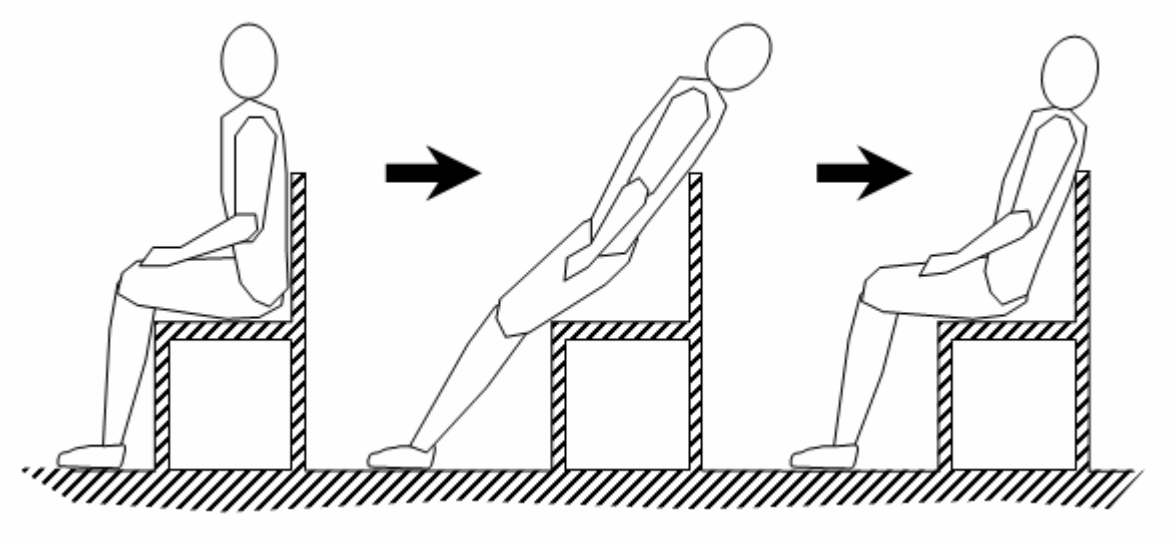

Figure 1: Progression of an Unconstrained Extensor Thrust in a Fixed Chair

Common examples of restraints include lap belts, some with anti-slip pads, chest straps and shoulder harnesses [2]. These are used to keep the occupant firmly seated during a thrust. Unfortunately, these restraints lead to other problems as the extensor thrust, instead of extending the body, creates large forces on the back, thighs, and feet. This is uncomfortable for the user, and also causes frequent breakage of the wheelchair components that are resisting these forces due to large moments and cyclical loading. Other problems from restraints include soreness from a constant seating position and moisture buildup from a lack of air circulation.

Other positioning devices are also used to maintain proper position when the user is not experiencing an extensor thrust. As users often lack muscle control, these supports help to keep the spine aligned, and the shoulders in a forward position to stabilize and increase arm movement range [3]. Extensor thrust wedges also exist with the specific aim to decrease the seat-to-back angle [4], which often reduces the frequency of extensor thrusts. One problem with these seating solutions is that they don't maintain proper

position after an extensor thrust. They keep the user from sliding out of the chair, but after the thrust episode is over, the user has moved to a more "slouched" position.

Extensor thrusts are common to people who have high muscle tone. Two groups who are impacted by this are those with cerebral palsy and spinal cord injuries. These two groups are the focus of the work done in this thesis.

Cerebral Palsy (CP) is a disease affecting somewhere between 500,000 and 750,000 people in the United States. It is a non-progressive disorder that is caused by damage to the muscle-control area of the brain. The damage to the brain most frequently happens before birth, but can also happen during and after the birthing process [5]. Common symptoms of cerebral palsy include unusual muscle tone. Tone can be thought of as a readiness to move, or the state of a muscle. People with normal muscle tone provide a normal level of resistance when someone attempts to move them. Those with cerebral palsy can have either low tone, where they are extremely "floppy", or they can exhibit high tone, where they are very stiff. Tone can also be variable, with a person having generally low tone, but change to very high tone at different times [6]. Extensor thrusts are an example of this change. Asymmetries of movement, or in other words, different tone for each side of the body, can also occur. This can lead to a rotation of the spine during extensor thrusts [7].

Treatment is generally effective for those with cerebral palsy, and some control can be gained over muscles. High-tone extensor thrusts, however, continue to occur in a spastic fashion for many affected with cerebral palsy. Botox injections directly into the muscle can help the muscle relax for certain individuals. Another treatment that is

effective involves using Baclofen, an anti-spasmodic drug [6]. While these can help reduce extensor thrusts, they do not eliminate the problem completely.

Spinal cord injuries, though different in nature than cerebral palsy, has similarities in the presence of extensor tone. When someone suffers a spinal cord injury leading to paralysis of a muscle, change in tone of that muscle almost always occurs. Either low tone or high tone can result, and the muscle can have spastic changes from low to high tone similar to that exhibited by those with cerebral palsy. These changes usually happen in response to the muscle being moved [8].

Because high-tone extensor thrusts are often linked to injuries of the brain and nervous system, some people have limited cognitive abilities and extensor thrusts are merely a result of uncontrolled changes in tone. Others, however, do have a great amount of cognitive abilities, and yet are still affected by extensor tone. These users suffer from involuntary extensor tone, but also have learned how to voluntarily use the same movement for achieving functional tasks, such as communicating. Another use for this voluntary extensor motion is to stabilize a muscle, joint, or body segment. For example, in order to extend the arm and reach for something, the shoulder blade must be stabilized. This is automatically done in those with normal muscle control. However, as users often do not have complete control over their muscles, a controlled extensor motion can be used to pin the shoulder blade against the back of the seat, and thereby gain the needed stability to accomplish the task. This dual nature of extensor thrusts is critical in the design of useful seating systems.

1.2 Dynamic Seating Systems

The negative effects of restraining users in a chair during an extensor thrust were mentioned previously. These included large forces on the chair components, and consequently, large forces pushing back on the user. The idea of a "dynamic seat" that moves with the user during an extensor thrust has been suggested [9]. Such a dynamic seat moves with respect to the wheelchair frame and contains both resistive and dissipative elements to absorb the energy during an extensor thrust. This naturally leads to a more comfortable experience for the user and also can lead to reduced breakage of chair components. An additional benefit of using a dynamic seating system is that is allows for the possibility of correctly repositioning the user after a thrust if the motion of the system can be designed intelligently.

1.2.1 Existing Concepts

Currently on the market, there are several wheelchair products that have dynamic seating components. One system, designed by Miller's Adaptive uses add-on components to existing wheelchair frames. The dynamic backrest and two-degree of freedom footrest are shown in Figure 2 and Figure 3, respectively. Both systems use gas shocks that provide resistance and damping to the motion of the user. The gas shocks are available with resistances of 15, 20, 40, 80, and 120 lbs of resisting force [2]. By using different combinations of gas shocks, discrete stiffnesses can be achieved. Additional types of dynamic footrests and headrests are also available.

Figure 2: Dynamic Backrest from Miller's Adaptive

Figure 3: Dynamic Footrest from Miller's Adaptive

Another dynamic seating solution on the market is offered by InterCo Gmbh. They make a dynamic wheelchair called Aktivline that is specifically designed for children with cerebral palsy and similar disorders. Rather than dynamic components that attach to existing chairs, their product is a complete chair with integrated dynamic components, shown in Figure 4.

The integrated design allows for potentially better control of the overall extensor motion, as the dynamic components have known relative distances. Additionally, the Aktivline features physiological hinges, located approximately at the same location as the point of rotation for each joint [10]. This reduces shearing forces that are caused during

Figure 4: Aktivline Dynamic Seating System by InterCo Gmbh

rotation, improving comfort and reducing skin friction. It also helps to keep the pelvis properly positioned during an extensor thrust, increasing the chances that proper positioning will be maintained at the end of the thrust, and thereby reduce the need for the caregiver to constantly reposition the occupant.

Aside from existing commercial products, several patents exist for dynamic seating systems or components. Some are related to the design of systems for extensor thrusts, while others are unrelated, but still reviewed here due to the potential similarities in design concepts developed in the thesis.

A figure from a patent assigned to InterCo Gmbh is shown in Figure 5. This appears to be the design concept from which the Aktivline came. Some things to note about this design are that it contains rigid seating components (i.e. the seatback, seat bottom, and footrest do not flex). All the elements work in a passive manner, and the seatback and seat bottom articulate together, while the footrest can move independently [11].

Another dynamic seating concept was patented by Susan Farricielli [12], as shown in Figure 6. In this design, all the elements are passive and appear to provide a more

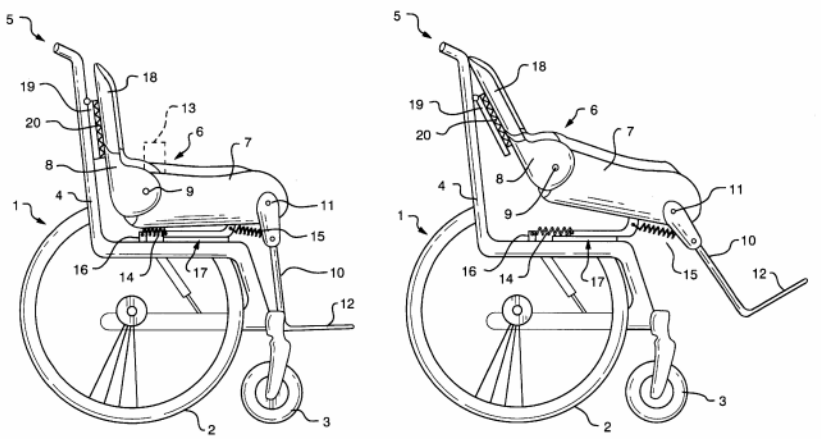

Figure 5: Traveling Seat Concept (US Patent 6,488,332), 2002

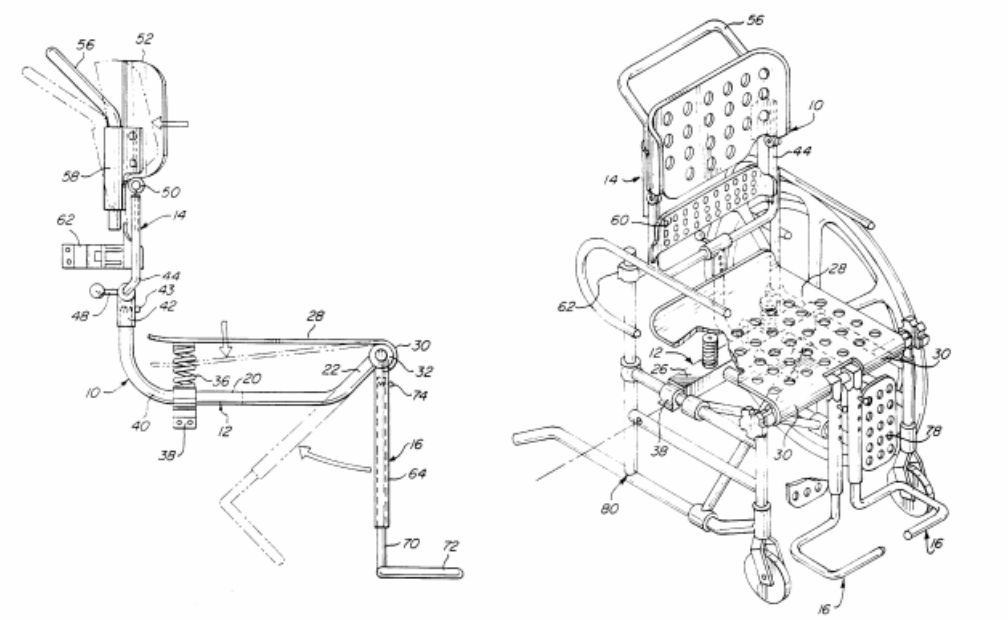

Figure 6: Ergonomically Designed Seat Concept (US Patent 5,904,398), 1999

comfortable ride during wheelchair use, rather than being used to absorb energy during an extensor thrust. The system does have a great deal of adjustability, which allows it to be fit to users with many different needs.

A third design, assigned to Sunrise Medical, focuses specifically on the headrest, rather than on an entire dynamic seating system. It is shown in Figure 7. This design provides needed support to the neck and head, while allowing one-degree of freedom

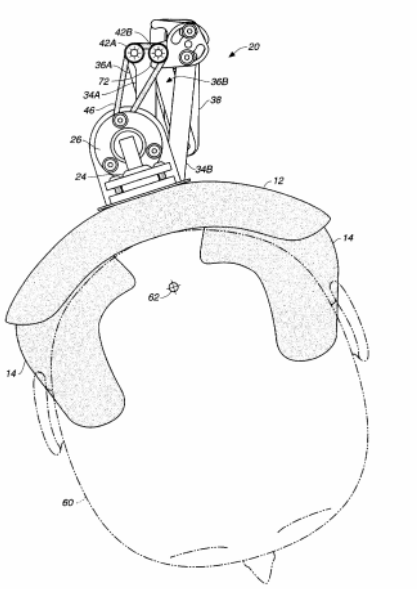

Figure 7: Headrest with Pivotal Support Concept (US Patent 5,791,735), 1998

motion for side-to-side movements of the head [13]. This is a passive system that does help reposition the head after rotational movements. While this does provide necessary support while allowing resisted movements, it unfortunately doesn't allow for neck extensions that are present in high-tone extensor thrusts.

Additional patents with dynamic components include one assigned to Salem Home, Inc. [14]. This wheelchair has a passive dynamic breaking system that engages when weight is removed from the wheelchair frame. This system only deals with controlled volitional movements, and has fundamentally different objectives than the goals of this thesis. Bellvis Castillo has a concept for a dynamic footrest that helps to achieve better posture [15]. This active system adjusts the angle of each foot independently, however it does not allow for full plantar flexion that occurs during extensor thrusts. Nor does it have resistive elements to absorb the energy from this action. Finally, a chair designed by Robert Jensen has continuous, passive dynamic motion of the seat bottom. This is intended to mimic the normal movements that the spine would feel during walking [16].

It does not account for the overall movements present in extensor thrusts, and has a different fundamental design goal than this thesis.

1.2.2 Dynamic Seating Survey

A dynamic seating system is an obvious choice to deal with challenges from high-tone extensor thrusts. Before beginning to design a system that will satisfy the needs of the user, it is important to find out what other factors are important from users and caregivers who deal with these challenges every day. These users and caregivers can also provide keen insight into the nature of extensor thrusts, which are not well understood. This insight will provide a useful starting point for the design.

With these objectives in mind, a survey was conducted by the Center for Assistive Technology and Environmental Access (CATEA) at Georgia Tech. Twenty-three stakeholders, including families with children affected by cerebral palsy, physical and occupational therapists, and wheelchair vendors participated in a survey about their understanding of the extensor thrust phenomenon, as well as what requirements they see for a dynamic seating solution. Important points will be discussed here, while the report is given in its entirety in Appendix A.

First, participants were asked to identify where they think extensor thrusts originate. Beginning at the pelvis and extending outwards in both directions, beginning in the lower extremities and extending upwards, and beginning in the upper extremities and extending downwards were the options. A few selected one of these options, but the majority felt that extensor thrusts initiate in different parts of the body, rather than always beginning in one location.

Second, participants were asked if a list of activities were accomplished with the help of purposeful, semi-controlled extensor thrusts. The list included accessing switches, assisting with chair-to-bed transfers, reaching for objects, communication, raising their head, changing position within the wheelchair, and driving the wheelchair. While not a unanimous consensus, the majority of respondents agreed that each task on the list is accomplished by the use of voluntary thrusts.

The next set of questions involved finding out about the nature of controlled versus uncontrolled thrusts. The majority of participants agreed that involuntary thrusts are faster than purposeful thrusts. They also felt that purposeful thrusts tend to last longer depending on the task. They did not, however, agree that involuntary thrusts are more intense (i.e. stronger) than purposeful thrusts.

A set of questions regarding certain requirements that a dynamic seat must have was asked. Participants desired portability of the chair, with either the seating system being removable from the frame, or at least having the frame still be collapsible with the seating system attached. Growth kits to allow the chair dimensions to extend were required, as the target group is growing children, and buying a new wheelchair every year is not a feasible option. Adjustability of the system without the need for specialized tools is also desirable. In addition, respondents want a chair that has features common to other advanced seating wheelchair designs, including tilt-in-space and manually adjustable recline angles. Aside from pressure relief, these functions also aid in transfers. Another requirement is the ability to disable the dynamic components with a single action for situations where dynamic movement of the chair could be dangerous to the occupant and those nearby.

These requirements are essential to a successful acceptance of a dynamic seating system in the marketplace, but are better suited to the final stages of design and engineering. This thesis focuses on the initial design concept and testing of a seating system to deal with extensor thrusts. Other factors that are standard on wheelchairs can be engineered to work with these designs at a later time, and are more suited to a commercial environment where detailed knowledge of government regulations and market acceptance are present.

Requirements that do fall under the scope of this work included a desire to have the dynamic components function independently from each other. When asked about the acceptability of electronic sensors and motors versus only mechanical devices, participants indicated that electronics are acceptable for advanced control functionality. They also want these electronics to be easily adjustable so that thresholds and parameters, such as rate-of-return of the system, can be fine-tuned throughout the day, if necessary.

This data is an invaluable aid in the design of a dynamic seating system. It can be looked upon as a specification list that the final product must meet, and will be useful as a basis for evaluating designs.

1.3 Pressure Ulcers

Pressure ulcers, also known as pressure sores and bedsores, are visible and painful evidence of reduced blood supply to skin and tissues under the skin [17]. When the oxygen and nutrients are cut off from the skin, it begins to die, and a pressure ulcer is formed. The stages of pressure ulcer damage run from slight discoloration of the skin all the way to an open sore that extends down to the bone [18], such as that shown in Figure

8. Pressure ulcers can happen quickly, in as little as 12 hours, and the injury may not show up for days or weeks afterwards [19]. Because the ulcer is a direct result of unrelieved pressure, pressure ulcers usually form under weight-bearing points, such as below the ischial tuberosities or under the heel. Shearing forces can also contribute to the formation of pressure ulcers [18].

Two of the most common groups to experience pressure ulcers are those with spinal cord injuries and the elderly [17]. Those with spinal cord injuries are often not able to feel the discomfort associated with prolonged pressure, and they may have difficulty shifting their posture in a wheelchair frequently enough to avoid pressure ulcers. This is particularly true for people with quadriplegia. The elderly population tends to spend a great deal of time sitting, and may also have difficulty repositioning their weight frequently enough as muscle strength deteriorates. In addition, they may have decreased sensation that reduces the body's ability to send warning signals about potential damage to an area. A smaller group that is also at risk for pressure ulcers are those affected by extensor thrusts, encompassing some of the aforementioned people with spinal cord injuries. The restraints used to keep occupants from sliding out of their chairs also restrict the ability of the user to reposition and readjust their weight in the wheelchair. If the belts are further tightened to reduce slouching after a thrust, the risk of pressure ulcers

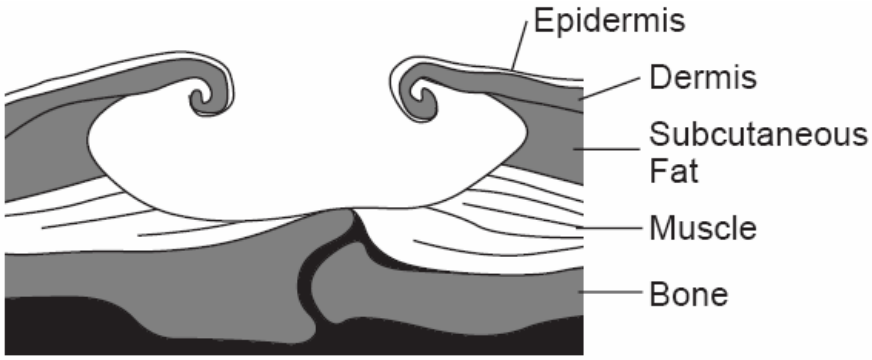

Figure 8: Stage Four Pressure Ulcer

is increased further.

Treatment of pressure ulcers involves removing pressure from the wound and allowing it to heal [20]. Friction should also be avoided, as it will aggravate the wound. The challenge of removing pressure to allow the wound to heal is difficult, as the sore was caused in the first place by unrelieved pressure. Care must also be taken to not cause pressure ulcers at other locations during this healing process.

Prevention is obviously preferred to healing. Suggested guidelines involve "repositioning chair-bound individuals every hour if they cannot perform pressure-relief exercises every 15 minutes" [21]. This is a time-consuming effort even in a fully-staffed nursing home, and severely limits the personal freedom of the user. Some of the pressure-relief exercises that allow a person to be more independent include tilting the wheelchair to 65° and leaning forward onto one's knees [18]. This effectively removes pressure from the buttocks where the majority of the weight of the trunk and upper extremities is carried. Other prevention guidelines for those in wheelchairs recommends that a trained healthcare professional select appropriate pressure relief exercises for wheelchair users [21].

These guidelines lead to the standard, accepted methods of pressure relief in a wheelchair, namely tilt and recline. Tilt maintains the seat-to-back angle constant while rotating the seating frame backwards. Recline opens up the seat-to-back angle, while maintaining the seat bottom at a relatively constant angle with respect to the ground. These methods are prescribed to aid in pressure reduction for wheelchair users. Another pressure reduction technique exists, that of standing, whereby the seat-to-back angle is opened up with the footrest and backrest angles remaining relatively constant with

respect to the ground. The relative effectiveness of these three techniques has not been fully studied, and is one of the goals of this thesis.

1.4 Research Goals and Thesis Outline

This thesis is part of a larger study at Georgia Tech involved in identifying the nature of extensor thrusts in greater detail, as well as designing seating systems that will hopefully reach a commercial market with the help of professional partners. The goals of this thesis focus on the seating needs of those with high-tone extensor thrust, and how to improve their comfort and quality of life

The first goal of the thesis is to test the basic assumptions of the dynamic seat, namely that a dynamic component will reduce the interaction forces between the user and the seat caused during a high-tone extensor thrust. To verify these assumptions, a single-hinged seatback is constructed to allow the experimental study of forces on the back during a thrust. The next goal is to effectively differentiate between voluntary and involuntary extensor thrusts, and have the chair respond appropriately. To accomplish this, the seatback is instrumented with sensors and active components. Two methods are developed and evaluated. These schemes use knowledge gained from the CATEA survey in their design. This is covered in Chapter 2 of the thesis.

Building on the first goal, an advanced dynamic seating system is developed that involves all the major muscle groups of the body that contribute during an extensor thrust. This is described in Chapter 3. This advanced system is designed to allow the body to extend against energy-absorbing components, while simultaneously putting the muscles at a weaker mechanical advantage, which helps to reduce forces. The design

takes into account the curvature of the spine and other knowledge to customize each element of the seating system for its functional task. The effectiveness of this seating system to reduce forces during an extensor thrust is analyzed.

The final goal of the thesis involves comparing methods of pressure reduction in wheelchairs. While tilt, recline, and standing are believed to be effective means of pressure relief, no side-by-side study has been done comparing the three methods on a single chair. Chapter 4 performs this study and reaches conclusions about the effectiveness of each method. One challenge in doing so is that no commercially available chair can do all three tasks. A mechanism is first designed and built that can effectively tilt a 350 lb. powered wheelchair, which itself has standing and recline capabilities. This allows for a comparison study of the three methods on a single chair. Laboratory methods are developed and data is collected from able-bodied subjects, with a future goal of testing those with spinal-cord injuries. A computer model is also developed and validated from the data to further the understanding gained through this study.

CHAPTER 2

SINGLE HINGED-BACK SEATING SYSTEM

In order to investigate the effects of a dynamic seating system on a user, a prototype was built involving a single-hinged seat back. This allows for the study into the effectiveness of a dynamic seating component to reduce forces during an extensor thrust. This prototype was also instrumented with sensors and active components to test the control schemes used to differentiation between voluntary and involuntary extensor thrusts.

2.1 Similar Studies

Before work began on this thesis, another study [22] was completed in a joint partnership between Georgia Tech and the Kumoh National Institute of Technology in Korea. This study developed a fundamental model that captures the essence of an unconstrained extensor thrust on a rigid seat. The body was modeled using three rigid links resting on a rigid seat frame. An extensor thrust motion was captured on video and input into the model. The forces at the points of contact, along with the torques of the knee and hip, were calculated using inverse dynamics. Sensitivity studies were also done on the effects of different coefficients of friction and uncertain body mass properties. This work resulted in general torque profiles during an unconstrained extensor thrust in a rigid chair.

Work on the project continued, with an effort to extend the model to include a dynamic seatback. The work focused heavily on modeling and used the model to drive the design of future prototypes. At the same time, the work in this thesis began with a

greater emphasis placed on building prototypes and evaluating their performance experimentally to drive the design of future prototypes. A single hinged-back dynamic seat was constructed as shown in Figure 9 for use in both studies, with the former study [23] using the seat to validate the model.

This thesis uses the hinged-back seat to verify that dynamic seating components can reduce forces during an extensor thrust. As well, it is used to study methods of sensing and differentiating between voluntary and involuntary tone. Inherent in the study of differentiation is the study of active and passive components to change the seat from a rigid to a dynamic state.

2.2 Hinged-Back Seat Components

The hinged-back design needs to fulfill three main functions. First, it needs to have a dynamic backrest that has resistive and dissipative elements, allowing the seatback to

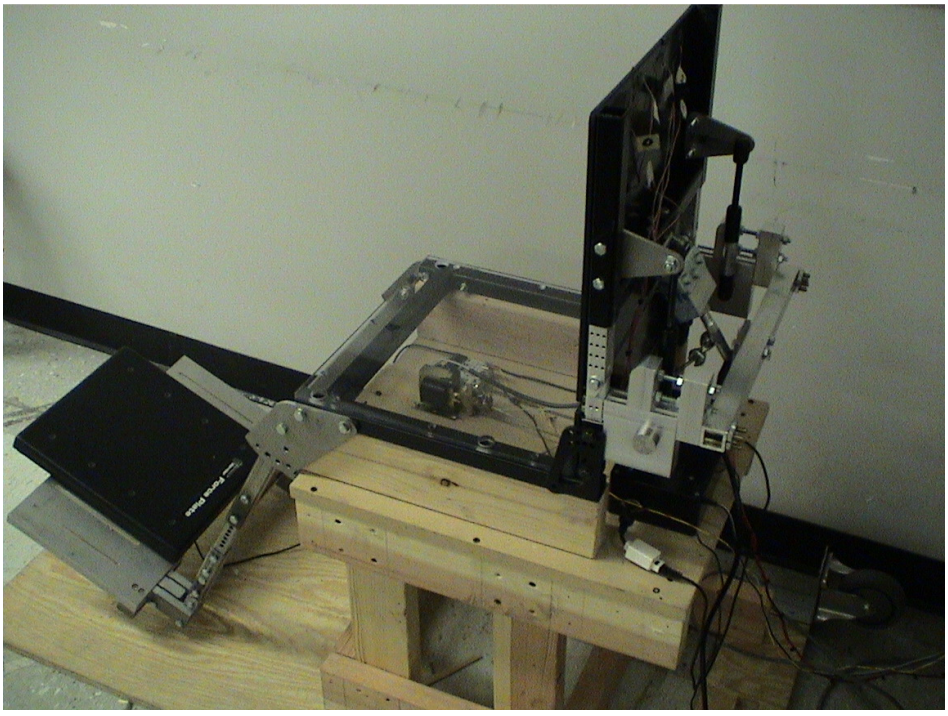

Figure 9: Dynamic Hinged-back Seat Prototype

move during a thrust, but keep the motion controlled. Second, it needs to have both a rigid and a dynamic configuration. Finally, it needs to have sensors and a control system to trigger the transition from rigid to dynamic states. Additional features are needed for stability and adjustability. Each component of the design is shown in Figure 10, and will be discussed individually.

2.2.1 Mounting Platform

The mounting platform, shown in Figure 11, has two main functions. The first is to provide overall stability for the prototype. It needs to create mounting surfaces for the seating frame to bolt on to and keep the system from tipping during an extensor thrust. The second function is to provide mobility for the system. In cases where participant transportation is difficult, the platform can be moved to meet their needs. This causes the

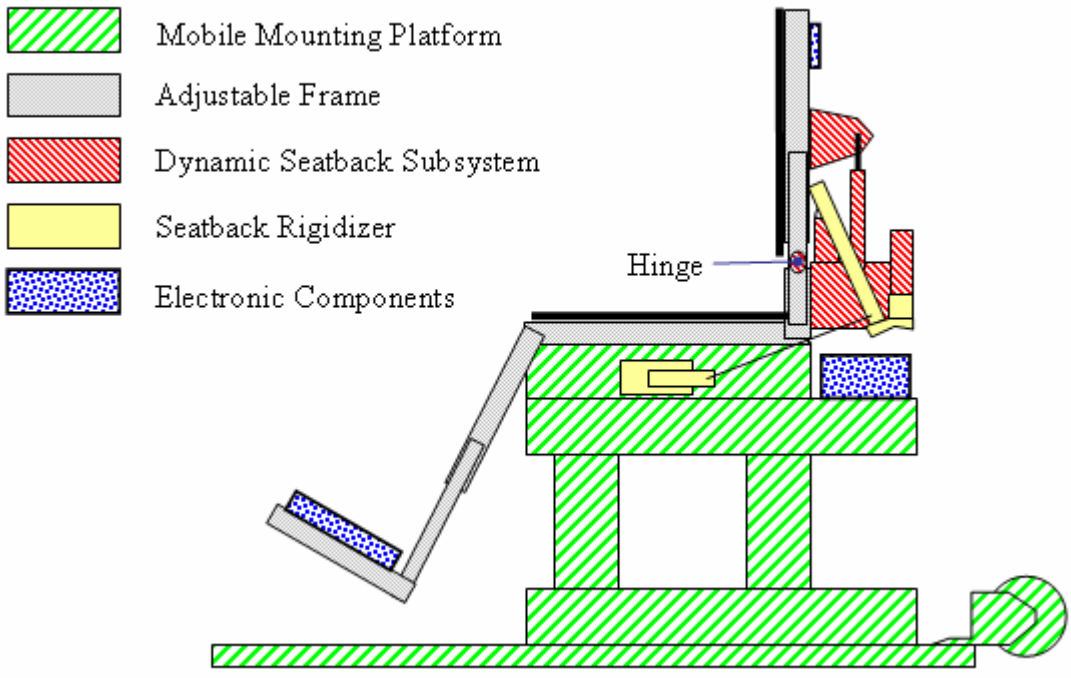

Figure 10: Dynamic Hinged-back Seating Components

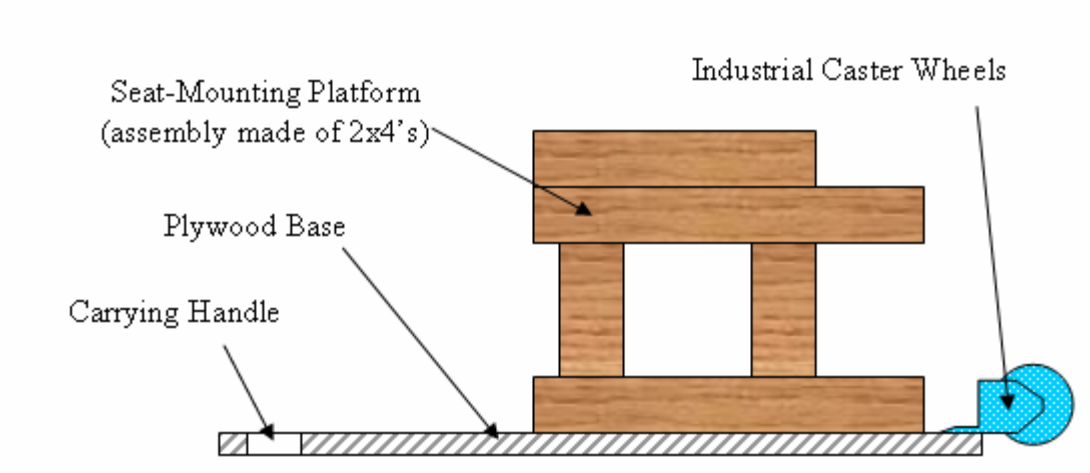

Figure 11: Mobile Mounting Platform

size and weight of the system to become important in the design.

To meet these needs, the mounting platform was constructed using 2x4's for the general framework. A plywood base was used to provide stability, into which a slot was cut to function as a carrying handle. Caster wheels were mounted to the opposite side of the plywood so that the entire system can be easily moved by a single person.

2.2.2 Adjustable Frame

Standard wheelchair seating systems are highly adjustable to accommodate the diversity of individual users. The hinged-back seating design needs similar adjustability. Figure 12 shows the adjustable parameters chosen for the system, including adjustments for leg length, torso height and joint angles. The hinge point is also adjustable, and is designed to pivot near the top of the pelvis where major lumbar extension begins. One known weakness of this design is that is does not allow for changes in seat depth.

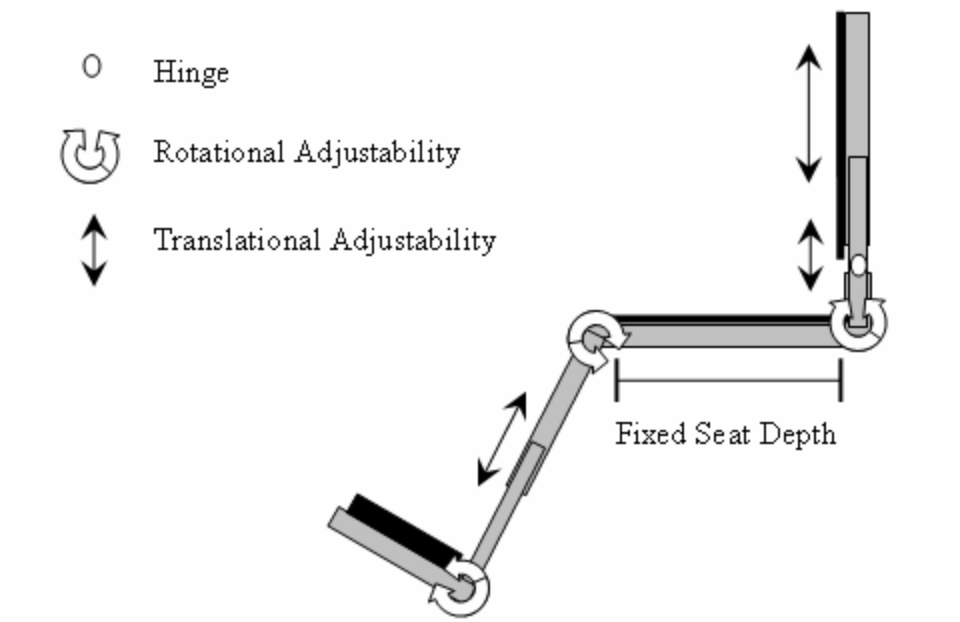

Figure 12: Diagram of Adjustable Components

2.2.3 Dynamic Hinged Seatback

The dynamic seatback is perhaps the most important part of the entire design, as it dictates the overall motion during an extensor thrust. Aside from the location of the hinge point, the most important piece affecting this motion is the choice of the spring. A nonlinear spring that increases its stiffness exponentially with distance traveled is desirable, making it impossible to ever reach a hard stop at the end of the move. Hard stops act like a discontinuous change in spring stiffness in the system, effectively replacing the stiffness of the spring by the stiffness of a metal bar. While metal bars do have inherent elasticity, they are dramatically more stiff than a coil or gas spring. This can lead to rebound effects and whiplash if the user is moving back quickly enough when the hard stop is reached. While such exponential springs could exist, they are likely expensive and challenging to design. A different approach was taken in this design with the use gas shocks, as shown in Figure 13. These have a built-in damper that only

functions during the last part of the stroke. This allows the user to push back quickly during most of the move, but if they are moving too quickly, the damper acts as an additional braking force before the gas shock is fully compressed.

Aside from the stroke length of the gas shocks, two other hard stops exist on the seatback. One acts to keep the seatback from returning past the upright position. The other is an adjustable hard stop that acts to limit the maximum angle that the seatback can

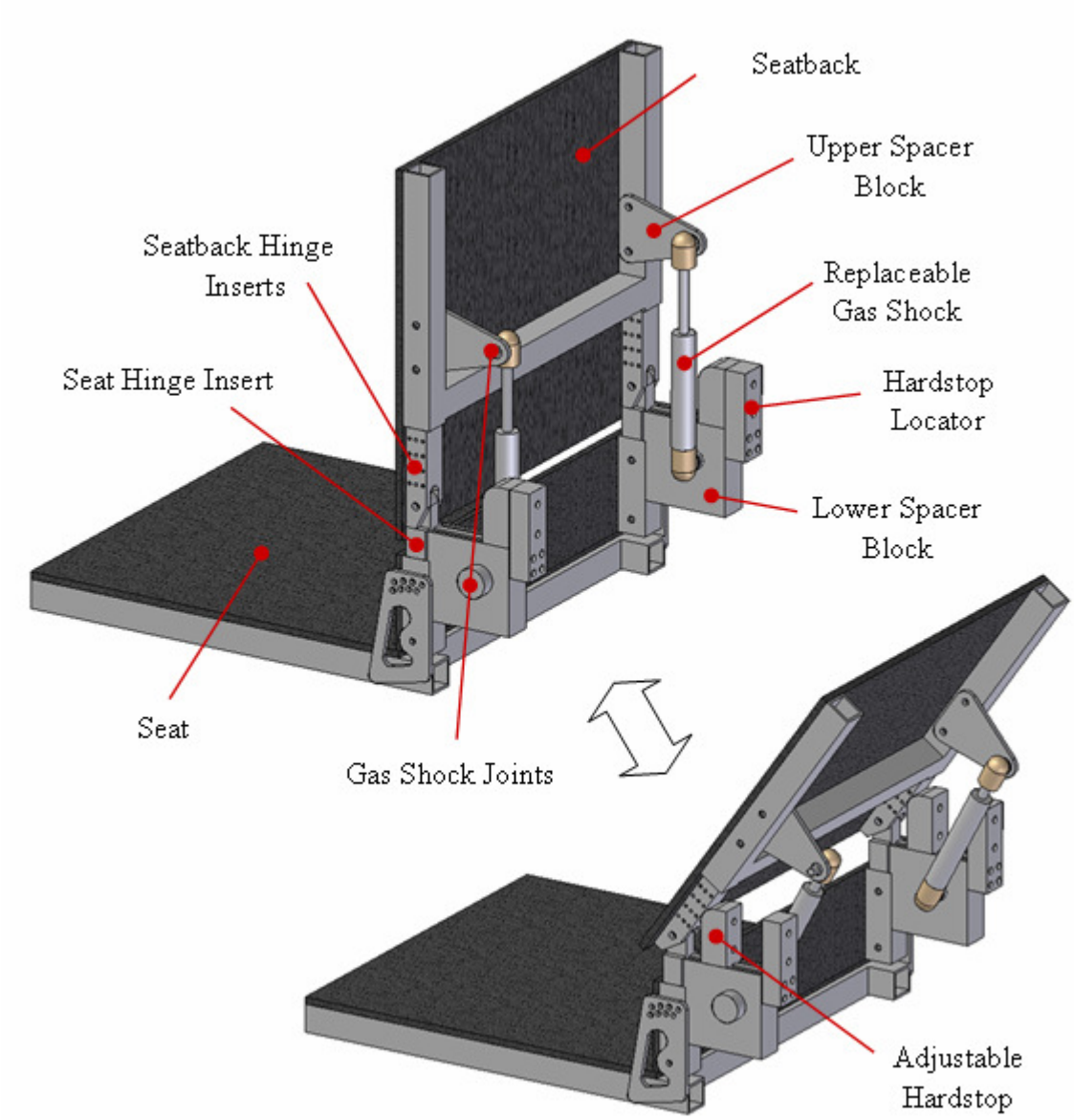

Figure 13: Hinged Seatback in upright and bent configurations

tilt back.

2.2.4 Seatback Rigidizer

In order to accommodate the functional tasks accomplished with volitional tone, it is necessary for all dynamic seating systems to have a rigid configuration along with a dynamic configuration. This presents a unique design challenge because the change from a rigid to a dynamic state can occur under loaded conditions. While this may not at first seem extraordinarily challenging, a few examples will help to illustrate the inherent challenge.

Many things are designed to change from a rigid to a dynamic state under no-load conditions. In fact, many things are specifically designed to make it impossible to make the change under loaded conditions. Consider a carabiner, shown in Figure 14. With no strain on the structure, the gate can be easily opened. Under load, however, the slight angle of the notch keeps the gate pin engaged as the C-shaped structure flexes outwards. This prevents ropes from slipping out of the carabiner during climbing. An additional

Figure 14: Carabiner (www.omegapac.com)

safety feature is the locking screw that encases the pin and notch and further keeps the gate closed. From this we see that it is easy to keep things from changing to a dynamic state under load.

The opposite is more difficult. Consider the simple example of a doorknob. With no load, it is very easy to turn the knob and disengage the latch from the door frame. Try pulling on the door while attempting to turn the knob. The door can still be opened, but it is much more difficult, and a sudden acceleration is felt when the latch breaks free. The resistance comes from the friction force, which is proportional to the normal force exerted on the door.

Another design consideration is that the system needs to be able to reset itself to a rigid configuration at the end of the thrust. In the case of the door, a spring pushes the latch out when torque is removed from the doorknob. Inclusion of a spring-damper linkage system attached from the door to the doorframe (very common on exterior doors) allows the door itself to be reset.

Although not the ideal setup due to the strong resistance under load and the sudden breakaway that occurs, the doorknob design is the basic concept used to make the seatback rigidizer, shown in Figure 15.

A rigidizer bar is mounted to the seatback by means of a preloaded spring hinge. In the rigid configuration, the end of the rigidizer bar rests in an L-stop and prevents the seatback from rotating backwards. This is shown in (a) of Figure 15. To provide enough force to pull the rigidizer out of the L-stop under load, a solenoid is used, attached to the rigidizer by way of a cable. Once the rigidizer is pulled free from the L-stop, shown in (b) of the figure, the seatback is free to rotate and the solenoid can be turned off.

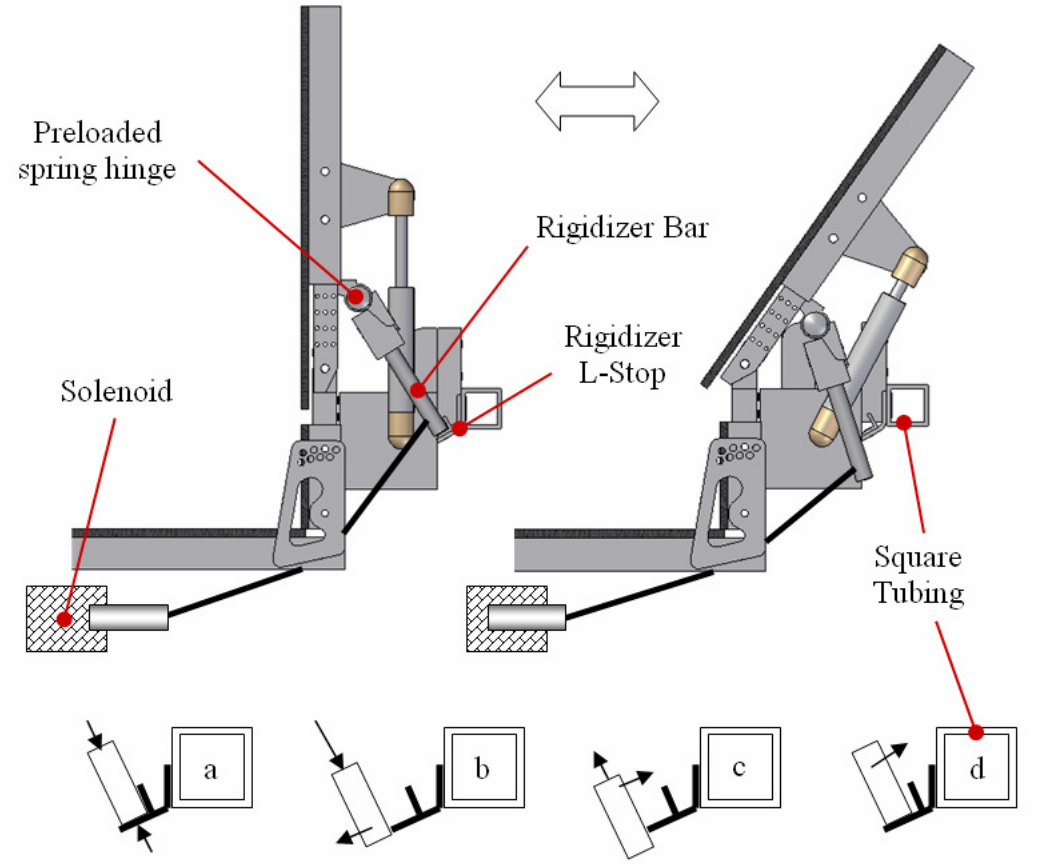

Figure 15: Action Sequence of Seatback Rigidizer

After the thrust, the gas shocks return the seatback to its upright position, and the torsional spring attached to the rigidizer bar functions to reseat the rigidizer in the L-stop, seen in (c) of Figure 15. When the seat back is fully upright, the rigidizer bar is returned to its original position, as seen in (d) of the figure. Thus, it uses power to change to a dynamic state, but has a fully passive return to the rigid state.

2.3 Methods for Sensing and Differentiating Thrusts

Sensing forces and differentiating between voluntary and involuntary extensor thrusts is critical to the success of a dynamic seating system. As discusses previously, the survey on dynamic seating systems conducted by CATEA (Appendix A) sheds valuable

light on this issue. The majority of participants believe that voluntary thrusting motions are used for functional tasks such as accessing switches, communicating, assisting with transfers, and driving the wheelchair. Thus, it is imperative that the seating system provide a rigid frame against which the user can push during these functional tasks. Having the seat always be in a dynamic mode would likely cause more harm to the user from frustration than any comfort gained during the involuntary extensor episodes.

This naturally leads to the question of how to differentiate thrust types in order to build this functionality into the chair. First, the participants in the survey indicate a lack of consensus for where in the body the thrust begins. This means that an ideal setup would have sensors in various locations to detect a thrust occurrence. If sensors were located at the footrest and the thrust began in the upper body, the system as a whole would react much more slowly than if the sensor had been placed at the backrest. This is not so much of a problem with being able to tell the difference between thrust types as a potential problem with delays in the system.

2.3.1 Options for Sensing Methods

Fortunately, the question of how to differentiate thrust types is addressed in the survey. The participants believe that involuntary extensor thrusts occur faster than their counterparts, while voluntary thrusts tend to last longer. They do not believe there is a substantial difference in the strength or force generated by each type of thrust.

Duration and rate of change of force are easily measured, so they can be used to differentiate. It should be noted that duration is something that is measured at the end of the thrust, so it is of limited use for initial differentiation, but might be useful with an

adaptive feedback control scheme as a check to see if the correct type of thrust was detected at the start. A rate of change of force (i.e. force gradient), however, can be tested at the start of a thrust, and so was tested for its ability to effectively distinguish between voluntary and involuntary thrust. With this method, the seat should become dynamic only if the rate of change of the force is high. Regardless of how much force is exerted on the back, if the force is applied slowly, the chair should continue to remain stiff.

A maximum force threshold can also be used, although its effectiveness is questioned by the survey participants. One of the strengths of this method is its simplicity. This method may work for some users, and so it was also tested for use as an available option in the final design.

2.3.2 Active Breakaway

Active breakaway involves using active components, such as motors and actuators, to change the seat from a rigid to a dynamic state. These are most easily controlled by a microprocessor. The processor also reads the current state of electronic sensors, such as strain gauges, load cells, and proximity sensors. These sensors usually have a voltage reading as their output.

One benefit to using a microprocessor is that it can perform advanced logic tests and improve the sensing methods. For instance, rather than having the need for a sensor that measures the rate of change of force, the force can be measured and the microprocessor can estimate the rate of change of force based on its internal clock and past readings of

the force. In this way, advanced control systems can be developed without the need for expensive sensors.

As always, there are drawbacks to using active breakaway. The main challenge is power. The motors and actuators, sensors and microcontroller all require power, which leads to the need for batteries on a mobile platform. Additional challenges include accounting for temperature effects and noise in the sensors.

2.3.2.1 Data Collection Setup

On the hinged-back seat, strain gauges were chosen to measure the force on the seat back. The strain gauges are mounted to the flexible seat back material in the configuration shown in Figure 16. The seatback consists of two vertical posts of steel square tubing, to which the seat back pivots are attached. Mounted to the vertical posts is a sheet of flexible polymer material. When a user's upper back pushes against the seat

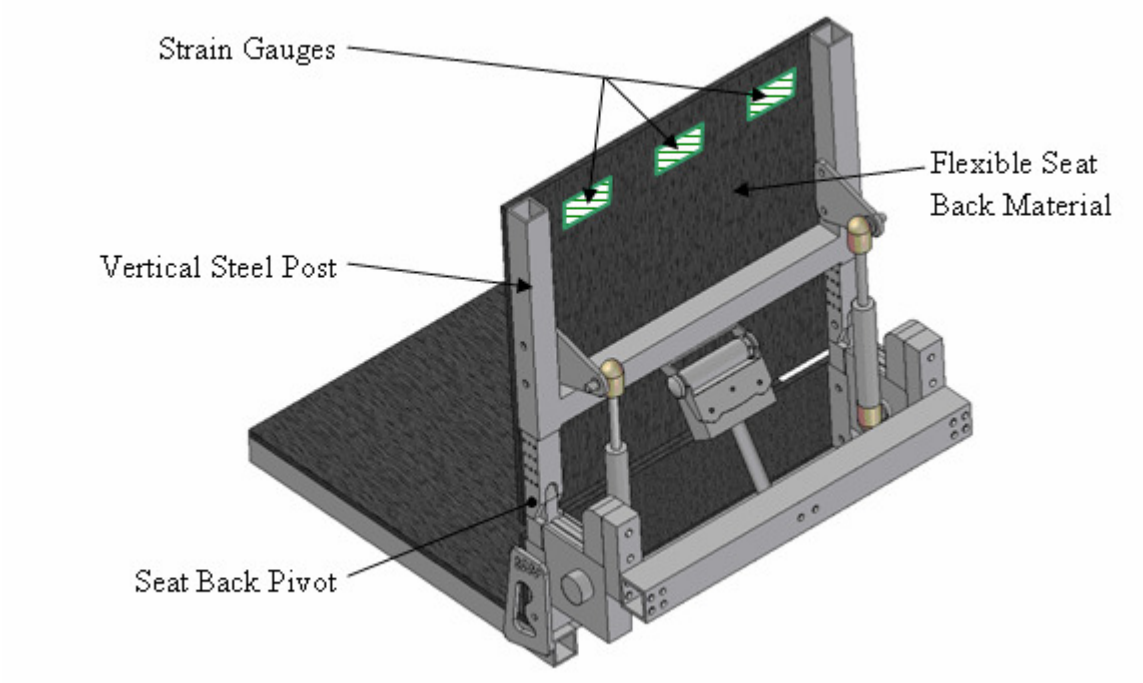

Figure 16: Strain Gauges on Flexible Seat Back

back, the polymer sheet will flex slightly between the vertical steel posts. This flexing can be detected as strain in the flexible material.

While it is difficult to compute an exact force from this strain measurement, increased force will always lead to increased strain. An additional sensor, a commercial force plate used to measure the force on the footrest, was schematically represented in Figure 10. The signals from the strain gauges are amplified with circuitry, and both the strain signals and the force plate signal are fed into a National Instruments analog-to-digital (A/D) data acquisition board, which is connected to a computer.

As the hinge-back seating system was also used for model validation in other work, a camera was also integrated into the data collection setup. It is used to record the motion of the seat occupant during simulated extensor thrusts by recording the location of tracking markers on the joints of the person and chair. A light source is placed in front of the camera and linked to the computer to allow synchronization of the force and motion data. This motion data is then processed by a Matlab program to extract the coordinates of each point throughout the motion. Figure 17 shows the tracking of each point as output by this program.

2.3.2.2 Control Setup

When the signals come into the computer from the data acquisition board, they are read by Labview at 1 kHz and used for a control algorithm. A schematic of the control logic is shown in Figure 18, with the Labview interface shown in Figure 19. In this logic diagram, two paths exist depending on the type of control desired. The force threshold path takes the three strain gauge signals from the first time sample, sums them, and

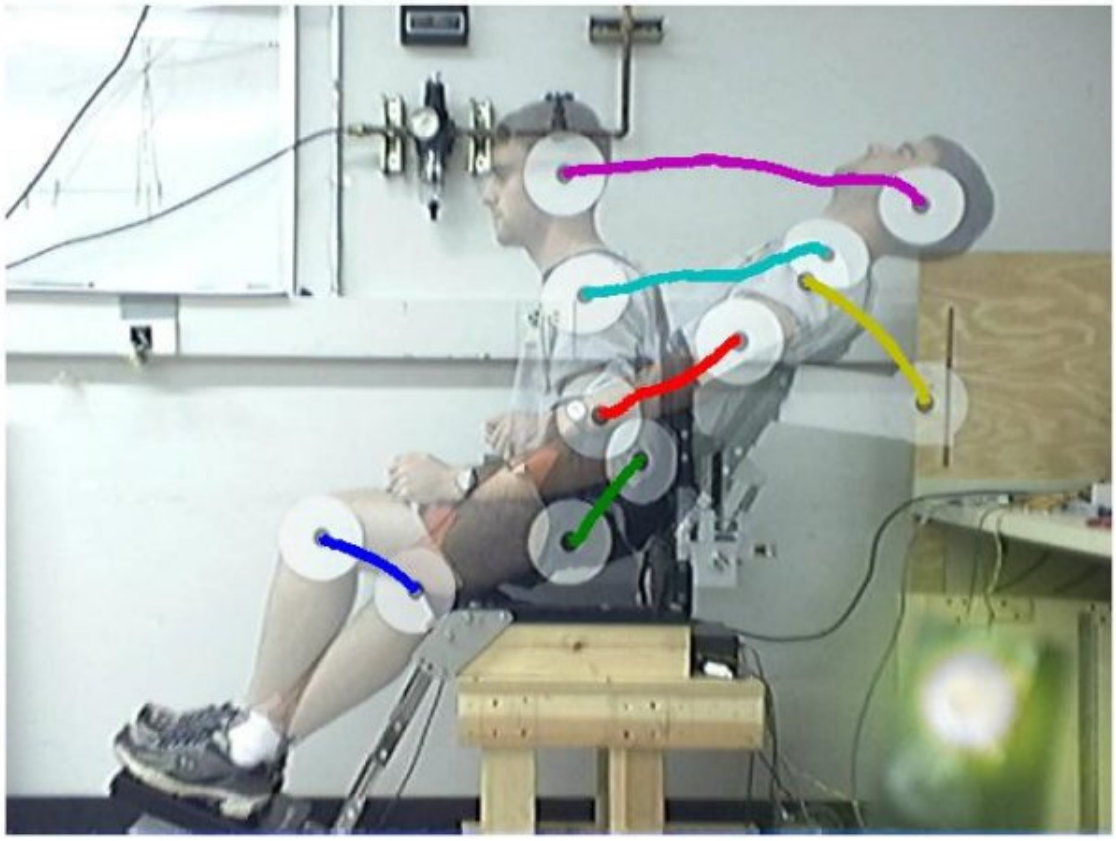

Figure 17: Motion Capture and Tracking

compares it to a threshold. If the sum exceeds the threshold, the solenoid is activated for three-tenths of a second, which is enough time to pull the rigidizer bar out from the L-stop (refer back to Figure 15).

The force gradient path in Figure 18 takes the sum of the strain gauge readings from the fifth time sample and subtracts the sum of the strain gauge readings from the first time sample. This is equivalent to the sum of the changes in strain over 5 milliseconds of time. This a simple way to calculate the force gradient. If the force gradient is greater than its threshold value, the solenoid is activated.

In either case, activating the solenoid also activates a three-second timed lockout that serves two purposes. One, it is necessary to ensure that the solenoid does not exceed its 10% duty cycle rating and risk overheating. The second reason is that, in many cases,

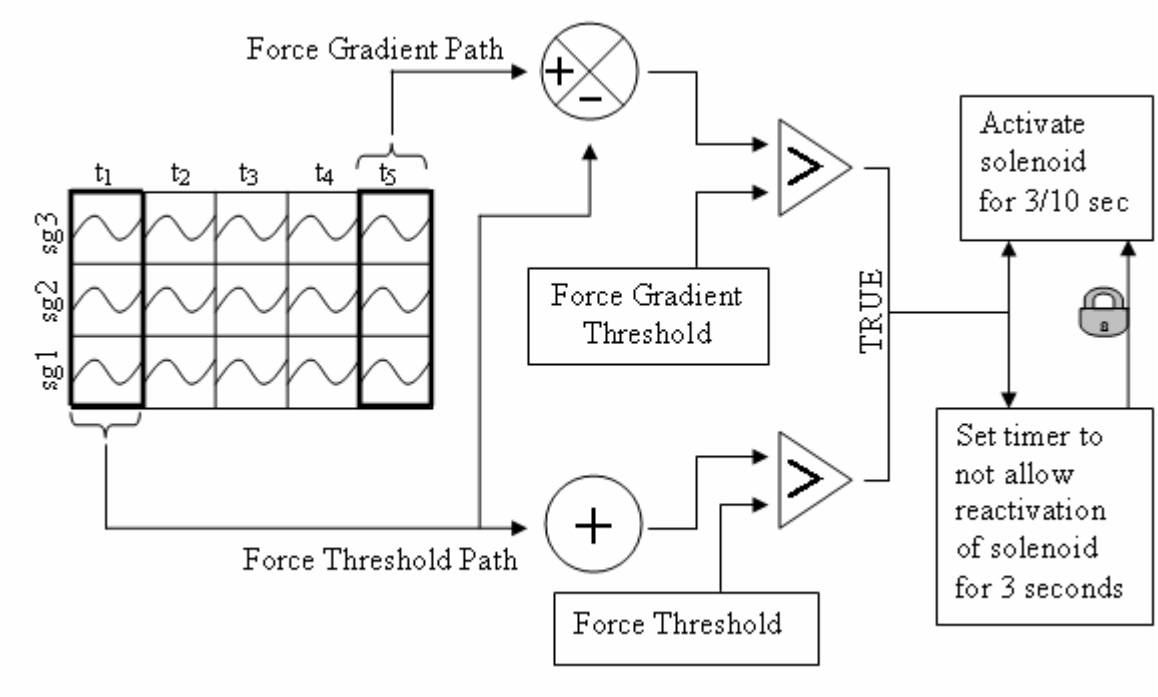

Figure 18: Labview Control Schematic

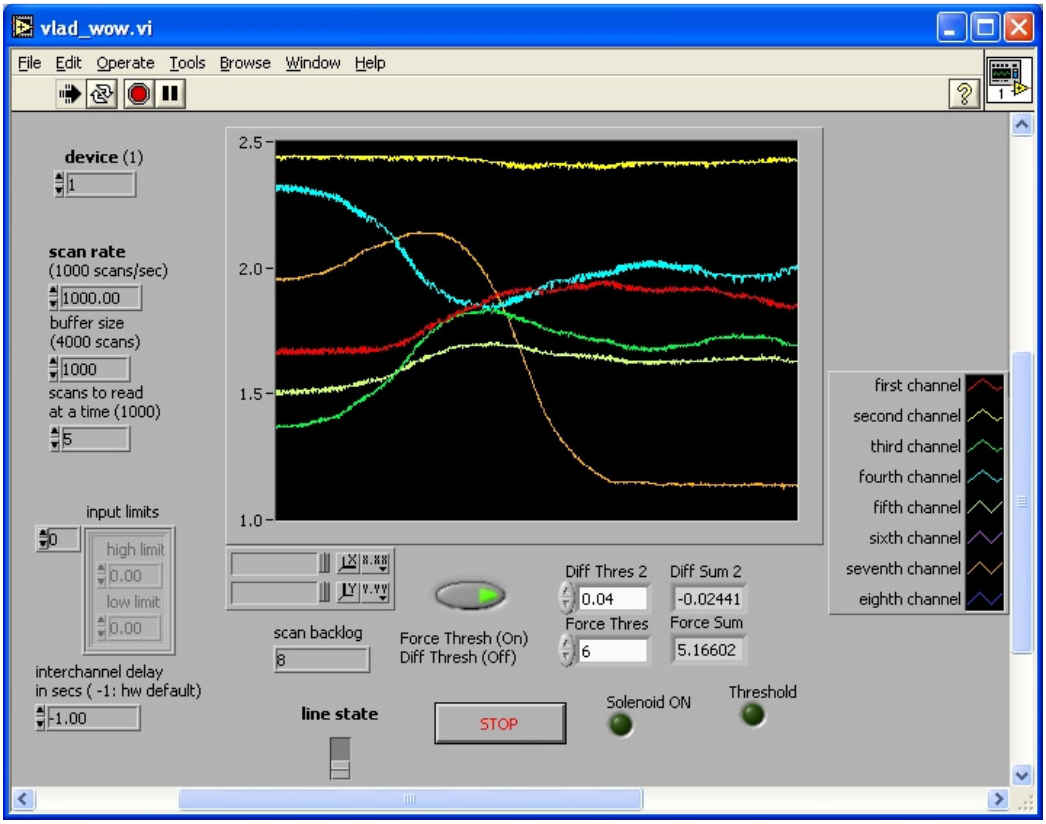

Figure 19: Labview Interface for Control Algorithm

the transition from the rigid to the dynamic state temporarily reduces the forces on the back as the rigidizing bar no longer resists motion, and the gas shocks have not yet begun compressing. As the springs are compressed, the force grows again, and the control logic may predict that this is another involuntary extensor thrust occurring and attempt to reactivate the solenoid. This leads to a second activation of the solenoid that accomplishes nothing, as the chair is already in the dynamic state. For these two reasons, a lockout is present.

While implementing the two methods of maximum force threshold and force gradient, slightly more advanced control schemes were created due to the inclusion of a timed lockout feature. This is to be expected as true simple cases are rarely effective for real-world situations. More advanced control schemes involving a combination of force thresholds and force gradient thresholds could also have been used. Indeed, a control algorithm could have been created which looks for a specific force-curve profile. These advanced possibilities could prove more accurate at correctly identifying uncontrolled extensor thrusts, but they also can introduce a time delay in the system, causing the chair to react slower. In the end, there is always a trade-off to be made.

2.3.3 Passive Breakaway

Passive breakaway involves detecting a change in the state of the system and reacting to it without the use of active components. The main benefit of using passive sensors is the lack of power or processing required. An example of effectively using a passive sensor is found in a slip clutch that has rollers that begin slipping at a threshold torque. This keeps the torque transmitted between shafts below a certain level. Once the

torque is reduced sufficiently, the rollers in the slip clutch stop and the full torque is again transmitted. This is a perfect use for passive breakaway.

One challenge to using passive sensors is that sensing and controlling the system are inherently integrated functions. In the case of a slip clutch, the sensing and transmitting of the torque are integral. For the case of active breakaway, sensing is done separately, and then active components are used to drive the system to a new state. This separation of functions often simplifies the mechanical design. Another challenge with passive breakaway is that adjustability is sometimes difficult. Instead of changing a threshold value in code, the change must be made in hardware. And, with the integrated nature of the sensor and breakaway mechanism, changing the threshold might add to the dynamics of the system as a whole.

For instance, a spring can be used passively to set the force required before the system will move. This is accomplished using a preload on the spring. This preload is often quite easy to adjust using a threaded plunger to compress the spring. However, this changes the dynamics of the system after the force is exceeded. The sensing of the initial breakaway force is tied to the amount of resistance the spring will provide throughout the move.

It is often necessary to separate this dependence so that the initial breakaway force can be adjusted without adding to the dynamic response. Figure 20 shows the difference between the breakaway of a preload and a decoupled type of breakaway. In the decoupled case, once the force exceeds the threshold, the system then pushes against a spring that is not dependent on the breakaway threshold. The stiffness of the spring could be independently adjusted without affecting the breakaway threshold, and vice versa.

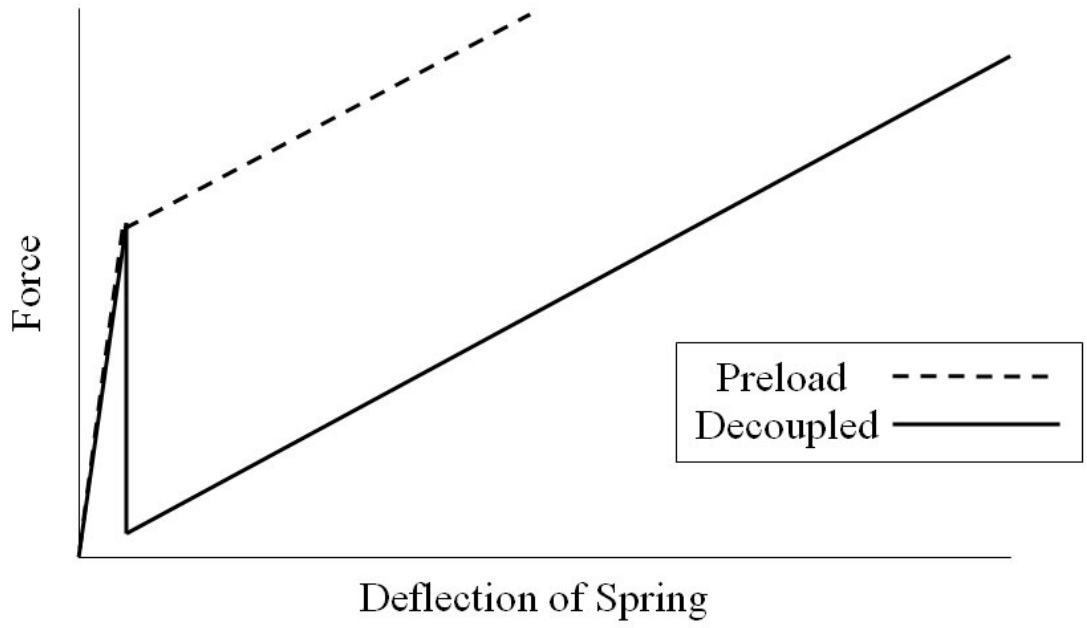

Figure 20: Spring Preload and Ideal Breakaway Curves

Given the advantages of passive breakaway, it is desirable to pursue this option assuming the inherent challenges can be overcome with a clever mechanical design. As the dynamic hinged-back seat was already setup for testing of the active sensing methods, a footrest was chosen on which to implement the passive breakaway concept. The goal of this design is the same as that of active breakaway, namely to remain rigid unless an involuntary extensor thrust is detected, and then to allow the system to move.

The attempted breakaway profile is the decoupled breakaway profile shown in Figure 20. One way to achieve this decoupling effect is to physically decouple the breakaway mechanism from the return spring. To do so requires that the breakaway mechanism is removed from the system after breakaway.

The general motion of the footrest is governed by plantar flexion. The motion is shown in Figure 21. The external spring shown is used for the return mechanism, but a lockout needs to be separate from this that is capable of breaking away and not adding to

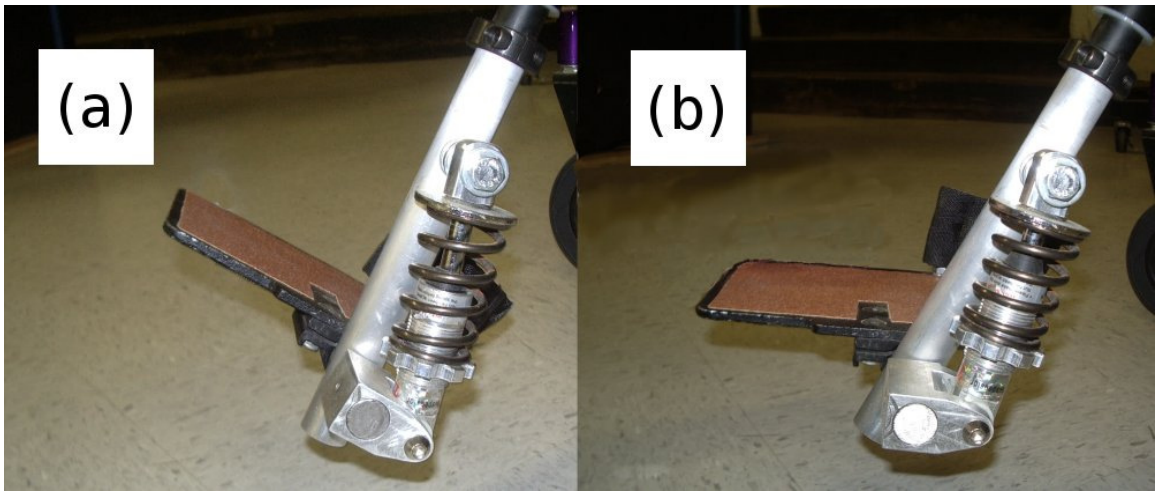

Figure 21: Motion of Footrest During Plantar Flexion

the dynamics of the system. The clever design to make this possible came from an undergraduate senior design project at Georgia Tech. The concept developed involves using a spring detent that is placed inside a groove in the shaft as shown in Figure 22. The detent keeps the shaft from rotating, and thus acts as a lockout for the system. Because the groove in the shaft has angled sides, some of the force is transferred axially to the detent. This axial force will eventually depress the detent into its housing and allow the shaft to rotate freely.

Calculations were performed by the design group to determine the angle of the groove necessary to create a reasonable force threshold, and are given in Appendix B. These calculations revealed a possible weakness in the design. The moment arm for plantar flexion is quite large compared to the moment arm for the spring detent. As the spring detent only needs a small axial force to become depressed, a small transfer angle is needed on the shaft. While this leads to a small axial force on the spring detent, it leads to a very large transverse force being applied to the detent as well. This has the potential to cause binding and impede the detent from being depressed in its housing.

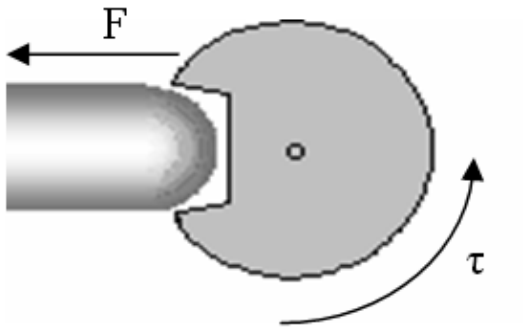

Figure 22: Interaction Between Shaft and Spring Detent

Though binding problems were a possibility, this spring detent design was built as seen in Figure 23. It satisfies the requirements for a passive breakaway component that is effectively removed from the system after breakaway.

The return mechanism is a custom designed spring-damper with an adjustable preload. The spring coil can be replaced to achieve different stiffnesses. This allows for a great deal of adjustability in the breakaway profile.

Figure 23: Footrest Prototype with Passive Breakaway

2.4 Experimental Data

Experiments were conducted to verify that a dynamic seatback reduces the forces during a high-tone extensor thrust. Experiments were also conducted to establish the effectiveness of using both active and passive breakaway schemes to differentiate between voluntary and involuntary thrusts.

2.4.1 Dynamic Seating Forces

To test the effectiveness of a dynamic seatback, the seatback rigidizer was removed, and the adjustable hard stops (refer to Figure 13) were used to set seven different maximum deflection angles for the seatback. For each maximum angle, a mock extensor thrust with an unconstrained pelvis was performed and data was recorded. Figure 24 shows the change in strain gauge voltage from an upright to a fully-extended posture for each seatback limiting angle. The profiles show that the strain gauge voltage first rises slightly and drops as the seat back is rotated. When the hard stop is reached, the voltage rises sharply, and plateaus as the user reaches the fully-extended state. As the seatback angle is increased, the maximum strain seen at the top of the seat back is reduced. A least squares line was fit to the maximum values for each deflection angle, as seen in Figure 24. The trend is downward, indicating that the dynamic seatback is reducing forces felt, although the force is not consistently lowered for every increase in deflection angle.

Another interesting result comes from the foot forces generated during the same conditions of varying seatback angles. The profiles and trends are shown in Figure 25, and appear to be even more pronounced than with the seatback strain. The profiles rise quickly and peak, falling off as the body is extended and rides up the seatback. This

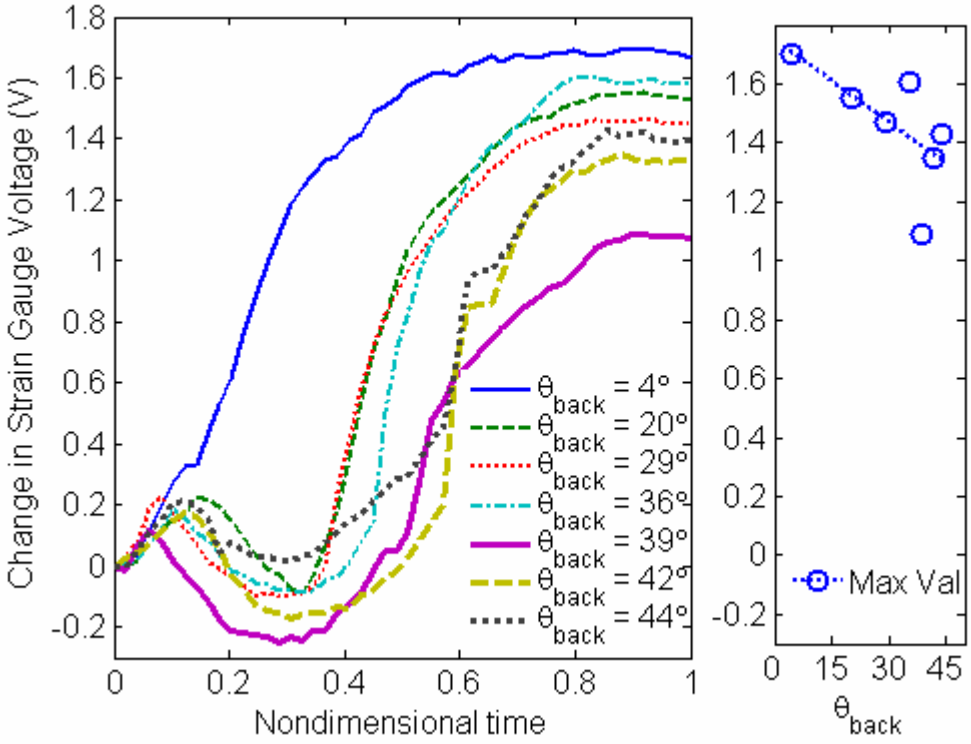

Figure 24: Strain Gauge Profiles and Trends vs. Maximum Seatback Deflection

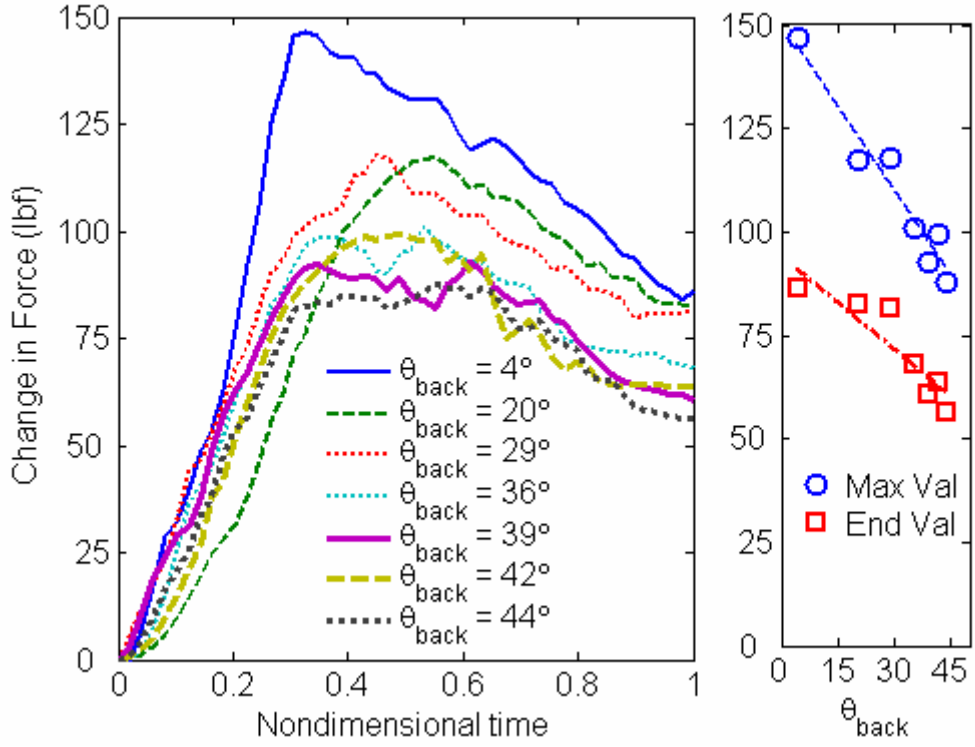

Figure 25: Foot Force Profile and Trends vs. Maximum Seatback Deflection

makes sense because the seatback supports the majority of the torso weight at the end of the extensor thrust. The feet, on the other hand, feel the initial force used to straighten the body and deflect the seatback, but as the seatback angle changes, the seatback supports an increasing amount of body weight.

The trends are consistent with those from the strain readings, indicating that allowing the seatback angle to change during an extensor thrust reduces forces, not only at the seatback, but also on the feet. This study provides good evidence that dynamic seating components are an effective way to reduce forces during an unconstrained extensor thrust, providing more comfort for the user and extending the life of the wheelchair components.

2.4.2 Active Breakaway Data

The next goal is to verify the ability of the control algorithms to properly detect a thrust based on certain criteria, specifically a maximum force threshold and a maximum force gradient threshold. To test the maximum force threshold, a mock extensor thrust was performed for three different force threshold values: 5.6, 6.0, and 6.4 volts. The user performed the thrust by pushing on the seatback and increasing the force until the solenoid fired and allowed the seatback to rotate dynamically. The strain gauge readings for the seat back during these runs are shown in Figure 26. As can be seen, the curve corresponding to each force threshold indicates a sharp decrease in strain once the threshold is reached. This is the moment that the solenoid is activated and the seatback is allowed to rotate backwards, relieving the stress and force on the back. This indicates that the method for detecting maximum force is effective.

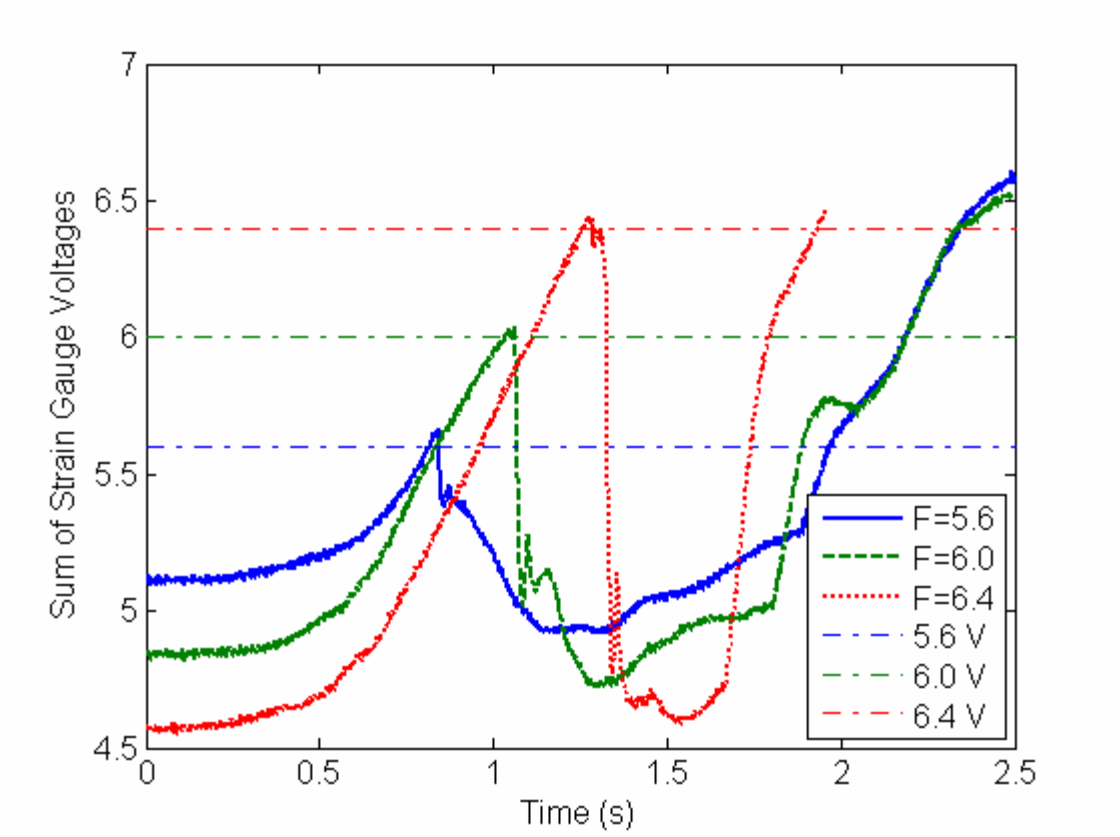

Figure 26: Force Threshold Activation Profile

There is an interesting phenomenon that occurs as a result of this detection scheme. After the initial sharp decline in seatback strain, the strain again quickly exceeds the level at breakaway. Exceeding the threshold force is expected, as the threshold was arbitrarily set to be lower than the maximum force for a rigid or dynamic thrust, seen previously in Figure 24. The interesting observation, however, is that after the breakaway, the strain exceeds the threshold value sooner for larger breakaway thresholds. This is attributed to the fact that larger forces are present when the seatback breaks away and begins rotating, causing the user to accelerate faster. By using the motion data captured from the camera, the horizontal velocity was measured to verify this conclusion. The horizontal velocity of the test subject's head during extensor thrusts at each force threshold is shown in Figure 27. As the force threshold increases, so too does the maximum horizontal velocity of the

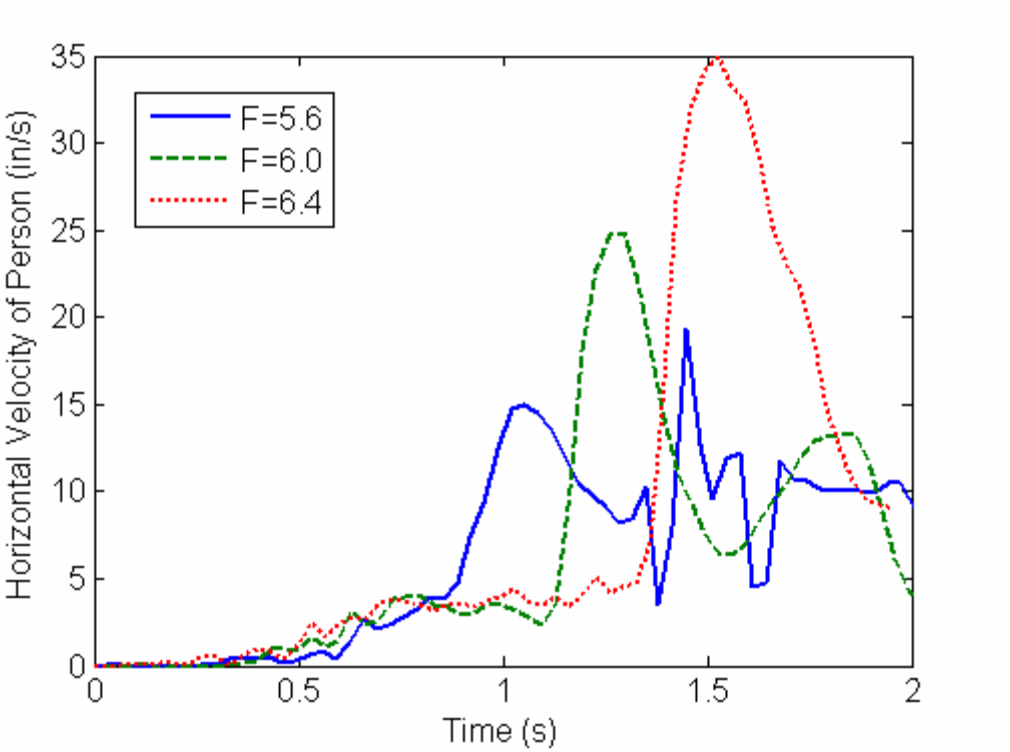

Figure 27: Horizontal Velocity During Force Threshold Breakaway

person's head. This sudden acceleration may be disconcerting for some, and is a definite weakness of the force threshold method. It should be noted that this prototype did not have a headrest, which might have reduced these horizontal velocities, but should not have changed the general trend.

The other control algorithm tested on the hinged-back seat was the force gradient threshold. The force gradient, approximated over five time steps, was compared to the gradient threshold. With the force gradient threshold set at 0.03, a test subject sat in the hinged-back chair and performed two thrusting motions. The first was slow and strong, while the second was fast and strong. The total force reading is shown in the top portion of Figure 28, with the force gradient appearing in the lower portion of the figure. The force reading shows that the first thrust was quite strong, yet the algorithm did not

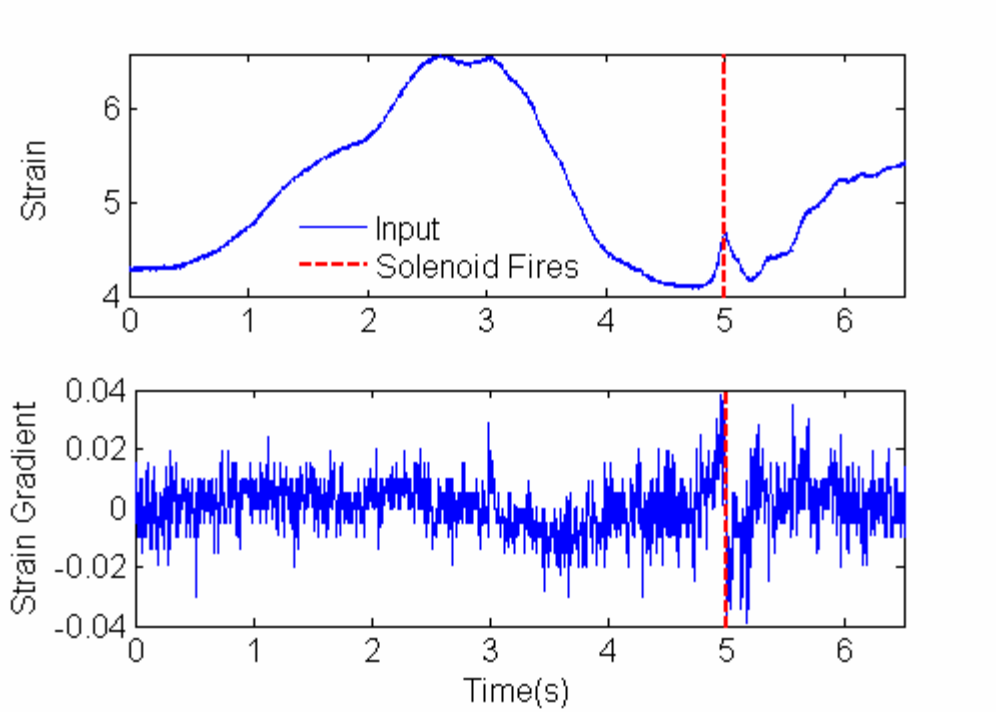

Figure 28: Strain Voltage and Gradient for Threshold = 0.03

activate the solenoid because the force gradient was small. The faster thrust did produce a force gradient large enough to trigger the solenoid around the 5-second mark.

Another test was performed with a threshold value of 0.062. The test subject performed three extensor thrusts, starting slow and increasing the speed with each thrust. The force reading is shown in the top half of Figure 29, with the force gradient appearing in the lower half of the figure. A small spike in force gradient is evident during the second thrust, but the threshold is not exceeded. The threshold is finally exceeded during the third extensor thrust, just before the 8-second mark.

One potential challenge with this method is the fact that the noise in the system is on the same order of magnitude as the threshold values we are testing against. This is not as noticeable in Figure 29, but is quite prominent in Figure 28, where a stray noise spike could reach the 0.03 threshold level and lead to a false positive detection. A spike near

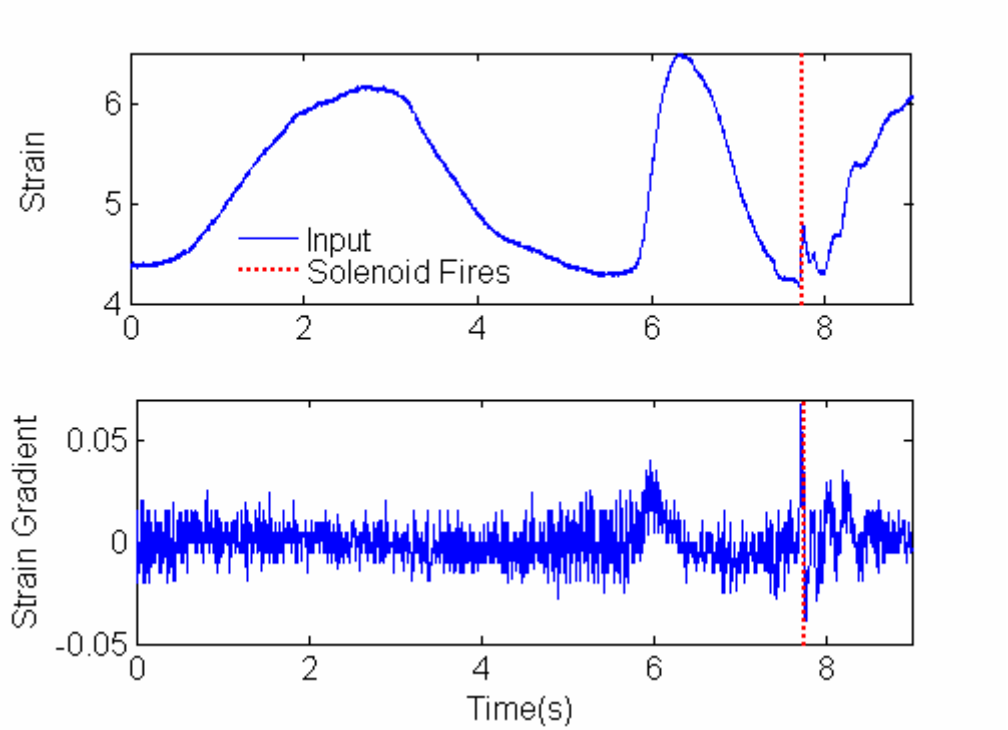

Figure 29: Strain Voltage and Gradient for Threshold = 0.062

the 3-second mark, for instance, was dangerously close to triggering the solenoid at an inappropriate time, as a single value larger than the threshold would have activated the breakaway components.

The problem with noise became especially apparent with no-load conditions, such as occur when the user stands up from the seating platform. Without the user to act as a damper in the system, transient vibrations often cause the force gradient method to predict that an involuntary extensor thrust has occurred. This phenomenon was duplicated by tapping the footrest of the seating system when no one was sitting in it. The resulting spikes in strain felt by the seatback are shown in Figure 30. These spikes are caused by transient vibrations in the seatback and possibly by motion of the wires or movement of the strain gauge amplifier, which is attached to the seating platform. These

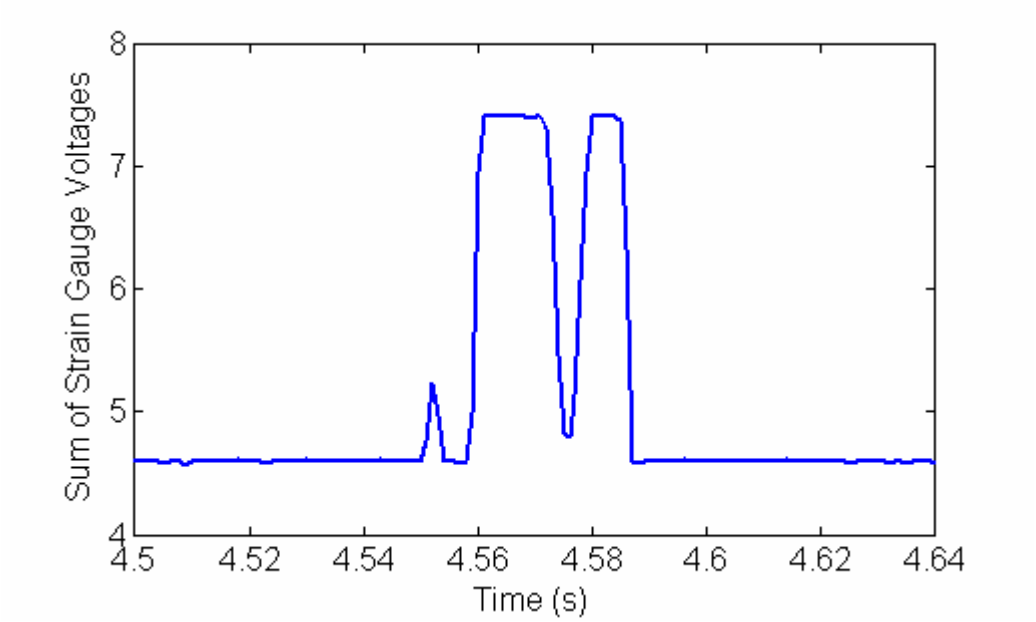

Figure 30: Vibration Spikes under No-Load Condition

transient vibrations cause the strain gauge voltage to oscillate several times in less than $1/20^{th}$ of a second.

Both the force and force gradient methods have weaknesses that must be dealt with. The large accelerations when breaking away under load are undesirable, but a system based only on the force gradient is too sensitive to noise. A possible solution would be to incorporate both systems into an advanced control algorithm, based on the force gradient, but with the addition of a minimum force required for system activation. This minimum force threshold, set at 5 V for instance, would guard against transient vibrations that occur under no-load conditions. By waiting until this minimum force has been exceeded for a few seconds before activating the force gradient check, the algorithm would guard against no-load transients. As well, it would guard against the user leaning forward off the seat back and then letting himself fall back against the chair. Additionally, a check could be done to ensure that the force gradient remains above the threshold for a certain amount of time before activating the breakaway system. This would guard against a

single noise spike which exceeds the threshold or vibrating transients. This would add a delay to the system, and a balance between robustness and activation speed would need to be found. Based on the transient vibrations in the no-load condition, 1/10th of a second seems like a good value to choose for the time delay.

2.4.3 Passive Breakaway Data

After concluding the tests of the active breakaway control algorithms, the passive breakaway footrest mechanism (Figure 23) was evaluated for its ability to differentiate thrust types based on a force threshold criterion. To do this, the depth of the spring detent inside the shaft's groove was adjusted. The force on the detent was calculated based on applied force on the footrest, measured with a force plate.

Past a certain depth, it became impossible to depress the detent. The resulting breakaway force curve is shown in Figure 31. As can be seen, the breakaway force of the detent is highly sensitive to the depth into the groove. For the first 0.15 inches, the force

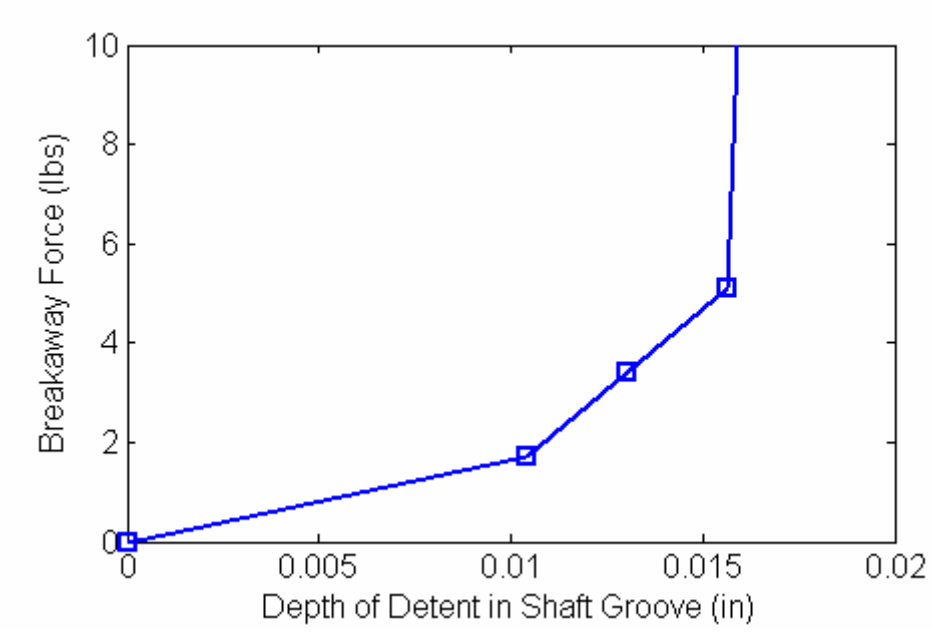

Figure 31: Passive Sensor Breakaway Force Curve

increases in a manageable way. After that, however, it became impossible to depress the detent. This was likely a binding issue, as discussed previously. While this indicates that the current setup doesn't work, it does not indicate that all passive breakaway systems are ineffective. It does, however, motivate the use of active breakaway because clever mechanical designs can still fail when attempting passive breakaway due to the coupling of the sensor and breakaway mechanism.

2.4.4 Summary

Looking at the data, we conclude that the hinged dynamic seat back is effective at reducing forces both on the seat back and on the foot rest. These findings are based on a limited amount of data, and were only done for unconstrained extensor thrusts. This is sufficient to motivate an advanced prototype that deals with constrained, full-body extensor thrusts. Further tests will be done with that prototype to verify its effectiveness.

We also conclude that the algorithms developed for use in the active breakaway system are effective means of differentiating, although each has a weakness. An improved design based on the force gradient method, combined with a minimum force threshold and time delay, should be used. The design chosen for the passive breakaway system, using a spring detent, is not effective. This is likely unique to this specific design, and not a general indicator of all passive breakaway systems.

CHAPTER 3

DEVELOPMENT OF ADVANCED DYNAMIC SEATING SYSTEM

The study of the hinged-back active seat component provided interesting insight and promising results. The next step is to study multiple dynamic seating components that target the major muscle groups in the body that fire during an extensor thrust. In doing so, the major focus will be on designing a system that can provide stability in its rigid configuration, and when in the dynamic configuration, effectively reduce the forces felt by the user during the thrusting episode. No attempt will be made to investigate the ability to sense the thrust and control the chair, as this was studied previously. It is assumed that the control concepts discussed earlier could be easily adapted to work with a multi-action seat, although some consideration would have to be taken regarding where the thrust is detected.

3.1 Guiding Principles

As stated in the beginning of Chapter 2, this thesis takes the approach of focusing on building prototypes and using the knowledge gained from experiments to drive future designs. Rather than developing a numerical model of the hinged-back component, and attempting to use that to drive the advanced design, general principles and knowledge of anatomy are used to generate concepts for prototypes. Knowledge gained from the CATEA survey is also used, along with concepts based on existing commercial products. These initial concepts involve how the seating system should move, and what motions will reduce the forces between the seating system and the user.

One goal of the seating system is to address full-body extensor thrusts, which comprises trunk extension, hip extension, knee extension, and plantar flexion. This can be accomplished by making the seat bottom and the leg rest, along with the seat back, into dynamic components. The seat back and seat bottom need to address trunk and hip extension, with the pelvis remaining stationary. The leg rest, and possibly the seat bottom, need to address knee extension. The leg rest also needs to address the issue of plantar flexion. The extension of the neck, motion of the arms, and possible rotation of the torso do not contribute significantly to the seated posture of the individual, and will not be addressed in great detail in the design.

The first guiding principle is to have some mechanical component absorb the energy during a thrust, instead of making the body absorb it. The hinged-back design uses this principle to store the energy from the thrust in the gas springs. Along with absorbing energy, these also act as a return mechanism for positioning. Besides gas spring, helical springs or even flexible beams can be used to absorb the energy and then return the user to the rigid configuration after the thrust.

The second guiding principle is to put the muscles at a mechanical disadvantage by the motion of the seating system. Because of the attachment points of muscles on bones and various interactions within the body, muscles can exert different maximum forces in different configurations. Anyone who has lifted weights or even pedaled a bicycle understands this effect. This principle allows us to find body configurations that will not allow the muscles to exert a large force against the wheelchair. This will reduce forces felt by the chair and, likewise, against the user. Fortunately, the position that the body wants to assume during an extensor thrust leads to a weaker mechanical advantage for the

major muscles. However, the body does not need to gain full supine posture before the effects are felt.

The final principle for the advanced seating system is that the chair should move in natural ways. This mainly applies to the spine. Because the spine is a flexible column, a user's back will arch during an extensor thrust. If the backrest is a rigid board, this will concentrate the force around the area of the shoulders and upper back, leading to high pressure. While the reduction of forces is the main issue addressed in this thesis, the real source of discomfort for the user is pressure. A better design than a rigid seat back would be flexible and follow the natural contour of the back in its dynamic state. This allows the forces to be more evenly distributed across the person's back.

3.2 Variable Stiffness Seating System

The prototype built to handle full-body motion during extensor thrusts was designed around the concept of a variable stiffness support surface. The fundamental idea behind the variable stiffness concept is the use of a flexible seating material combined with a moving flexure point. Force at the end of the seating component will cause the material to bend over the flexure point. As the flexure point is moved to different locations, the seating component resists forces with different stiffnesses. As the flexure point is moved directly under the force, the seat effectively become rigid. This is shown schematically in Figure 32. Because the stiffness of the material changes continuously from the rigid to the dynamic configuration, this design has a much smoother transition under loaded conditions than the hinged-back breakaway design.

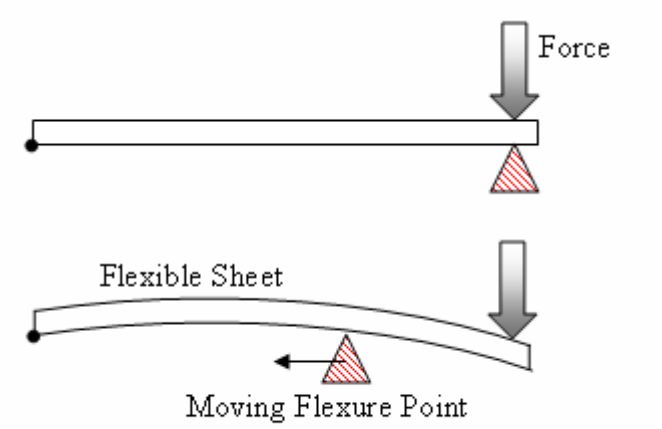

Figure 32: Variable Stiffness Concept with Moving Flexure Point

Two implementations of this variable stiffness concept were developed. The first uses a roller wheel as the moving flexure point, driven along a fixed track. This is equivalent to the motion shown in Figure 32. The position of the roller wheel can be moved by a drive belt attached to a motor. This design is used for the seat back of the advanced dynamic seating system.

The second implementation of this design has a fixed flexure point, with an additional rigidizer bar that tilts away from the material and allows it to bend over the fixed flexure point. This is shown schematically in Figure 33. When the rigidizer is tilted upwards under the seat edge, the seat becomes rigid. An actuator is used to rotate the rigidizer bar away from the seat. While the flexure point does not move in this design, it still captures the essential ability of changing the stiffness of the flexible material. This design is used for the seat bottom in the advanced seating system.

The footrest does not use a flexible material with changing stiffness, but instead builds on the design developed in Section 2.3.3. Knee extension is added to this previous design, which only allowed for plantar flexion. This gives two degrees of freedom for

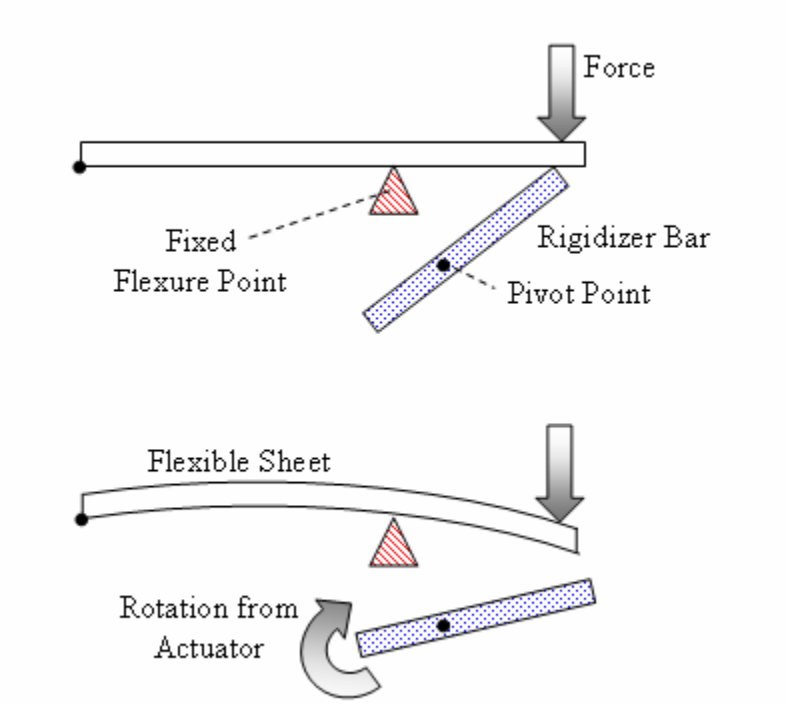

Figure 33: Rigidizer Tilt-Away Concept with Fixed Flexure Point

the new footrest design. The breakaway system for the footrest is done with a single lockout point that disables both degrees of freedom. A magnetic breakaway system is developed, and will be discussed later in the chapter.

The motion of the advanced dynamic seating system, showing both the rigid and dynamic configurations, is shown in Figure 34. The workings of the three main components of this design are summarized in Table 1.

Table 1: Advanced Dynamic Seating Components

Seat Back	• Roller wheel on fixed rail functions as moving flexure point • Roller wheel driven by motor using drive belt
Seat Bottom	• Fixed flexure point with tilt-away rigidizer bar • Rotation of rigidizer bar controlled by actuator
Footrest	• Two degrees of freedom (knee extension and plantar flexion) • Single magnetic lockout for both degrees of freedom

Figure 34: Full-body Motion of Variable Stiffness Prototype

3.2.1 Roller Seat Back Design

The design of the roller seat back is shown in Figure 35. The seat back uses a roller wheel as a moving flexure point. This moves along two parallel support rails using linear bearings. The bearings and roller wheel are connected with an interface plate. The support rails are held in place by the overall support framework. This framework extends outward to allow two tension support bars to be mounted free from interference by the flexible back rest.

A drive belt, attached to the motor, is used to drive the roller assembly up and down. The motor is held in place by the motor mount, which is itself fixed to the support framework. The vertical position of the motor can be adjusted on the motor mount to increase the tension in the drive belt.

The support framework for the prototype was built using 8020® extruded aluminum and hardware to connect the pieces together. The roller extension was also constructed using 8020® aluminum. Other attachment components were machined by the designer.

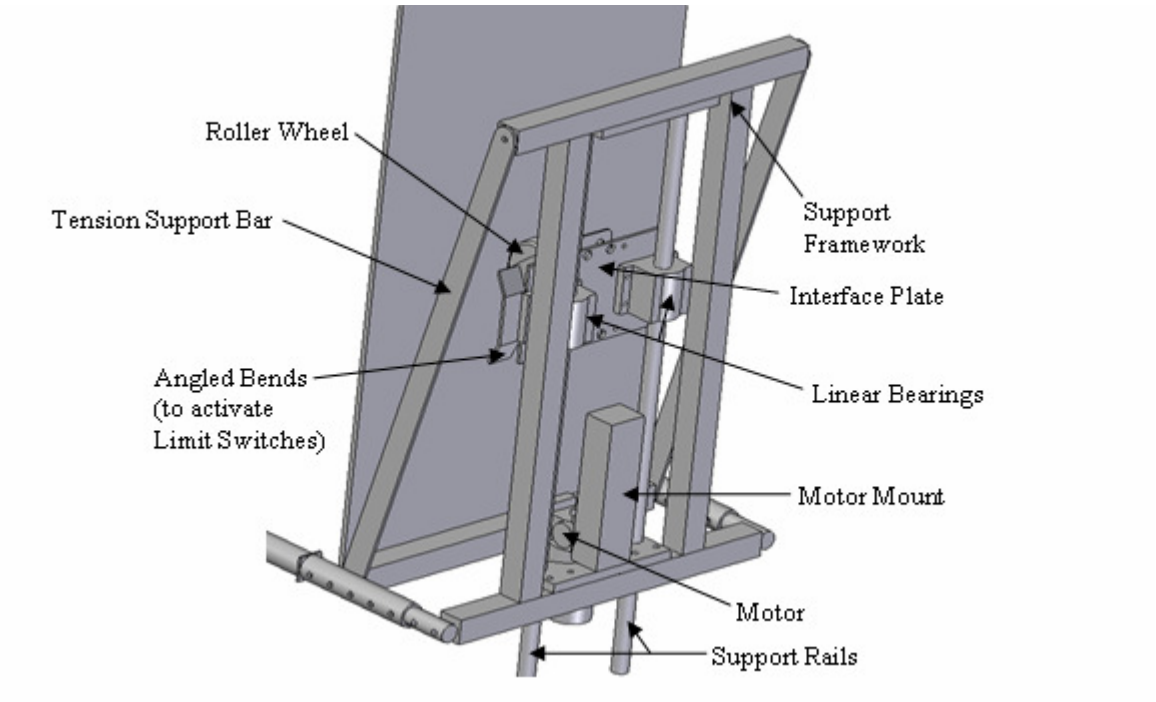

Figure 35: Diagram of Double Rail Design

The finished prototype, shown in both the rigid and dynamic configuration, is seen in Figure 36. The height of the system allows for the roller wheel to be situated near the height of the occupant's shoulder blades. The depth of the framework, while significant, is needed for the large maximum deflection before the seat back makes contact with the framework. The extension for the roller wheel is needed to keep the roller in contact with the seat back at this seat depth.

Figure 37 shows a side view of the final prototype, along with several more prototype components. First, magnets and a steel attachment surface are used to keep the roller assembly at its highest point when the motor is turned off. Because the motor does not have a power-off brake, the weight of the roller assembly will back-drive the motor and cause the bearings to slide down the support rods. The best fix for this problem would be to replace the current motor with a power-off braking motor. Because the

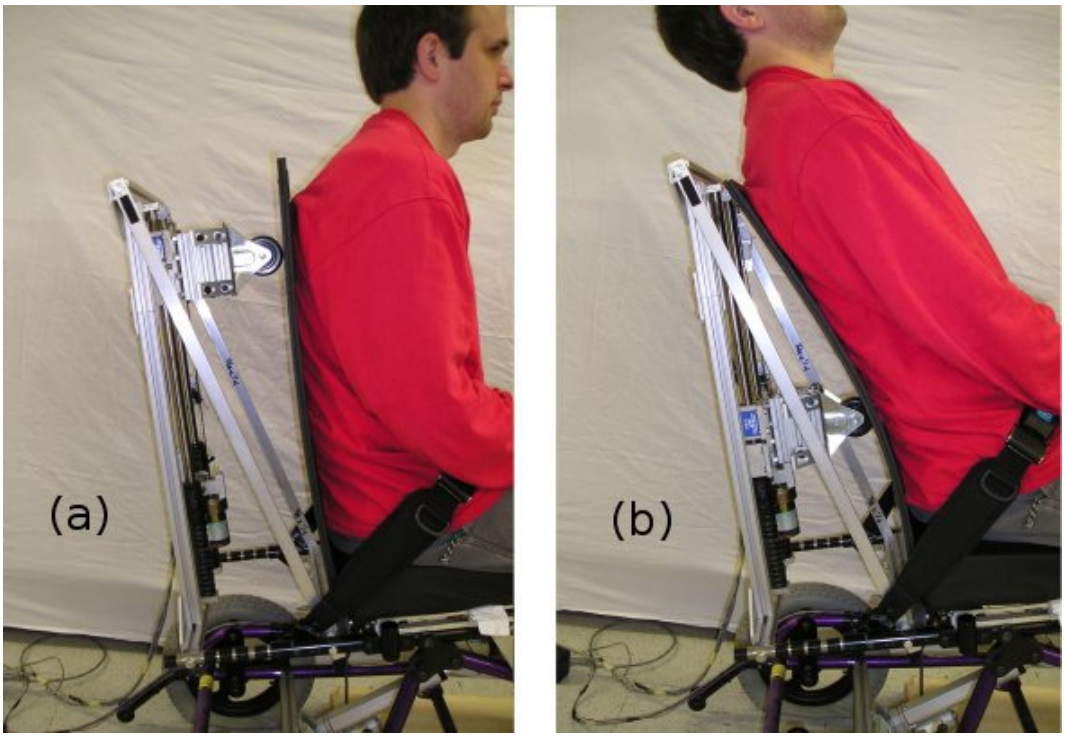

Figure 36: Rigid and Dynamic Configurations of Double Rail Design

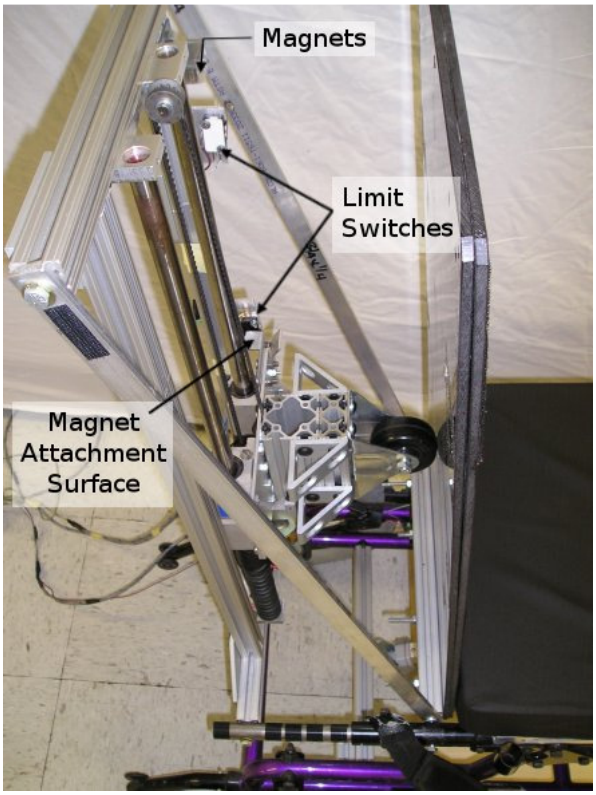

Figure 37: Side View of Improve Double Rail Design

roller only needs to remain stationary at its highest or lowest point of travel, a simple solution was to use magnets to create a holding force at the top of the system. The motor is sufficiently strong enough to pull the roller assembly free from the magnets when needed.

Another feature of the design is the use of limit switches. The interface plate in the roller assembly already has the angled bends needed to activate the limit switches. These allow the addition of a control box which will drive the motor, without allowing the system to be driven through the stops at the top or bottom of its travel.

Figure 38 shows a back view of the prototype, along with several more features of the design. A control box is used to control the motor. This controls both the seat back motor as well as the actuator for the seat bottom. The limit switches are integrated into the system so that the motor cannot drive the system up when the upper limit has been reached. The limit switch does not stop the motor from driving the system down in this

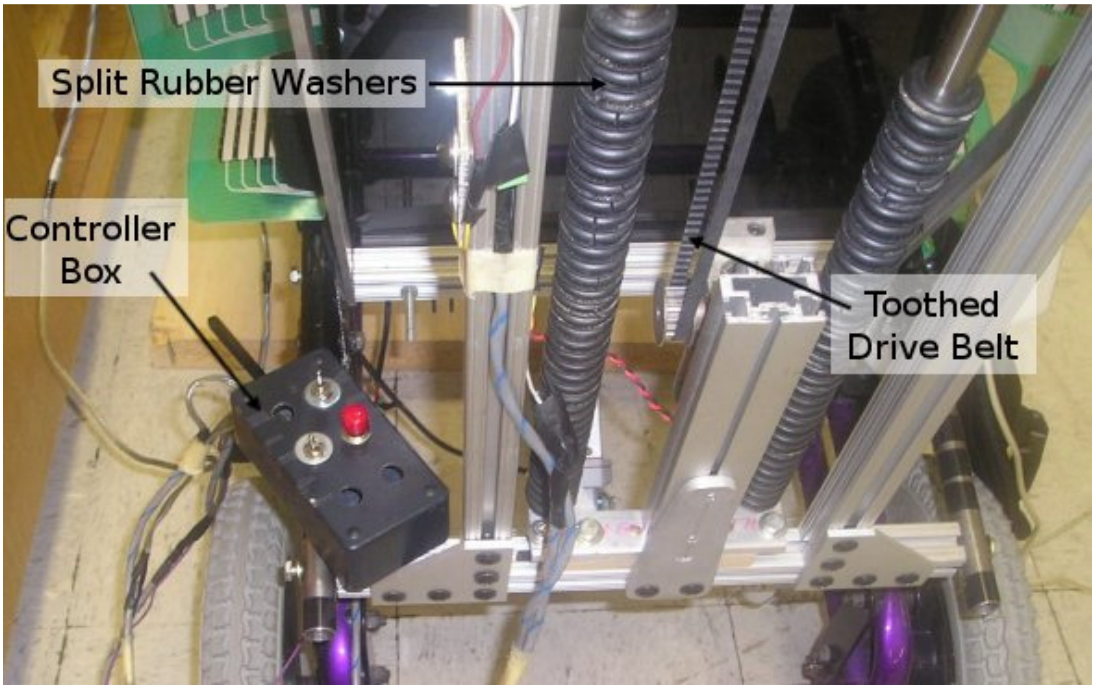

Figure 38: Back View of Improved Double Rail Design

position, so the system does not get stuck at its extremities. The same functionality is provided at the lower limit.

As mentioned earlier, the design uses magnets to hold the roller assembly at its upper limit. The roller assembly must also be held fixed at its lower limit. This lower limit must to be adjustable to allow for different levels of stiffness in the seat back. If a brake motor had been used, this would be trivial. By choosing to use a less expensive motor, however, another solution for adjustable height was needed. The solution was to use split rubber washers. These fit around the support rods and can be easily added or removed as needed. These washers act both as a lower limit for the system as well as a shock absorber at the bottom of the stroke, when the roller assembly has its greatest momentum. The placement of the lower limit switch is adjustable to match the height of the split washers. This keeps the motor from attempting to drive the system past the lower limit.

Another feature of the design is a toothed drive belt. This allows the motor to drive the roller assembly back up the seat back under load without the belt slipping. This enables the motor to be used for repositioning the occupant after an extensor thrust.

One final design feature, shown in Figure 39, allows for adjustability in the rotational stiffness of the seat back. A roller offset block allows the roller wheel to be adjusted transversely two inches in either direction. This can be useful for those who exhibit spinal rotation during extensor thrusts. The roller can be moved off-center to provide more stiffness in one direction or the other.

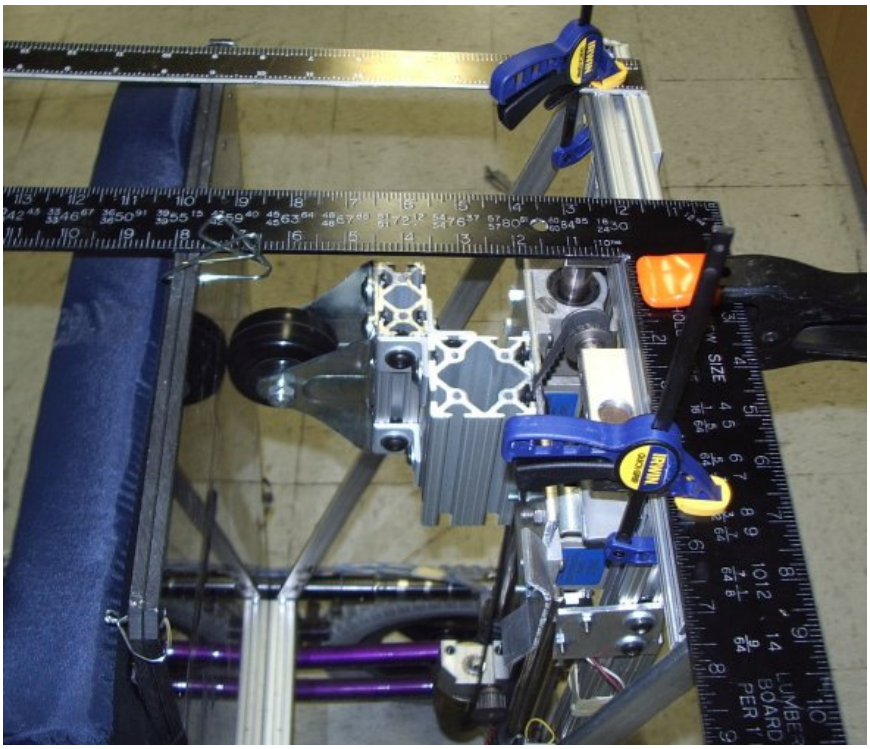

Figure 39: View of Offset Roller on Seat Back

All of these design features add to the adjustability and functionality of the design, but the essence of the design still lies in the motion of the roller wheel relative to the seat back, allowing a continuous change in stiffness from the rigid to dynamic configuration.

3.2.2 Tilt-Away Seat Bottom Design

The seat bottom incorporates the variable stiffness concept by having a fixed flexure point and tilting a rigidizer bar away from the front edge of the seat bottom to change from a rigid to a dynamic state. This was shown schematically in Figure 33. The fixed flexure point is actually a semi-fixed flexure bar in the prototype, as seen in Figure 40. This flexure bar can be moved by loosening the clamps on either end and sliding it along the track.

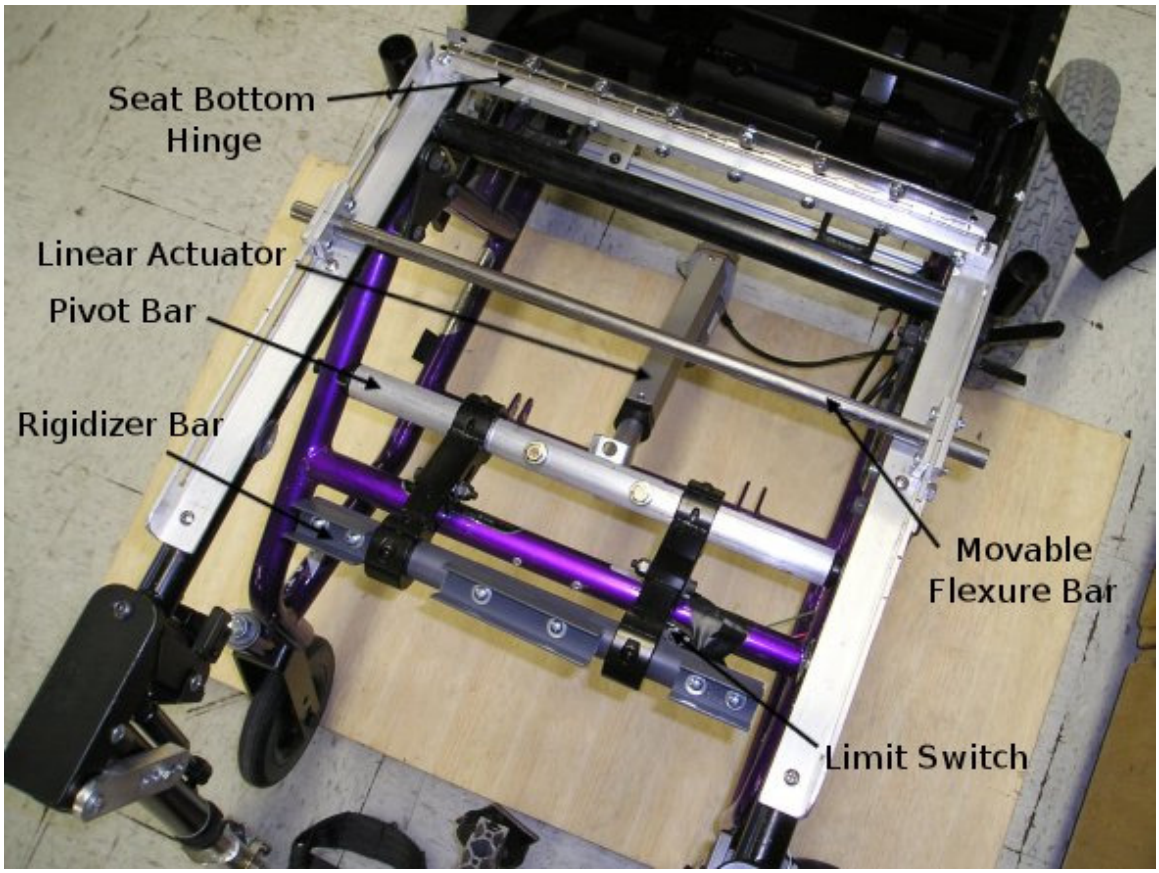

Figure 40: Overhead view of Tilt-Away Mechanism

The rigidizer bar rests under the front edge of the seat bottom in the rigid configuration. To switch to a dynamic configuration, this rigidizer bar is tilted away using an actuator, and the seat bottom is allowed to bend over the flexure bar. When the thrust is over, the linear actuator is also able to push the rigidizer bar back into position to keep the seat bottom in a rigid configuration.

The tilting of the rigidizer bar is done using a lever system to reduce the mechanical advantage of the actuator. The linear actuator is attached with a short lever arm, and the rigidizer bar is attached with a longer lever arm. This allows the rigidizer bar to move through a large arc for very little motion of the actuator, as seen in Figure 41. The reason

Figure 41: Motion of Tilt-Away Mechanism

this is important is that the linear actuator is quite slow compared to the motor and drive belt system. However, the linear actuator is much stronger than the motor.

One benefit of using the linear actuator is that it effectively has powered-off braking capabilities. This means that the use of holding magnets and rubber washers is not necessary. Instead, it can be raised to any height and held at that position indefinitely without power.

3.2.3 Two Degree of Freedom Footrest

The variable stiffness concept works well for the seat back and seat bottom because the spine and thigh only travel a short distance in one direction during an extensor thrust. This makes the use of a flexible system practical. In the case of the footrest, the shank and foot undergo a large motion. The overall footrest system needs to account for these two large angle motions. A flexible system becomes impractical for this. Instead, the

footrest designed previously in Section 2.3.3 will be used to build an improved footrest capable of two degree-of-freedom motion, as shown in Figure 42. The breakaway mechanism will also be improved and studied.

3.2.3.1 2 DOF Design

The previous footrest prototype (Figure 23) focused only on the motion of the ankle during extensor thrust. It was designed to fit into a standard wheelchair leg rest extension. A quick way to obtain the second degree of freedom needed for motion of the knee is to fit our prototype into the footrest system designed by Miller's Adaptive (Figure 3). The Miller's system actually has two degrees of freedom itself: rotation about the knee pivot and elongation of the shaft. These motions are needed when the knee pivot of the mechanism does not line up exactly with the knee joint of the user. This configuration creates a four-bar mechanism, and elongation of the shaft is necessary during knee extension.

While this allows for greater freedom in the system, it complicated the issue of a

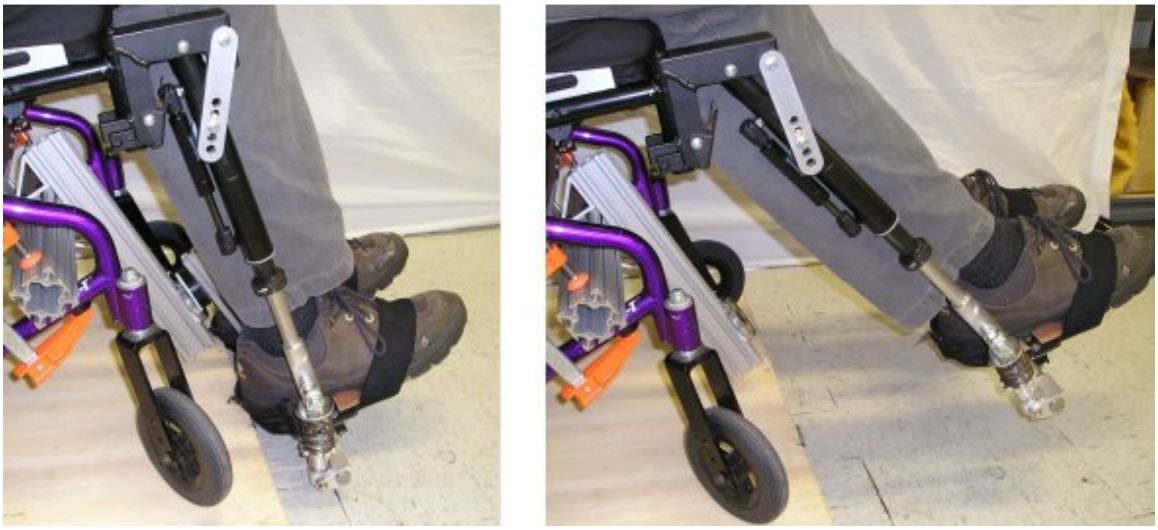

Figure 42: Motion of the Improved Footrest

lockout mechanism. To simplify this need, the slider bar in Miller's product is replaced by a coupling bar as shown in Figure 43. This eliminates one degree of freedom from the Miller's product, but still achieves knee pivot and shaft elongation in a fixed, coupled manner. This coupling effect can be adjusted by moving the pin into different holes along the coupling bar.

The system is further reduced in complexity with the addition of a footrest connector. This synchronizes the motion of both feet and does not allow for independent motion of each foot. While this is a limitation, it allows for a single breakaway point in the system, hopefully simplifying any future control implementations. A separate breakaway could be used for each degree of freedom if desired. A single lockout was

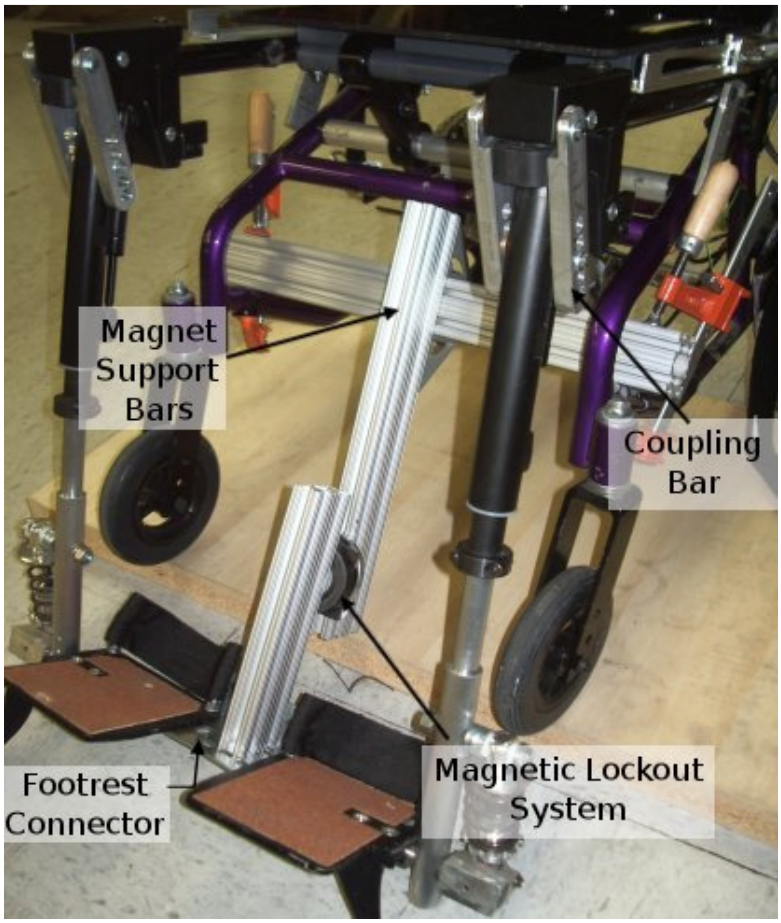

Figure 43: Improved Footrest Prototype

chosen for this design for convenience only.

Breakaway is accomplished using a magnetic lockout system. The magnet is held fixed by the magnet support bars. A steel plate is fixed to a bar extending from the footrest connector. This arrangement effectively lockout out both knee extension and plantar flexion while the magnets are connected. Once the connection is broken, both degrees of freedom are unlocked.

3.2.3.2 Electromagnet Breakaway

After seeing the benefits of using active components to change the dynamics of the system in Section 2.3.2, it was decided to try to use an active breakaway system with the footrest. One option would be to use an electromagnet to create the necessary holding force, and then release the lockout bar when appropriate. While this option would work well, it would also require the power to be on whenever the chair is in its rigid state. Because this is the state of the system most of the time, this is not a very efficient method.

A possible alternative would be to use a permanent magnet to attach to the steel core of an electromagnet. Then, when the electromagnet is turned on, it should repel the permanent magnet if the poles are properly aligned. That is the theory, at least. To test this theory, a permanent magnet was created as seen in Figure 44. A single cylindrical permanent magnet is seen attached to the electromagnet. This is the ideal location for the permanent magnet to be repelled by the magnetic field when the system is powered up. The field comes out the central core and into the out ring, which lines up with the direction of the field of the cylindrical magnet.

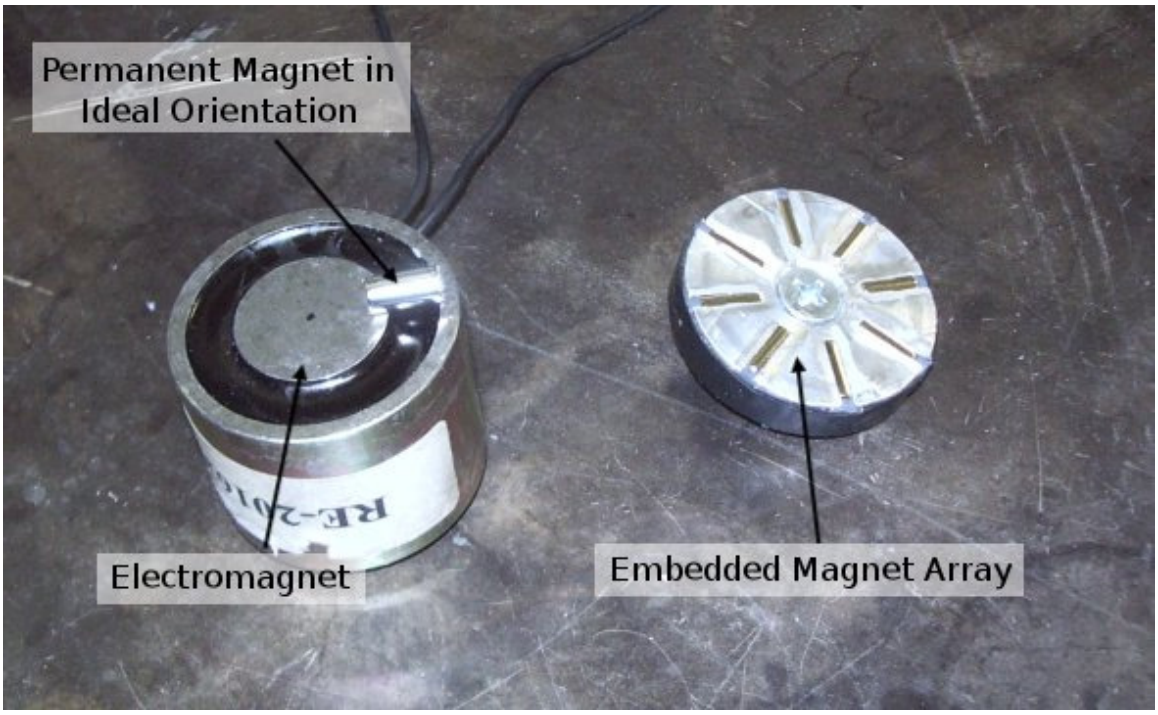

Figure 44: Electromagnet with Permanent Magnet Array

To create a stronger permanent magnet, eight cylindrical neodymium magnets were embedded in an aluminum disk with the proper orientation to form a permanent magnet array. This array of magnets will achieve maximum repulsion by the electromagnet when it is turned on, but will also create a holding force with the core of the electromagnet when the power is turned off.

During preliminary tests, the attraction between the permanent magnet array and the core of the electromagnet was weakened when power was supplied, but the two components were still attracted. Upon separation, however, a noticeable repulsion was felt. To quantify these effects, force profiles were generated using a Zwick/Roell Z005 tensile testing machine. Constant velocity tests were performed with the electromagnet powered on and off, and with different plastic spacers between the magnets. The results are seen in Figure 45.

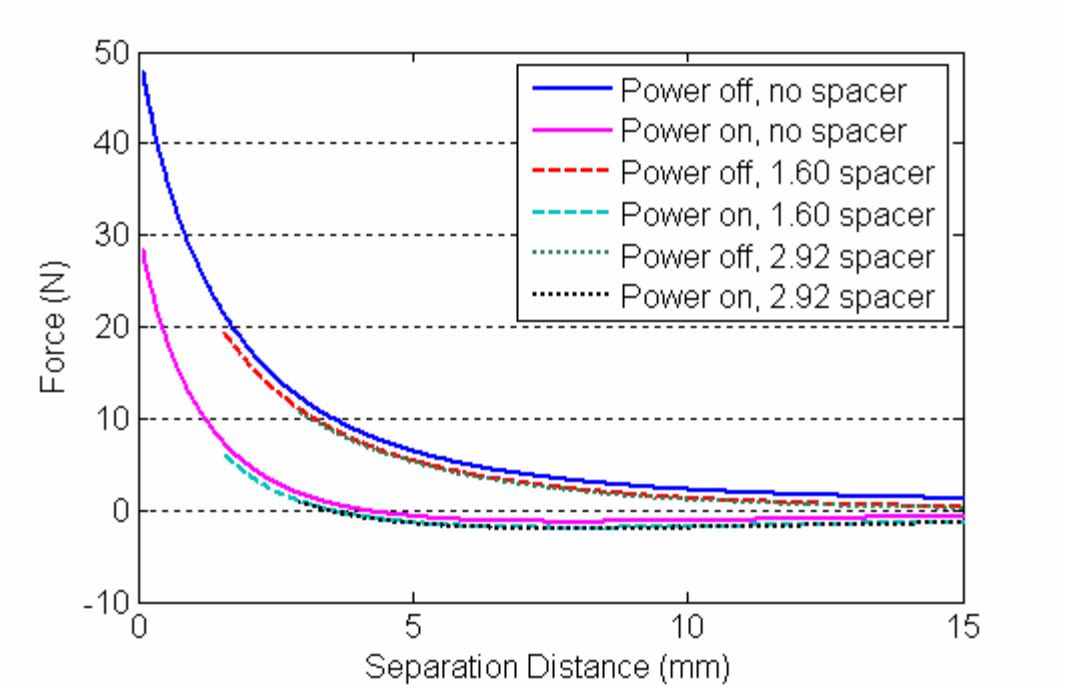

Figure 45: Force Profiles of Electromagnet

As can be seen, the attraction force is reduced by roughly half when the electromagnet is turned on, but the two are still attracted by more than 25 lbs. of pull. The effect of the spacers is negligible, as it merely moves the starting point of the force curve. One interesting thing to note is that with the electromagnet turned on, a repulsive force does occur starting at around 4 mm. The repulsion is not large, but is present. Unfortunately, this does not occur at 0 mm, as this would be the ideal case for active control of the system.

After quantifying the holding force of the system, the two magnets were attached to the footrest design. The motion of the footrest during breakaway is shown in Figure 46. While the strongest holding force of the permanent magnets is nearly 50 lbs. of pull, this is not enough for forces felt at the breakaway point during normal activities. The permanent magnet broke free with nearly zero effort from the user.

Figure 46: Footrest Motion during Electromagnet Breakaway

Thus, with only marginal results from the change in holding force and the weak maximum pull, the electromagnet design was removed from the system and replaced by a much stronger permanent magnet solution.

3.2.3.3 Permanent Magnet Breakaway

While the spring detent breakaway system performed poorly in Section 2.3.3, this was an isolated design failure, and not a general reflection on all passive breakaway systems. Indeed, after replacing the electromagnet in the 2 DOF footrest system with a 150 lbs. permanent magnet, the system performed remarkably well. The setup is shown in Figure 47. The permanent magnet acts as a force threshold above which it will break away freely. The resetting of the system is automatic. As well, the magnitude of the breakaway threshold can be adjusted by changing how much of the magnet and steel plate overlap.

While the passive breakaway is not synchronized with the active breakaway mechanisms of the seat back and seat bottom, it is still an effective means of changing the

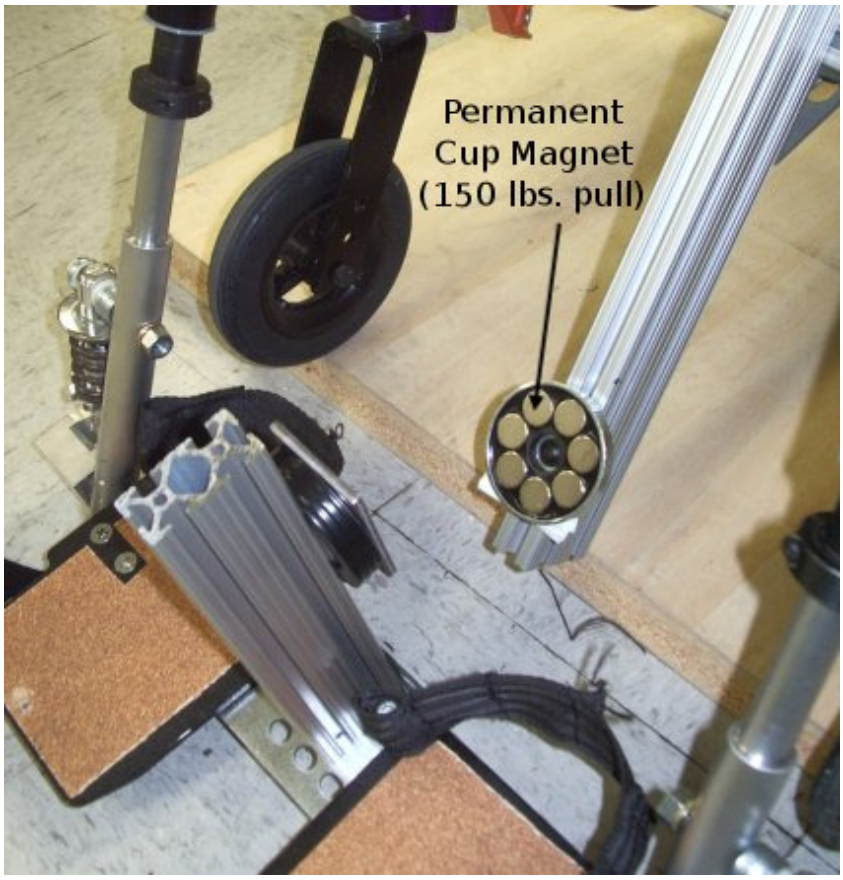

Figure 47: Footrest with Permanent Magnet

dynamics of the seating system. It also helps to highlight the benefits of a passive system. While not as versatile in how it differentiates (it cannot look at force gradient), it consumes no power and is very robust. If this will meet the basic requirements for a certain user, it should be chosen as the superior method unless needs are such that more advanced differentiation methods are required.

Because there is a single lockout point for both degrees of freedom, a test should be performed to see how the breakaway force is affected when one of degree of freedom dominates the initial breakaway. To do this, a force plate was attached to the footrests and three trials were performed. For each trial, breakaway was accomplished by attempting to use strictly plantar flexion, then strictly knee extension, and finally a combination of the two. These were repeated with different plastic spacers separating the

magnets at breakaway. The force profiles for the runs with no spacers are shown in Figure 48. The peak forces for all the runs with the different spacers are summarized in Figure 49.

A clear trend is present in the summary data. As is expected, with the inclusion of more initial space separating the magnets, the breakaway force is reduced. Additionally, the force to breakaway the footrest using both the feet and knees is consistently higher than using either motion separately. This is likely due to the fact that the magnets are most difficult to pull apart when the plates are parallel. Rotating the plates apart is much easier. Using plantar flexion or knee extension alone creates more of a rotating separation of the magnet from the steel plate, while using both forces the plates to remain more parallel during separation. This explains the higher force.

One other thing to note is that the force for using either plantar flexion or knee

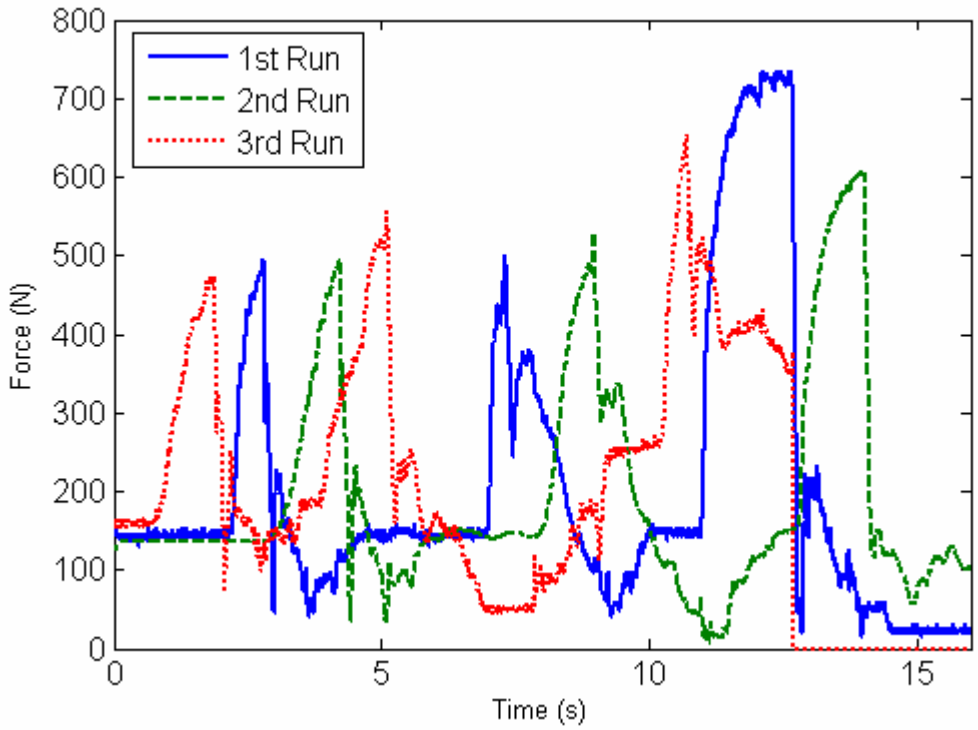

Figure 48: Force Reading During Breakaway with No Spacing

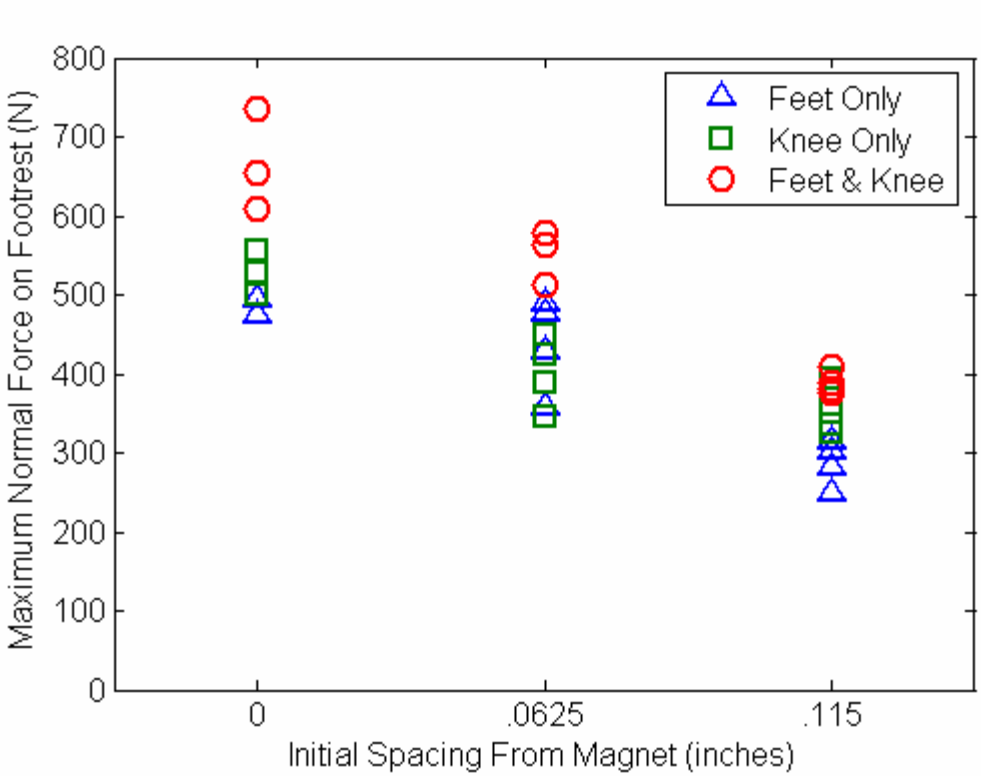

Figure 49: Peak Normal Force During Footrest Breakaway

extension is roughly the same. This can be adjusted by moving the magnet lockout up or down on the magnet support frame. This changes the moment arm for each axis of rotation. If a user has a stronger knee extension, the magnet lockout can be moved down to create more resistance to that motion, while simultaneously decreasing the force required to breakaway the system with plantar flexion. Using this, in combination with the spacers, allows a high degree of customizability in the footrest breakaway requirements.

3.3 Alternate Designs

Several alternate designs were proposed for the advanced dynamic seating system. Some were merely discussed, while other designs were made into a prototype.

3.3.1 Seat Lifting Concept

The Aktivline seating system was the inspiration for an alternate seat back and seat bottom concept. The Aktivline couples the motion of the backrest with the seat bottom in a manner that allows the seat-to-back angle to open up during a thrust. This is accomplished by allowing the seat bottom to pivot about a fixed point below the seat while the backrest slides up two rails. The general motion concept can be seen in Figure 5.

The seat lifting concept couples the motion of the seat back and seat bottom in a manner similar to the Aktivline system, but focuses on forcing the combined motion to raise the seat bottom during a thrust. This uses gravity to our advantage as the person is required to lift their own weight during an extensor thrust, absorbing and storing the energy from the thrust. The height increase can then be used to return the person to the pre-thrust configuration after the spasm is over.

The combined system is broken into three separate components: the seat back, the pelvis platform, and the seat bottom. The user is belted to the pelvis platform, which is designed to support and stabilize the pelvis during the entire motion. The seat back and pelvis platform are linked in a four-bar kinematical relationship that causes the pelvis platform to translate along an arc without rotating. This motion is shown in Figure 50.

The seat bottom is attached to the front of the pelvis platform and has a pin-slot connection that prescribes its motion. The complete system causes the height of the pelvis platform to increase during an extensor thrust.

A prototype was built to test this concept in hardware. The seat back, pelvis platform, and seat bottom were constructed from wooden boards. The positioning bar,

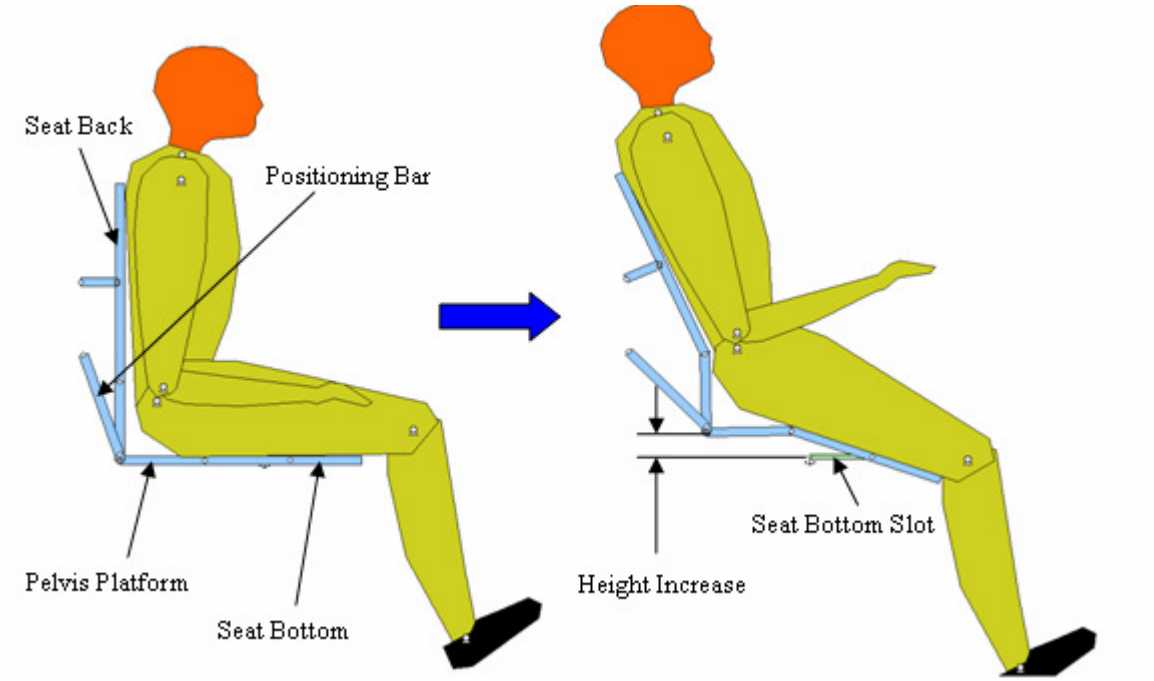

Figure 50: Motion Profile of Four-Bar Concept

which completes the four-bar system, was also constructed from a wooden board. Two large sheets of plywood were used as framework for the system, into which holes for the pins were drilled and the seat bottom slot was cut. These two plywood sheets were fixed to each other to stabilize the entire system and allow the seating components to move within the outer framework. The prototype is seen in Figure 51, with the motion of the system shown schematically. A front view of the prototype in its actuated position is shown in Figure 52.

The prototype was tested on several individuals. All of them were able to successfully lift themselves by using an extensor motion. Unfortunately, the seat bottom slot created a large amount of friction, which made the overall motion of the system quite rough.

This concept is good in its ability to absorb energy during the thrust and allow the body to move to a position where the muscles are at a mechanical disadvantage.

Figure 51: Four-Bar Prototype with Component Diagram

Figure 52: Four-Bar Prototype in Actuated Position

Unfortunately, the system does not match the contours of the body very well. The seat back does not conform to the spine as well as the flexible seat back design, causing an area of high pressure at the upper back instead of a more distributed pressure. The bend between the pelvis platform and the seat bottom can be moved to best fit the natural bend at the joint of the pelvis and femur, but this bending point will cause high pressure on the soft tissues of the leg.

One possible way to overcome these challenges would be to overlay the seating frame with a flexible material, cantilevered from the pelvis platform. The system still undergoes a similar motion as before, but the addition of the flexible materials helps to better match the contour of the spine. The flexible material on the seat bottom will eliminate the sharp transition point. This solution ends up looking very similar to the variable stiffness design, although the new system would still have a coupled motion that raises the user's center of gravity during an extensor thrust.

3.3.2 Double Roller Variable Stiffness Concept

Another concept looks to improve the design of the roller assembly for the variable stiffness seat back. This alternative design would use the concept of non-parallel support rods as shown in Figure 53. By removing the parallel requirement of the support rods, rotational stiffness of the seat back can be increased at the top of the seat back, while allowing the seat back to twist when the rollers are at the lower limit. Of course, this requires two separate roller assemblies, which complicates the drive belt interface with the motor. However, if the challenges could be overcome, this design would allow for a high degree of adjustability for the needs of those with rotational components during

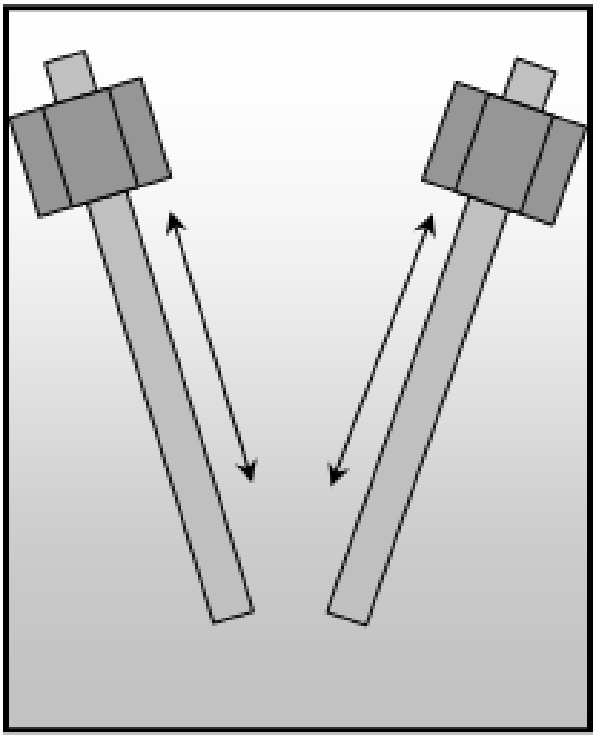

Figure 53: Schematic of Non-Parallel Support Rods

extensor thrust. For instance, the heights of the two rollers could be different, creating different torsional and bending stiffnesses across the surface of the seat back. This would likely be an improvement over the roller offset functionality of the current roller back design.

3.4 Experimental Data

The goals of this chapters included designing a dynamic seating system which reduces forces during a full-body extensor thrust while maintaining positioning of the pelvis. This could be accomplished by absorbing the energy from the thrust, putting the body's major muscles in a mechanically weak configuration, and letting the system conform to the natural shape of the person.

3.4.1 Seat Back Stiffness

The first analysis of the seating system investigated the ability of the seat back to conform to the natural curvature of the spine during an extensor thrust. To do this, we needed to analyze how the seatback deflection is affected by different configuration changes in the design.

Figure 54 shows the deflection curves for different applied forces when changing the roller height. The deflection is measured at the top of the seat back to reflect the maximum deflection for the force. The force was applied using a spring force gauge, attached to a hook at the top of the seat back. The gauge was pulled until the appropriate force for each measurement was achieved. As can be seen in the figure, the curves approximately follow a 1/x trend. When the roller is at the top of the seat back, the

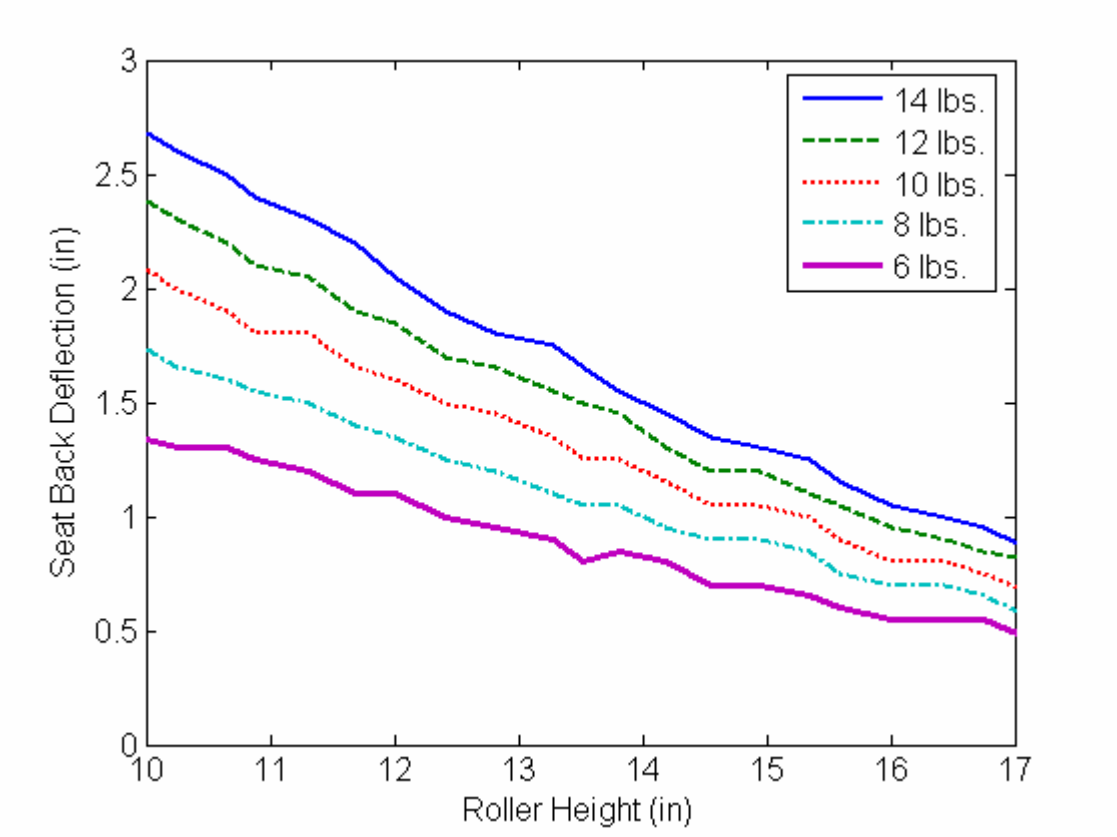

Figure 54: Force-Deflection Curves of Seat Back

deflection should be near zero. And when the roller is at the same level as the seat back hinge, the deflection should be very large.

The next study demonstrates how changes in the seat back material affect the seat back stiffness. The standard seat back consists of two sheets of PVC, each 0.233" thick. The addition of other flexible sheets to create a sandwiching effect was used to increase the stiffness of the seat back. The materials used are listed in Table 2.

As can be seen in Figure 55, the deflection curves from a 10 lbs. load again follow a 1/x trend. This shows that a variety of different stiffnesses can be achieved by using a

Table 2: Seat Back Materials Used

Label	*Material*
A	PVC, .233" Thick
B	PVC, .125" Thick
C	Lexan, .107" Thick

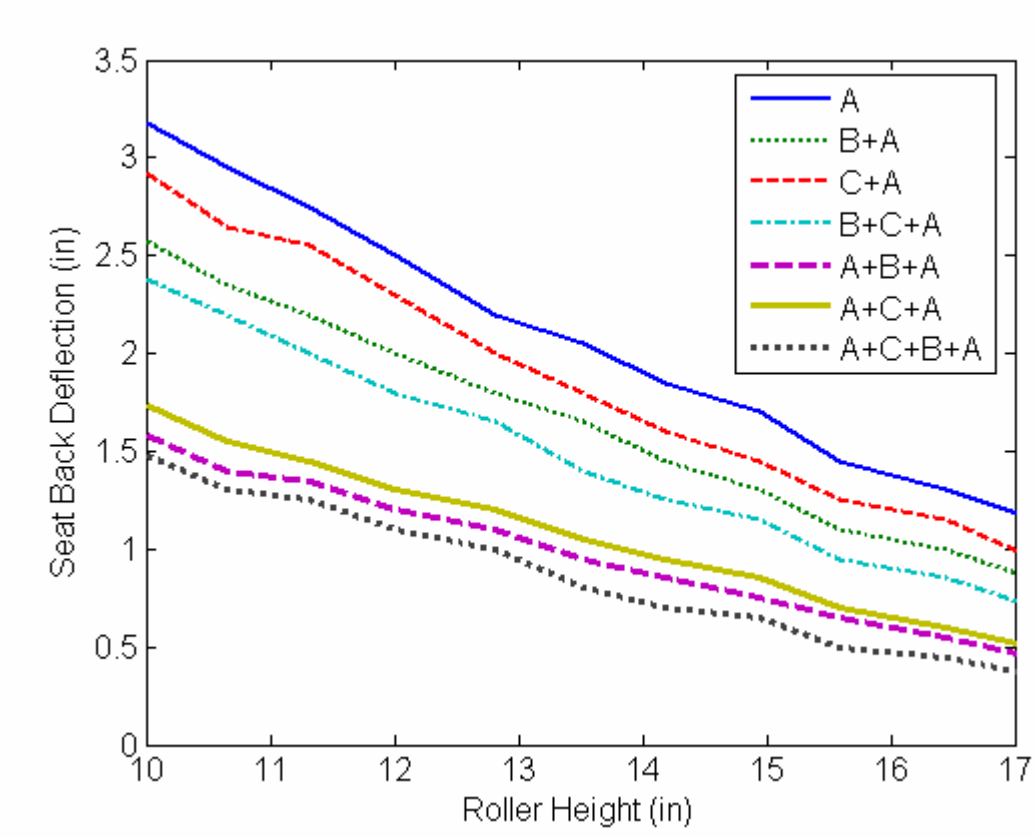

Figure 55: Material Thickness-Deflection Curves of Seat Back

combination of these materials.

PVC and Lexan were used for the flexible seat back due to their useful material properties. PVC is a good choice for a seat back material because it is inexpensive and is easily blended with additives to get a wide range of stiffnesses. It is also lightweight and has good fatigue properties for the amount of bending required by this design. Lexan and other polycarbonates are generally stronger than PVC and have higher impact resistance. They have good fatigue properties, but are generally more expensive than PVC. Both would work well for the seat back material, and the choice would be determined by those working on the final manufactured design.

Using the methods of adjusting the roller height and changing the seat back material and thickness allows for different seat back stiffnesses and shapes. A user with a sharp spine curvature might want to have a less stiff seat back material, but not allow the roller to move down as far in its lower limit position. Another user, perhaps who has had a portion of his or her spine fused, might choose to have the roller move down much further in its travel, but increase the material stiffness. These two systems could have the same deflection at the top of the seat back, but a very different curvature profile, suited to the needs of the individual user.

Another way to customize the seat back stiffness is in the area of torsional stiffness. As was mentioned previously, some users experience a rotation of the torso during extensor thrusts. With the addition of the transverse offset for the roller, seen in Figure 39, we can easily change the torsional stiffness profile.

A spring force gauge was again used, set to 10 lbs. of force. The force was first applied to the upper right corner of the seat back, and the deflection of the same corner

was measured for various roller positions. The height as well as the offset position were adjusted. The results for this study are shown in Figure 56.

Next, 10 lbs. of force was applied at the center of the seat back, and the deflection at the center of the seat back was measured. The roller height and offset position were again adjusted. The resulting deflection curves are shown in Figure 57.

As can be seen in the corner deflection curves, offsetting the roller by two inches changes the seat back deflection by approximately a quarter of an inch for 10 lbs. of force. Looking at the center deflection curves as the horizontal offset is changed shows that there is only a small effect, which makes sense. By offsetting the roller to the right, the stiffness should be able to change in a way that allows the entire top edge of the seat back to have a constant deflection, even in the presence of the rotational tendency to the right. The same could be done for those with a rotational tendency to the left. Whether

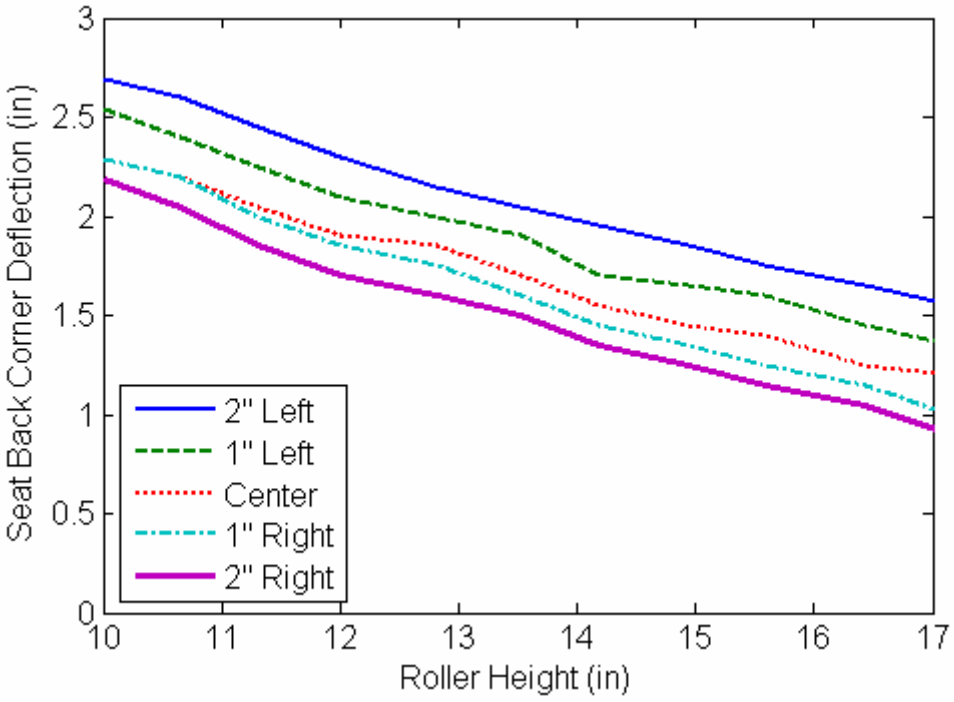

Figure 56: Effect of Offset Roller on Seat Back Corner Deflection

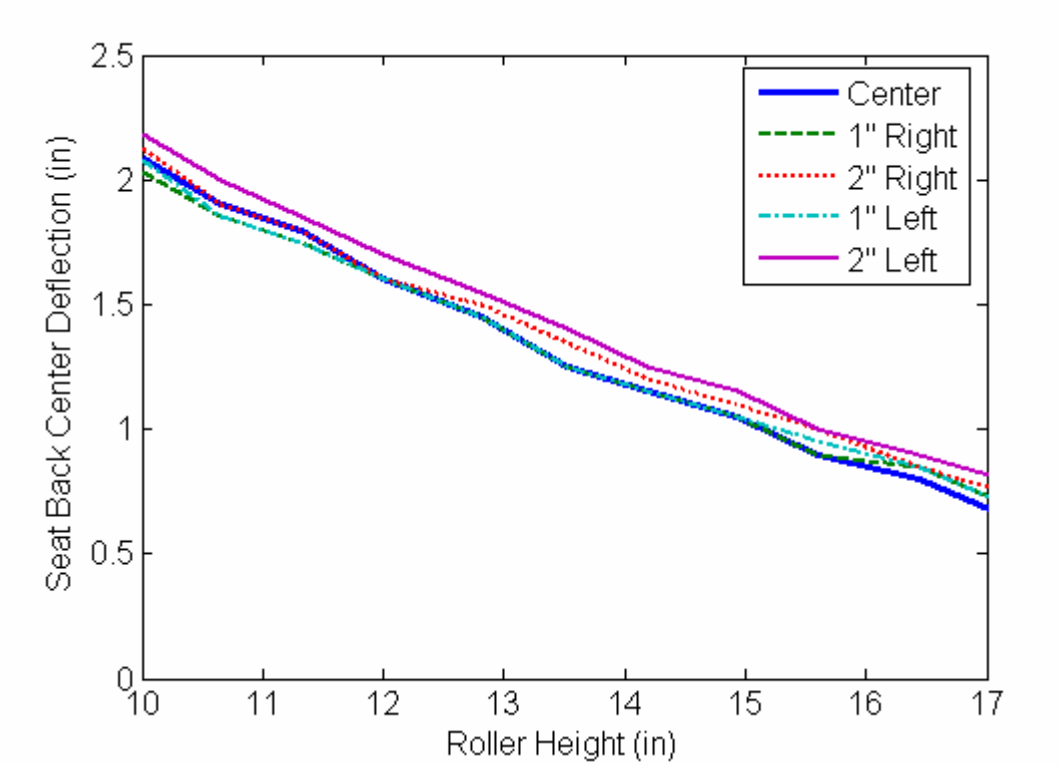

Figure 57: Effect of Offset Roller on Seat Back Center Deflection

this change in rotational stiffness is desirable is debatable, but at least the functionality is provided if a clinician feels it will be beneficial to the wheelchair user.

3.4.2 Motor Speeds

The next variable to investigate in the variable stiffness design is the speed of the seat back motor and the seat bottom actuator under load. The seat back and seat bottom designs were chosen to highlight different possible implementations of the variable stiffness concept, and the most unique difference in their operations is the speed at which they are able to change from the rigid to the dynamic mode. The speed at which each system is able to become dynamic and also the speed at which it is able to return to the rigid mode are examined. The speed at which the system becomes dynamic is important,

while the ability to push against the weight of the person is more important in returning to the rigid mode.

The first test was performed on the seat back. The chair was tilted backwards and different amounts of weight were attached to the seat back in roughly the area where the shoulder blades make contact with the seat back. A camera was then used to record the position of the roller as a function of time. This test is not completely true to the actual setup because the weight of the roller assembly is neglected. However, this setup is the easiest way to have a consistent normal force on the backrest throughout the test. Two trials were performed, one that went the full travel of the drive belt and one that went from the top to halfway down the possible travel. The difference shows up in the return stroke, as the initial moment arm of the load is reduced in the half-travel case.

The results of the tests are shown in Figure 58. The graph shows a consistent speed of roughly 17 in/s on the downward stroke of the roller. The extra force at the tail end of the stroke that should come from curvature in the seat back seems to have little effect in this case. The average speed drops rapidly, however, when weight is present during the up stroke. This is likely due to the motor having to start from rest and accelerate the roller assembly against the maximum resistive force it will encounter during the move.

In some cases the motor is unable to overcome the initial resistive force from the weight on the bent seat back. With 25 lbs. on the seat back at the full travel length, the motor stalls and is unable to complete the move. This is an important consideration in how far down the roller is allowed to go, as it affects the ability of the motor to return the occupant to the upright position.

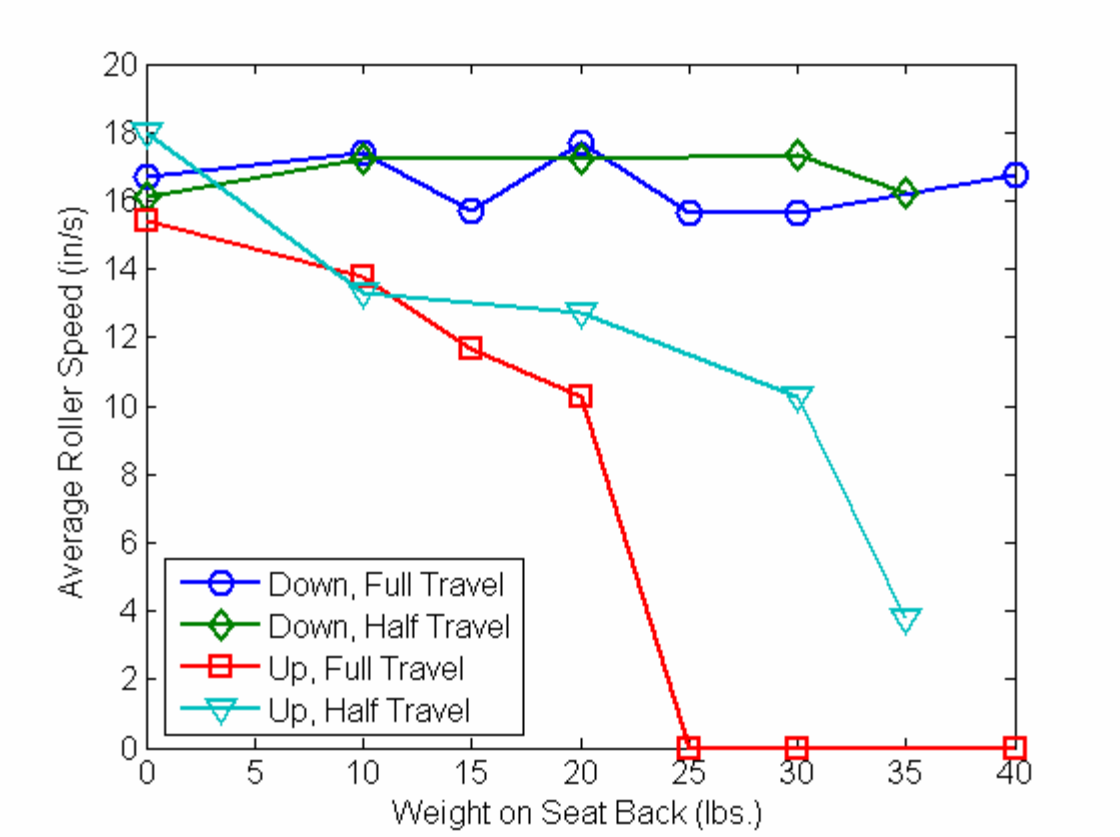

Figure 58: Roller Speed vs. Load on Seat Back

This inability to return the user to the upright configuration is a significant weakness in the current design. An estimate of the backrest angle when the roller is in its lowest position is 69°. By looking at the contribution of the upper body weight (approximately 60% of the total body weight) on the normal force seen at the seat back, a stall at 25 lbs. in Figure 58 equates to stalling under the weight of someone who weighs only 116 lbs. While that may be realistic for small children, this motor size would not work for teenagers or young adults. The correlation between motor size and stall weight was not measured, but this is a factor that would need to be considered in designs for specific users.

The next test looks at the seat bottom and the speed at which the linear actuator is able to rotate the rigidizer bar away, and also to return the rigidizer bar to the original

position. The test was performed by placing weights on the front edge of the seat bottom and driving the actuator. The results are shown in Figure 59.

While driving down, the rigidizer moves at approximately a constant rate of twelve degrees per second. The total travel is 30°, so this equates to more than 2.5 seconds. This is quite slow compared to the roller assembly, which completes its downward move in about 0.5 seconds. However, the actuator is much stronger, and is able to return the seat bottom to its starting configuration easily for 60 lbs. of weight on its front edge. Because the bulk of the user's weight will be distributed across the seat bottom, this makes the tilt design better suited for the seat bottom than the roller design.

The slow speed is a weakness in the design, as the ability to quickly change configurations is needed when a thrust is detected. To solve this problem, a different actuator should be used that travels at least three times as fast as the current 0.5 in/sec. This should be accomplished by using a more powerful actuator rather than changing the

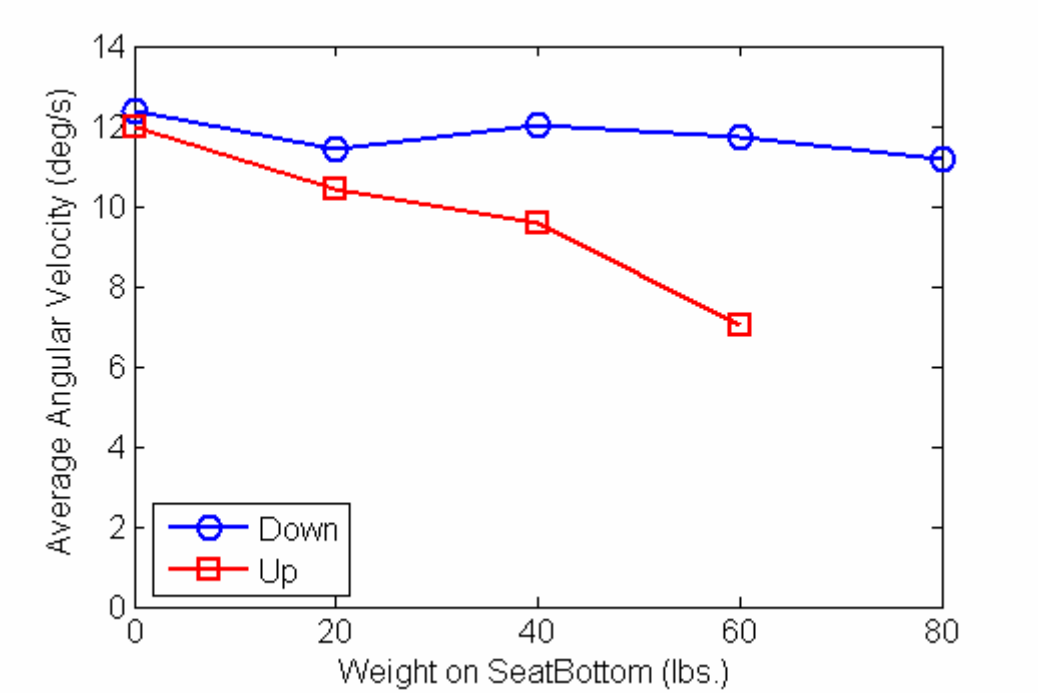

Figure 59: Rigidizer Speed vs. Load on Seat Bottom

gear ratio of the current actuator, as this would limit the lifting power when returning the seat bottom.

3.4.3 Thrust Interaction Forces

After looking at the properties of the variable stiffness seating system, we investigated how the motion of the system affects the forces that the user feels during an extensor thrust.

3.4.3.1 Methodology

To study these interaction forces, two Conformat® pressure mats by Tekscan were attached to the chair, one on the seat back and one on the seat bottom surface. A 2" piece of foam was then placed on the mat to allow for a more distributed pressure reading at the interface. Data from these mats was recorded using computer software with a sampling rate of 5 Hz.

In addition to the two pressure mats, a 200 lbf digital force gauge was mounted inline with the seatbelt to get a tension reading during the thrust. The gauge was mounted with a freely pivoting hinge to guarantee true axial readings of the tension. The readings were also recorded in software with a sampling rate of 5 kHz.

Five able-bodied test subjects were chosen to perform mock extensor thrusts in the seating system. For each subject, the height of the footrest was adjusted to reduce any pushing on the footrest in the fully extended position. The seatbelt was tightened by the user according to their level of comfort, and was used to keep the pelvis constrained

during the thrust. This is a different setup than used previously in the hinged-back seat, in which the mock extensor thrusts were done with an unconstrained pelvis.

A total of five wheelchair configurations were tested, as shown in Table 3. For the first two positions, forming the first group, the seat bottom and feet were allowed to move dynamically, with the location of the flexure bar changing from 6" to 8". The backrest was also dynamic, with the roller height being kept at 11", its lowest position. The second group kept the seat bottom and feet locked out. The three positions differ in the height of the seat back roller, ranging from 11" to nearly rigid at 22".

Table 3: Wheelchair Test Configurations

Group 1		*Group 2*		
Configuration 1	**Configuration 2**	**Configuration 3**	**Configuration 4**	**Configuration 5**
Seat & Feet dynamic, 6" flexure bar, 11" roller height	Seat & feet dynamic, 8" flexure bar, 11" roller height	Seat & feet locked, 11" roller height	Seat & feet locked, 16" roller height	Seat & feet locked, 22" roller height (rigid mode)

The reason for locking out the seat bottom and feet together is because the motion is inherently coupled between the two subsystems. Keeping the footrest fixed keeps the location of the knees relatively constant. Thus, the thighs will not move down into the seat bottom, even if it were allowed to be dynamic. On the other hand, allowing the feet to move while keeping the seat bottom fixed would create a very sharp edge of pressure as the thighs want to rotate downwards, but are not able to.

For each test subject, the order of the configurations was randomized by group, and then randomized within each group. For each specific configuration, three mock extensor thrusts were performed sequentially. After the person achieved as much full-body extension as possible in each configuration, data recording ceased. The person was then

allowed to relax. By stopping the data collection in full extension, it was easy to analyze the data for the full-body position, which is the position of greatest interest.

The analysis of the data looked at several factors that could be extracted from the pressure mats and the force gauge. From the pressure data, the peak pressure index (PPI) was calculated. This was done by finding the maximum pressure on the mat, and looking at the four averages of the surrounding cells on the mat. The highest average is the PPI. The PPI is a more robust measure of the peak pressure than looking at a single pressure cell reading. In addition to the peak pressure index, the total mat force, the center of pressure on the mat, and the contact area were calculated. For the contact area, the threshold was set at 10 mmHg, below which the readings were assumed to be noise. The force gauge was used to measure the belt tension in the fully extended position, along with the amount of preload before the thrust began.

By collecting data from three mock extensor thrusts for each configuration, anomalies in the mock thrusting could be detected. For the analysis, the median data for the three runs was used to draw conclusions, according to the following graphs. The complete data, showing the variability of the forces between trials in the same configuration is given in Appendix C.

3.4.3.2 Seat Back Forces

The first set of data that we consider is the normal force felt at the seat back. This was calculated by converting the mat pressures to a force reading when the user was in a fully extended position for each different configuration. The force reading has been

adjusted to remove the contribution due to the weight of the upper body. The results are shown in Figure 60.

In the most rigid configuration, the normal force is due solely to the extensor thrust force. When the seat back is allowed to bend backwards, some of the normal force comes from the weight of the person's upper body on the seat back, and not from the thrust force. To get a reading of the thrust force, we removed this contribution. The estimated angle for configurations 1-3 is 69°, for configuration 4 it is 77°, and for configuration 5 it is 90°. The estimated weight of the upper body is 60.28% of the total body weight for males and 58.23% of the total body weight for females [24]. The person's weight is multiplied by this percentage, as well as by the cosine of the estimated angle. This contribution due to gravity was then subtracted from the normal force

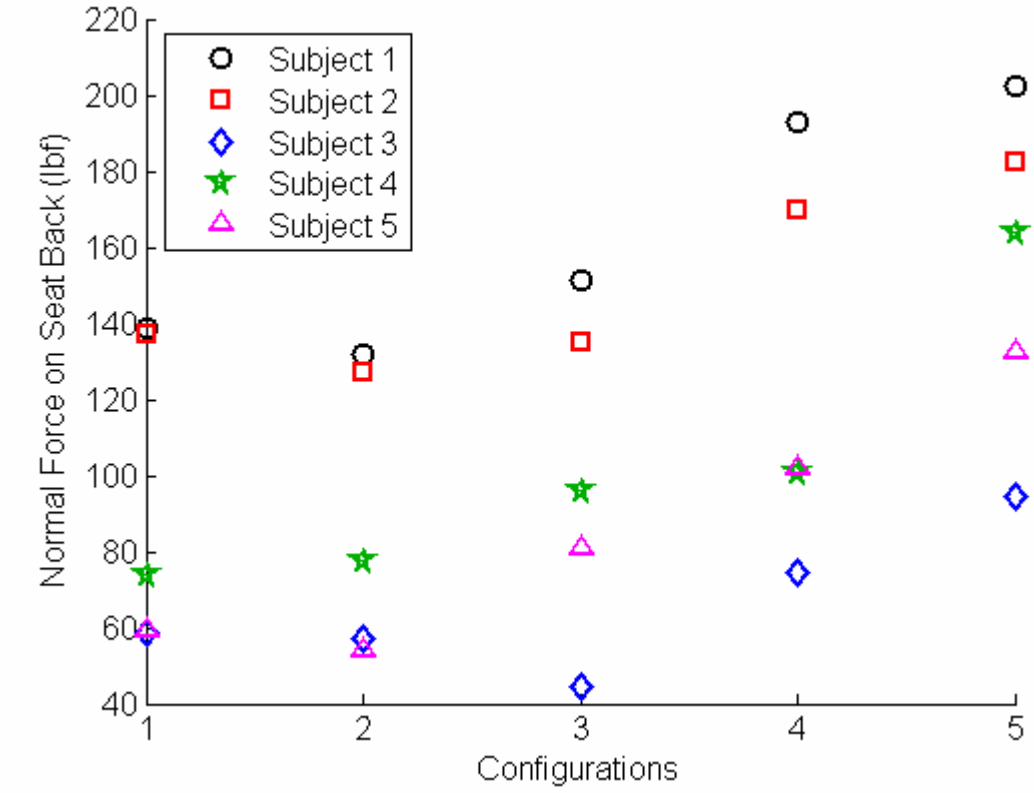

Figure 60: Seat Back Normal Force in Full Extension (Gravity Contribution Removed)

reading on the seat back to get the final normal force readings shown in Figure 60.

As seen in the figure, the adjusted normal force is highest in Configuration 5, the rigid mode configuration. An analysis of variance (ANOVA) was performed on the median forces across the different configurations, and found that there are significant differences in the median forces. A Tukey post-hoc comparison [25] was then run to determine the source of the differences. The results are shown in Table 4, with statistically significant differences shown as nonblank entries.

Table 4: Significant Differences in Seat Back Normal Forces

Configuration	1	2	3	4	5
1				.0018	.0000
2				.0006	.0000
3				0.168	.0000
4					.0136
5					

The statistics show that Configurations 1-3 were not different, but each one was different from Configurations 4-5. Furthermore, Configurations 4 and 5 were different from each other. This indicates that Configuration 5 certainly has the highest normal force on the seat back, with Configuration 4 having the next highest loading. This shows that the dynamic components are effectively reducing the normal force felt at the seat back.

The contact area at the seat back in full extension was also examined. The contact area was defined as the area on the pressure mat where the pressure exceeded a minimum of 10 mmHg. Below that threshold, the pressure cannot be distinguished from the noise in the sensors. The results are shown in Figure 61. These results are best analyzed together with the vertical center of pressure data for the seat back, shown in Figure 62. Figure 62 shows the vertical location of the center of pressure, together with the location

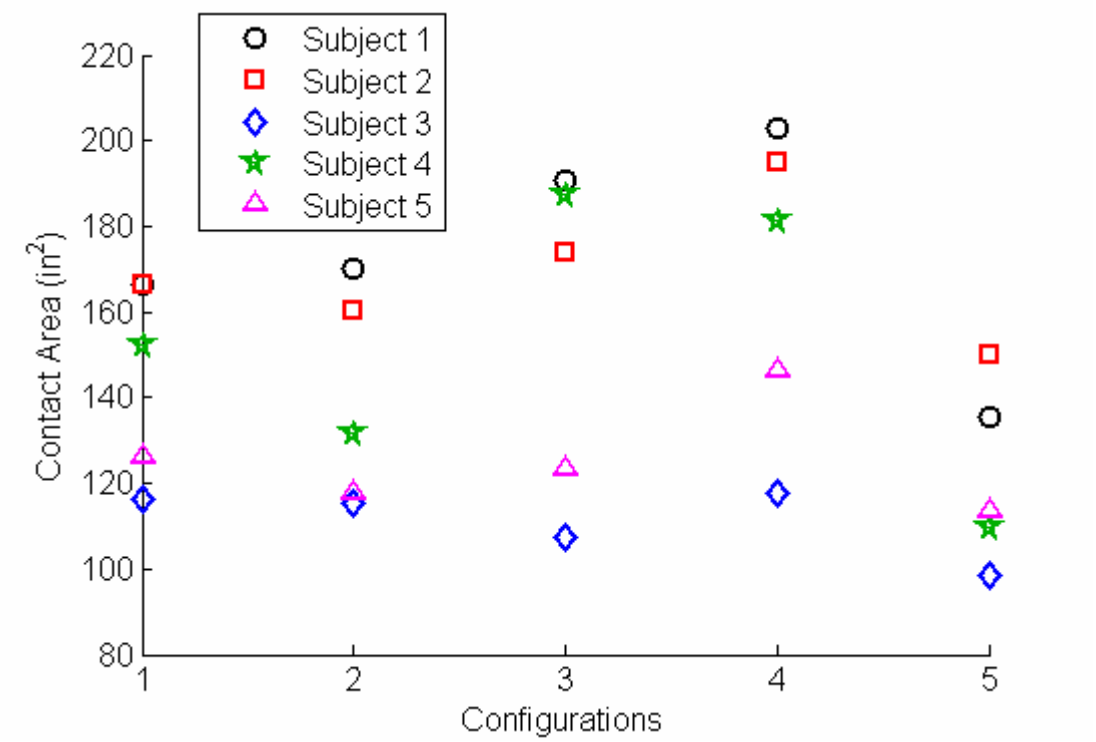

Figure 61: Seat Back Contact Area in Full Extension

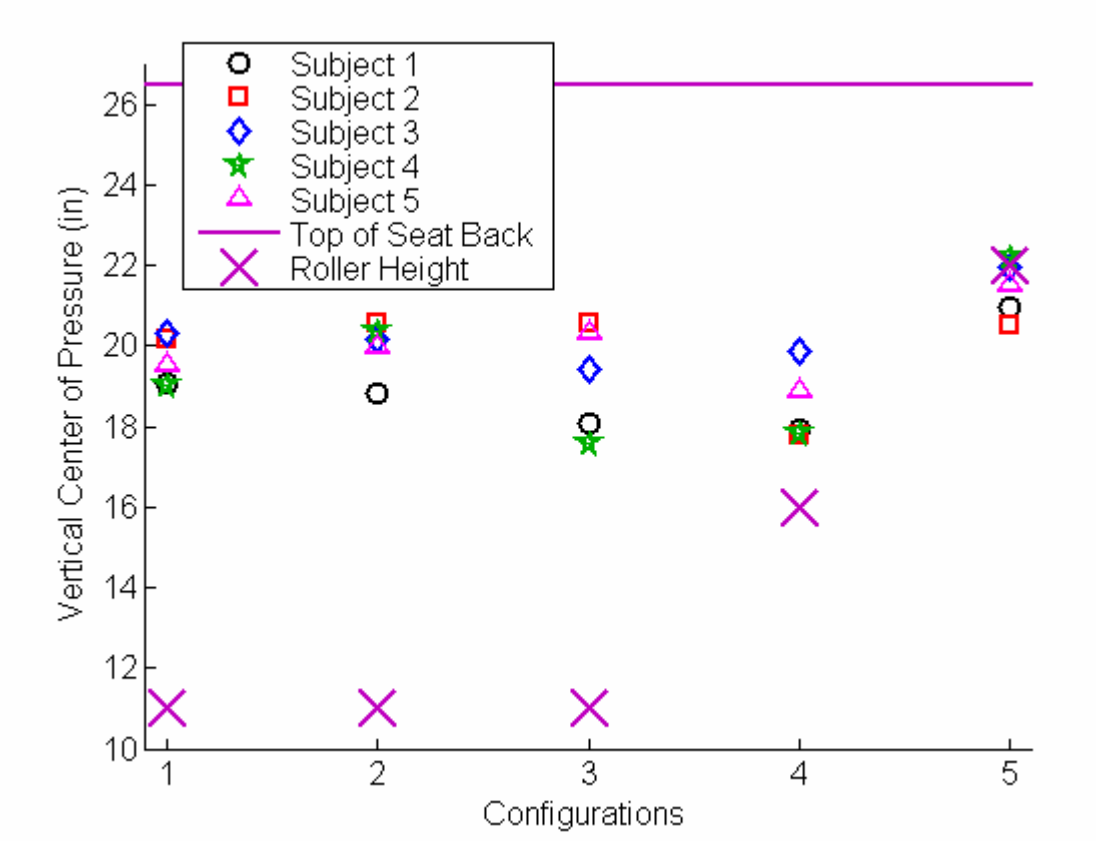

Figure 62: Seat Back Vertical Center of Pressure in Full Extension

of the seat back roller and the top edge of the seat back. This allows for a visual interpretation of where the center of pressure lies in relation to important seating components.

As can be seen, the rigid configuration (Config. 5) has the smallest contact area, and the center of pressure is located the furthest up the seat back, near where the roller is positioned. This is a good result, indicating that the roller is properly positioned to resist the extensor thrust and keep the seat rigid. The small contact area is due to the force being concentrated on the shoulder blades.

The contact area is largest when the seatback is dynamic, but the feet and bottom are locked out (Config. 3 & 4). The center of pressure does not appear any higher, so it seems that the person is not extending up the seat back like they would in an unconstrained extensor thrust. Instead, keeping the feet locked causes the lower back of the person to remain close to the seatback during a thrust, thereby increasing the contact area. When the knees extend (Config. 1 & 2), the lower portion of the person's back moves away from the seat back, reducing the total contact area.

The peak pressure index in full extension is shown in Figure 63. We see that the PPI is highest for the rigid mode (Config. 5), as expected by the large normal force and small contact area. The first three configurations have the lowest PPI, indicating that these dynamic configurations produce less pressure points that would cause discomfort and injury to the user.

A correlation was done on the contact area, center of pressure, and peak pressure index of the seat back. The results are given in Table 5. The most significant correlation was between the contact area and center of pressure. The correlation indicates that with

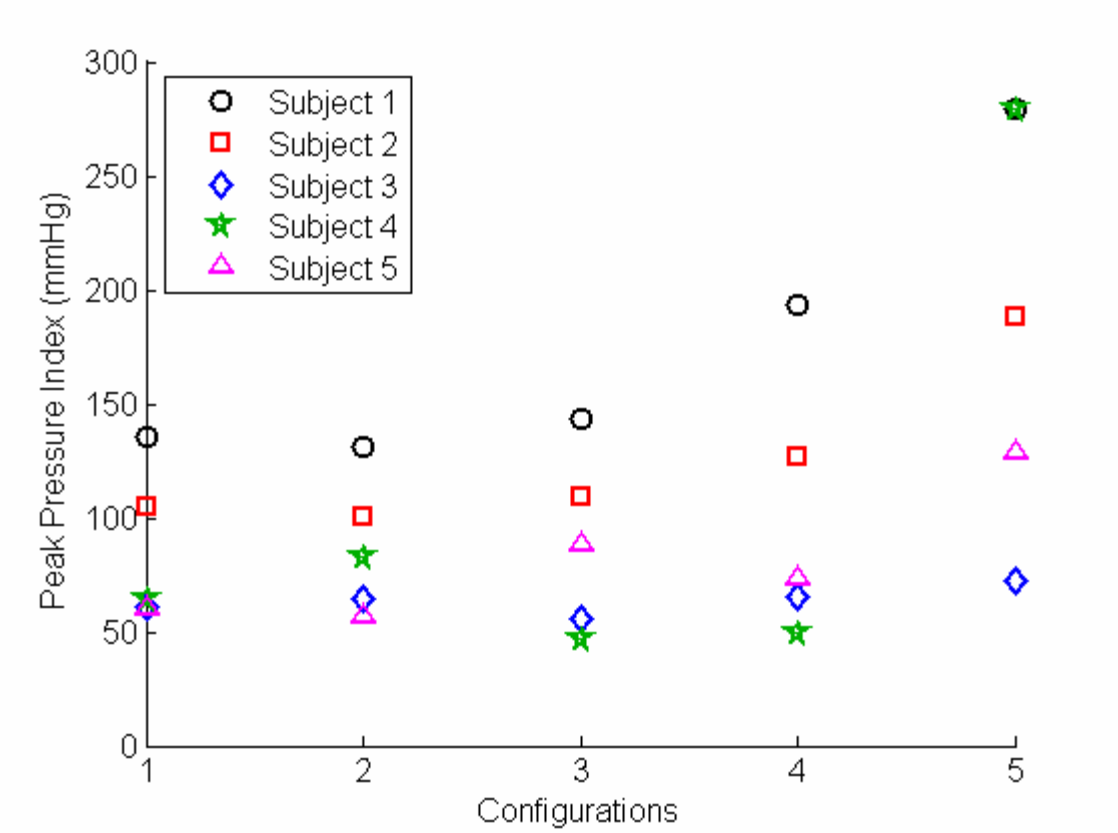

Figure 63: Seat Back Peak Pressure Index in Full Extension

Table 5: Correlations Between Seat Back Data

	Contact Area	Center of Pressure	Peak Pressure Index
Contact Area		-0.730433806	0.138810116
Center of Pressure			0.283680382
Peak Pressure Index			

increased contact area, the center of pressure moves further down the seat back. This agrees with the previous conclusion that the increase in contact area was at the lower back, due to the lower back being constrained when the feet and seat bottom are locked.

Overall, the data indicate that the dynamic components are very effective in reducing interaction forces at the seat back, and improving comfort by reducing the peak pressures. No strong conclusions can be drawn about the best configuration, although the

rigid mode clearly gives the highest forces, the smallest contact area, and the highest peak pressure index.

3.4.3.3 Seat Bottom Forces

A parallel analysis on the seat bottom interaction forces in the fully extended position was also performed. We first looked at the normal forces on the seat bottom, shown in Figure 64. No correction factors were needed for the seat bottom, as all configurations have a nearly equal contribution due to the weight of the user.

From the figure, Configuration 2 seems to have a significantly higher seating force than the other configurations. An analysis of variance (ANOVA) was also run on this normal force data, with a Tukey post-hoc comparison shown in Table 6. The nonblank

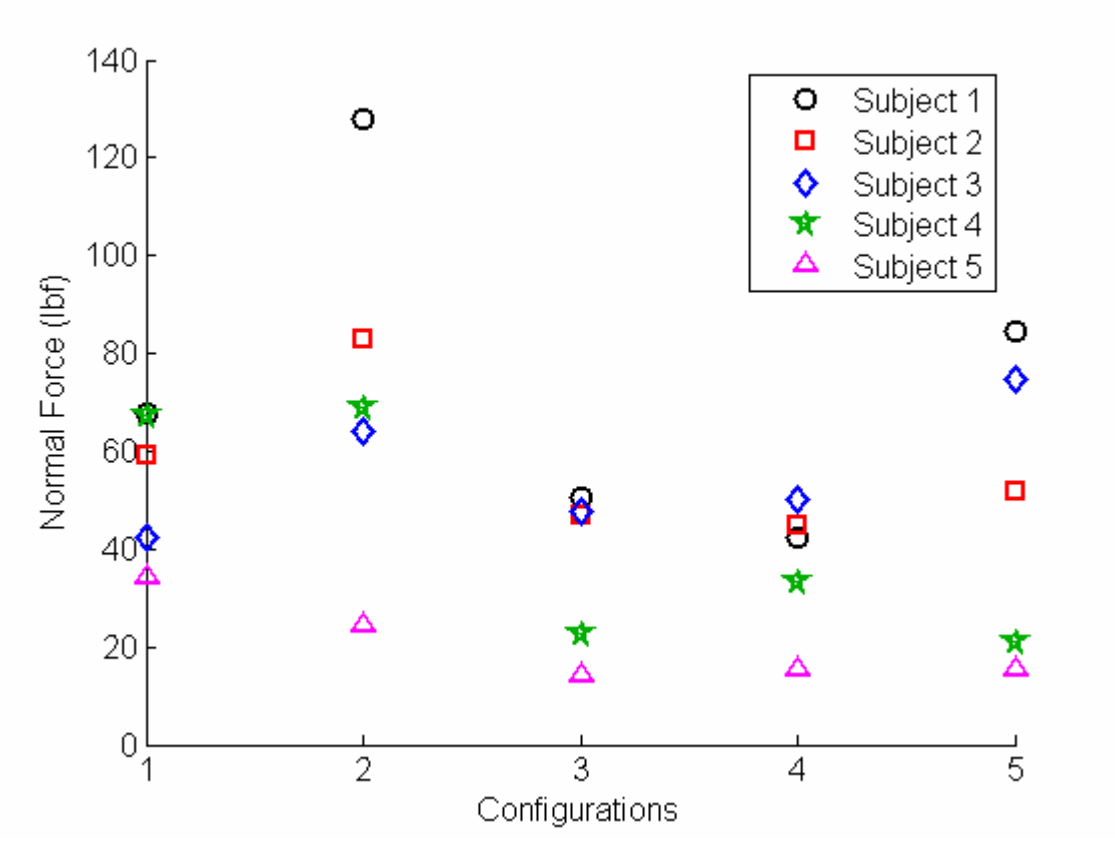

Figure 64: Seat Bottom Normal Force in Full Extension

Table 6: Significant Differences Between Seat Bottom Normal Forces

Configuration	1	2	3	4	5
1		.0056	.0218	.0222	
2			.0000	.0000	.0002
3					
4					
5					

entries show statistically significant differences between the normal forces across the five subjects. The table shows that Configuration 2 is different than all other configurations. Thus, we conclude that the forces are, in fact, the highest in this configuration. The table also indicates that Configuration 1 is different from all but the last configuration, with the last three configurations not differing significantly.

This analysis indicates that allowing the seat bottom and feet to move dynamically tends to increase the normal force on the seat bottom. This makes sense when one considers that keeping the feet locked allows the user to "bridge" off the seat bottom during an extensor thrust. By allowing the feet to move, this "bridging" action is decreased, and the force at the seat bottom is increased. This is not a weakness of the design, rather it is a natural and desirable outcome of allowing full-body extensions to occur.

The contact area on the seat bottom is shown in Figure 65. The contact area appears largest for the 8" flexure bar position (Config. 2). Configurations 3 and 4 have the smallest contact area. The lower contact area for Configurations 3 and 4 can be explained by the bridging action off the footrest.

The increased contact area for Configuration 2 is due to the change in curvature of the seat bottom. In this configuration, the seat bends up more under the pelvis before it curves down towards the knees. Thus, with a higher amount of curvature under the

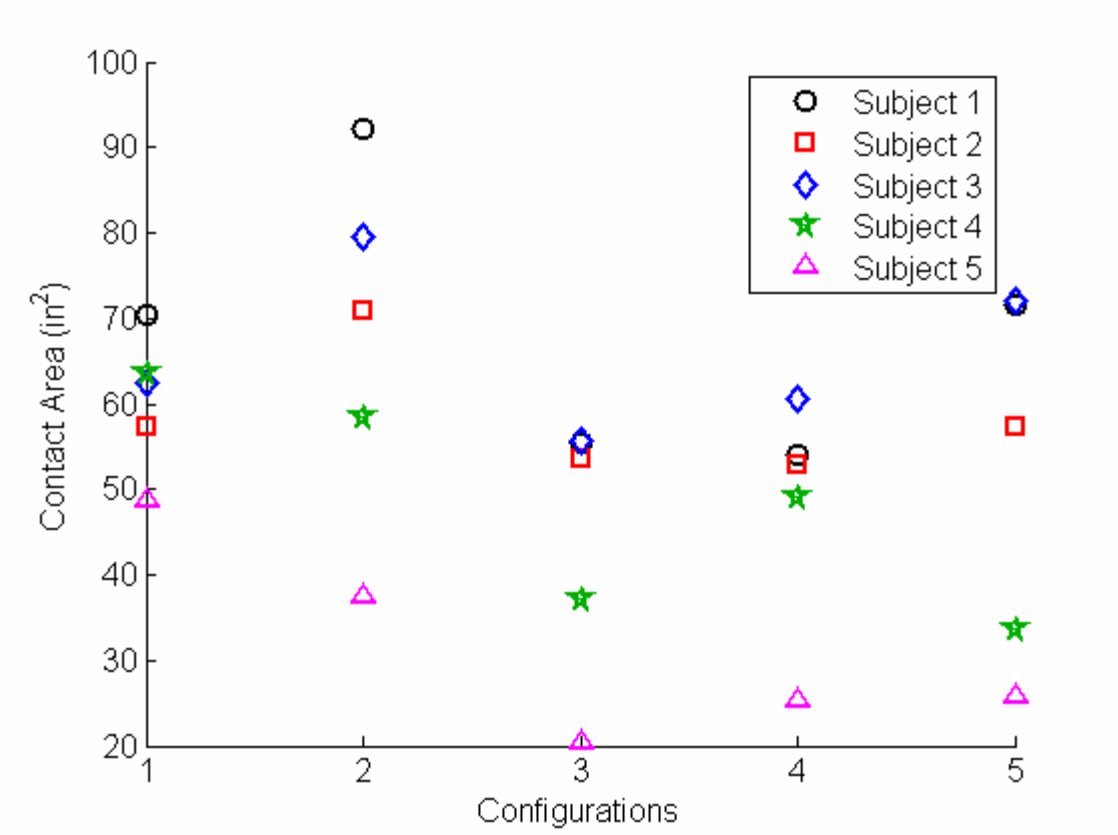

Figure 65: Seat Bottom Contact Area in Full Extension

pelvis, more contact will occur. This is similar to the increased contact area with the seat back with a 16" roller height (Config. 4). Increased curvature allows more contact at the lower back, and similarly with the pelvis for the seat bottom.

The data for the center of pressure on the seat bottom is shown in Figure 66. The center of pressure is measured in the horizontal direction, away from the seat back. The front edge of the seat is shown, along with the location of the flexure bar, for reference.

The center of pressure does not vary much with the configuration changes. It is slightly lower for the 8" flexure bar (Config. 2), due to the increased contact area toward the rear of the seat bottom. The center of pressure is quite near the edge of the seat, indicating high pressure concentration at the edge.

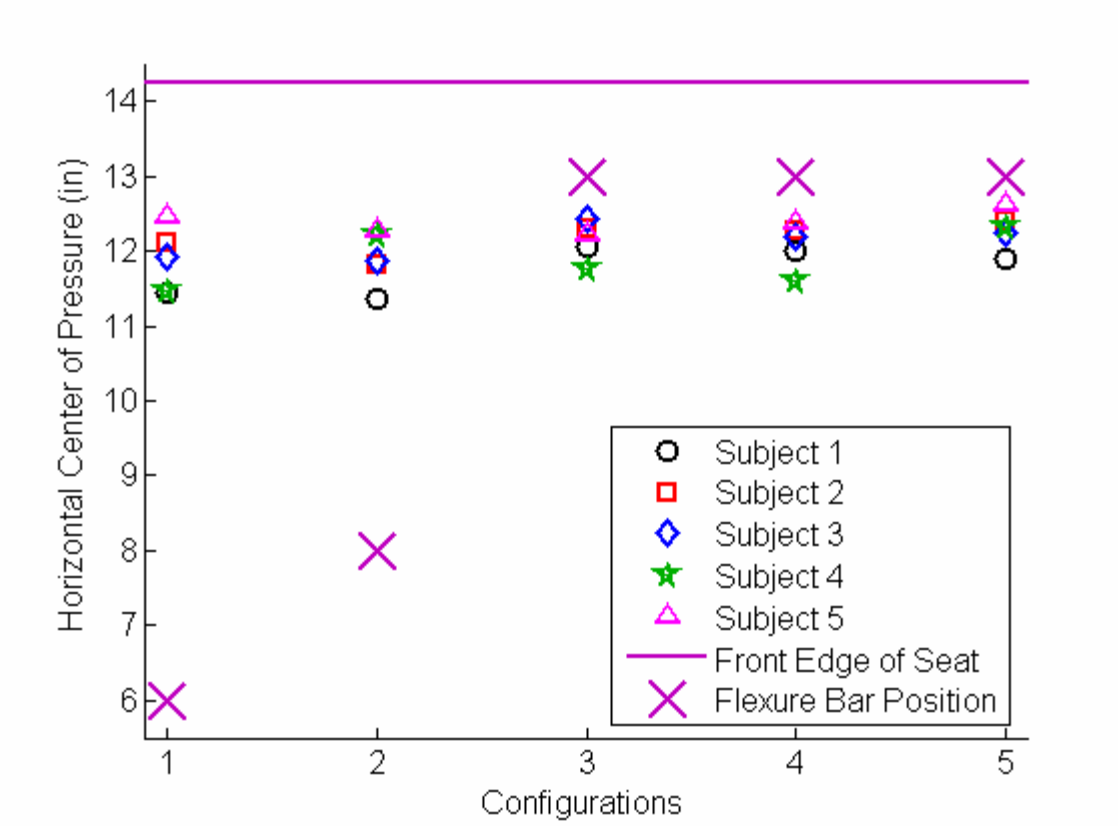

Figure 66: Seat Bottom Horizontal Center of Pressure in Full Extension

We also looked at the peak pressure index on the seat bottom to see which configurations caused points of high pressure. The results are shown in Figure 67. Configuration 2 has the highest PPI. This is a troubling result. Rather than assuming that the larger contact area caused the higher seat forces, this seems to indicate that there are higher pressures on the seat bottom in this configuration.

A correlation was also run for the contact area, center of pressure, and peak pressure index on the seat bottom. This data, given in Table 7, indicates a significant correlation between the contact area and the center of pressure, with an increase in contact area causing the center of pressure to move rearward. While the differences in center of pressure between configurations are small, these differences are correlated to differences in the contact area of the seat bottom. The data also indicates a strong correlation

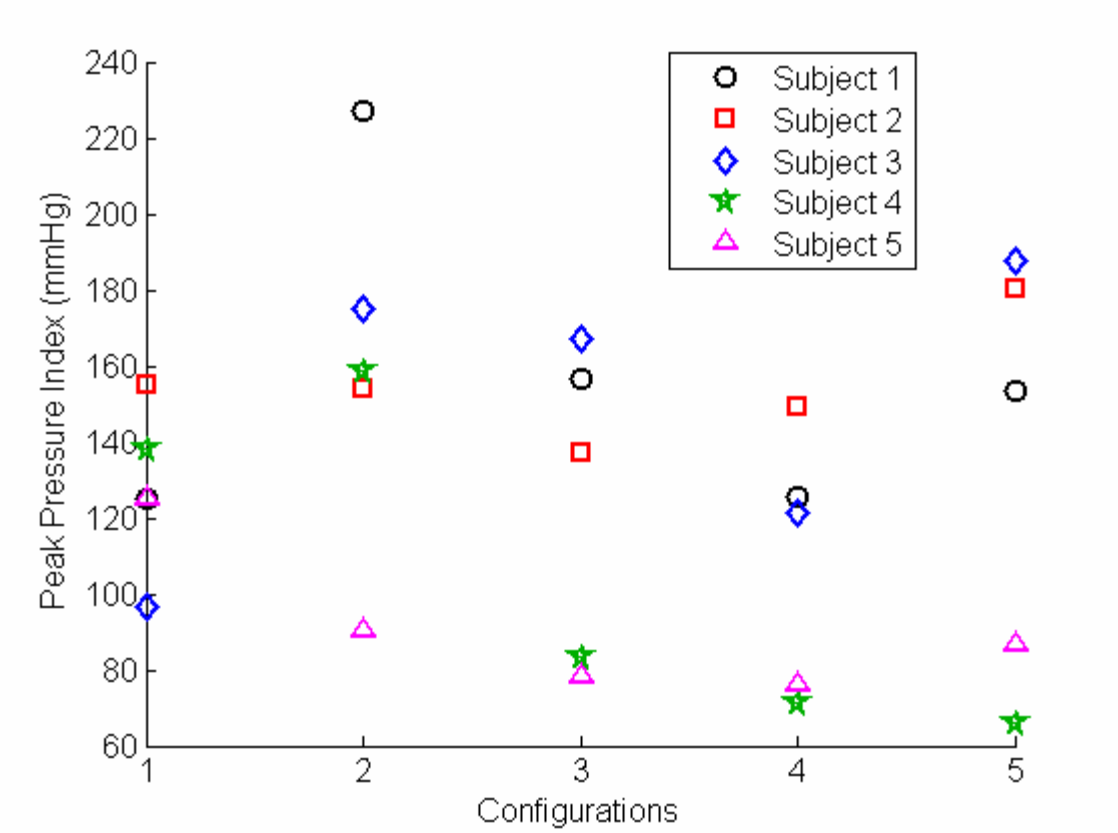

Figure 67: Seat Bottom Peak Pressure Index in Full Extension

Table 7: Correlations Between Seat Bottom Data

	Contact Area	Center of Pressure	Peak Pressure Index
Contact Area		-0.569999787	0.79325687
Center of Pressure			-0.176176429
Peak Pressure Index			

between the contact area and the peak pressure index, indicating that an increase in contact area causes an increase in peak pressures.

This data makes a case for not using Configuration 2, as the increased contact area is linked with increased peak pressures. This causes localized discomfort and large normal forces – a bad combination. The best configurations appear to be configurations 3 and 4, based only on the seat bottom data. Configuration 1 is not so bad, indicating that the dynamic footrest and seat bottom do not always cause poor results for seat bottom

interactions. Even so, the "bridging" that happens from a locked footrest seems to be an effective way to reduce forces and peak pressure on the seat bottom.

3.4.3.4 Seat Belt Forces

The seat belt sensor could not analyze any pressure readings, and could only look at the tensile forces in the seat belt. The force in the belt was analyzed at both the start of the thrust and the end of the thrust. This gave an upright, relaxed preload tension measurement, as well as the tension in the fully extended position. The preload forces are shown in Figure 68, and the forces at full extension are shown in Figure 69.

The preload data shows that allowing the user to set their own belt tightness gives a wide range of preloads. The preloads differ between configurations due to how the person was repositioned at the end of the previous thrust. Additionally, some

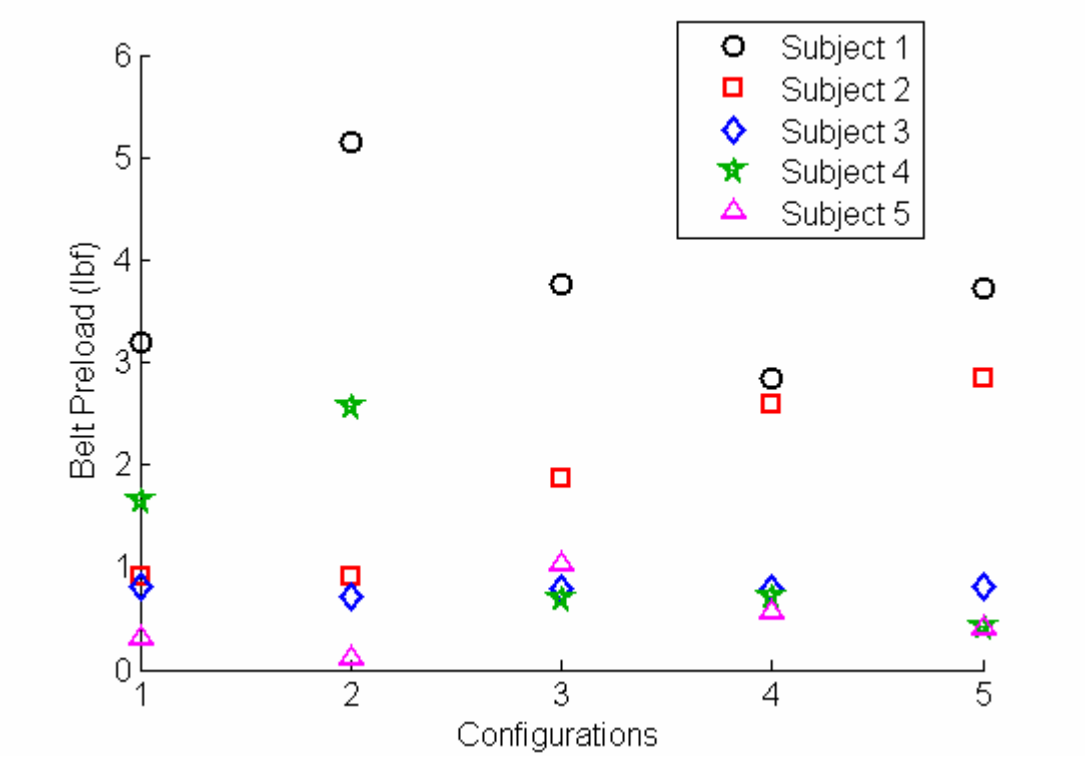

Figure 68: Seatbelt Preload Forces

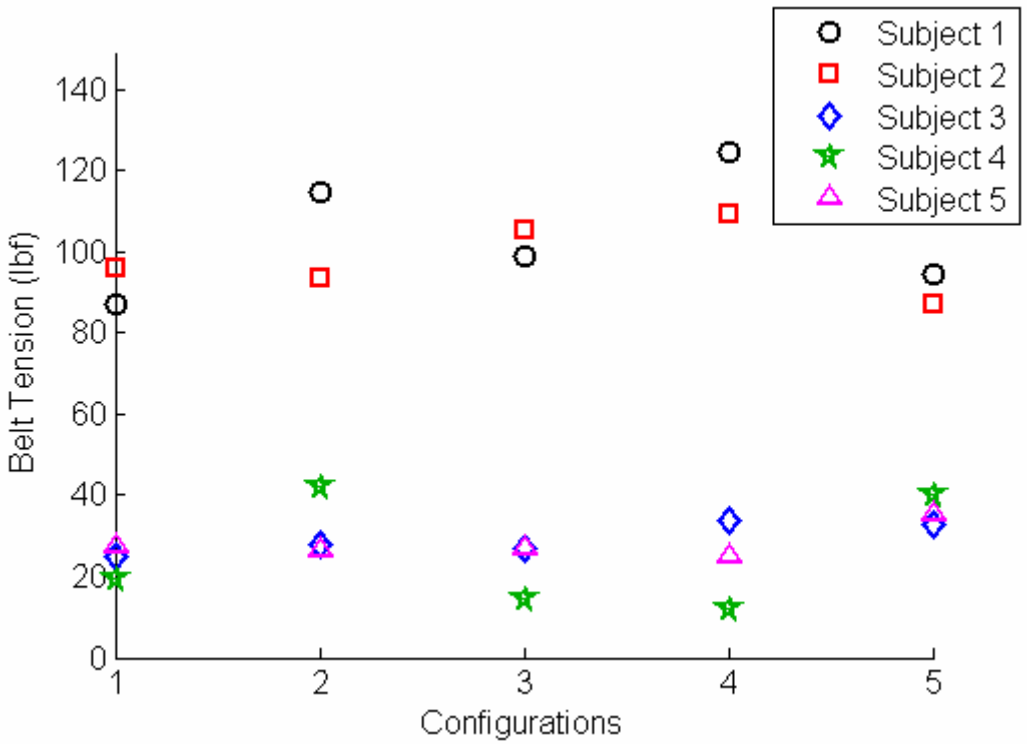

Figure 69: Seatbelt Tension Force in Full Extension

configuration changes required the user to come out of the chair while a component was adjusted. When the subject reattached the belt, they might have applied a different tension. In any case, it appears that the preload does not have a significant impact on the belt forces in full extension.

The seat belt tension measurements provide interesting results. For both Subjects 1 and 2, the belt forces were significantly and consistently higher than for the other subjects. This does not seem to be due to the higher preloads, as Subject 4 has a larger preload than Subject 2 in Configurations 1 and 2. Instead, the higher forces seem consistent with the higher forces seen previously in Figure 60 when examining the seat back normal forces. It appears that Subjects 1 and 2 were actually pushing harder during the extensor thrust, and this led to higher back forces and higher belt tension forces.

While the belt tension forces seem to lack any trends, a statistical analysis was done. The Tukey post-hoc comparison chart is given in Table 8, and shows a significant difference between Configuration 1 and Configurations 2 and 4. This indicates Configuration 1 is better than either of those configurations, but not necessarily any better than Configurations 3 and 5.

Table 8: Significant Differences Between Seatbelt Tension Forces

Configuration	1	2	3	4	5
1		.0466		.0798	
2					
3					
4					
5					

The seat belt data is interesting in that it has no major trends in the forces, indicating how strong a subject was pushing during a thrust, but not changing very significantly between configurations. This is an important finding because it means that the same forces are used to keep the pelvis constrained during an extensor thrust with minimal impact from the dynamic components. Thus, reducing interaction forces at the seat back and seat bottom will not cause the pelvis to become unconstrained. This is critical to the success of the dynamic seating system design as the pelvis must remain constrained for it to have any chance of being properly positioned in the seat at the end of the thrust.

3.4.3.5 Combined Force

One final analysis was done by combining the three sets of force data into a combined force reading (with the contribution in the seat back force due to gravity being eliminated). While each force interaction is important, a reduction in the total force is one of the goals of the dynamic seating system. The combined force results are shown in

Figure 70. A statistical analysis was performed to give an unbiased representation of significant differences in the data. A Tukey post-hoc comparison is given in Table 9, with the significant differences shown as nonblank entries.

The data indicates that the rigid mode (Config. 5) is significantly different than all other configurations, and has the highest total force. This is a powerful result because it shows that any of the combinations of dynamic components gives a lower total force during the thrust than with the rigid configuration. The data also indicates that Configurations 1 and 3 are not any different, and Configurations 2 and 4 are not any different, with the latter having a higher total force than the former. Thus, the lowest forces are achieved with either Configuration 1 or 3. Both of these configurations performed well when looking at the seat back, seat bottom, and seatbelt individually, and

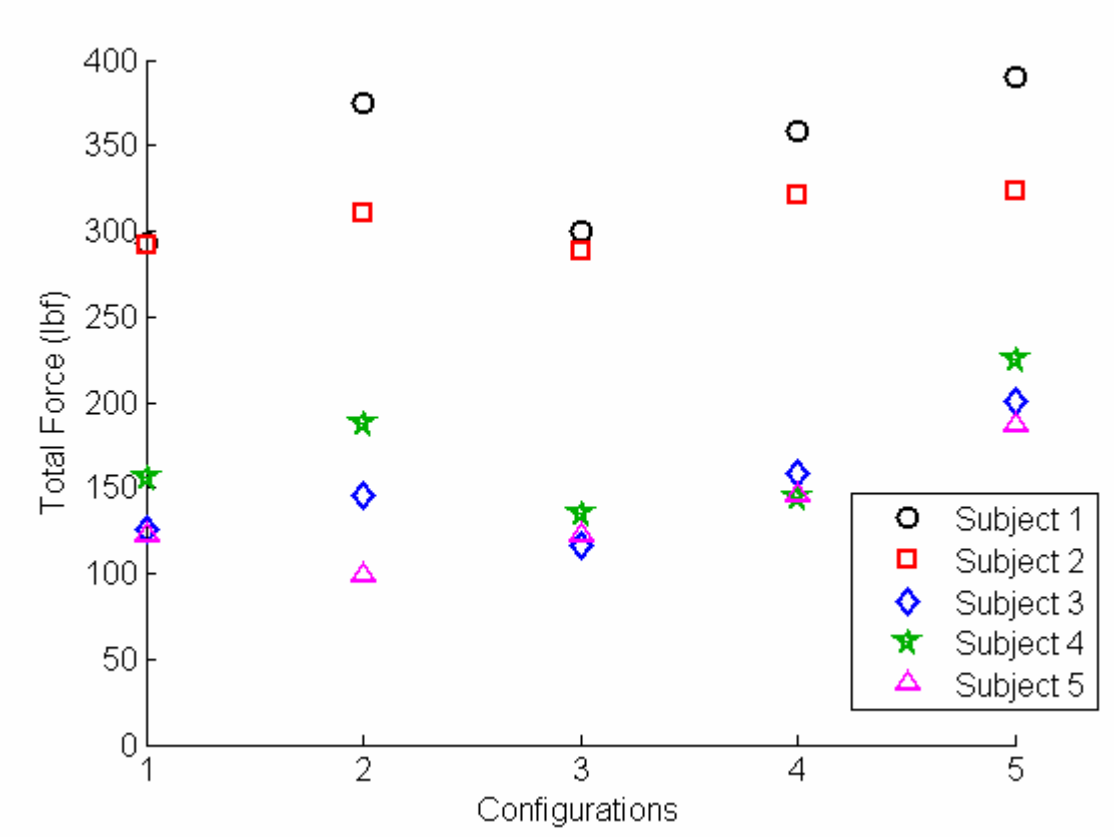

Figure 70: Combined Seat, Back, and Seatbelt Force in Full Extension

so they seem like good choices for best overall performance.

Table 9: Significant Differences Between Combined Interaction Forces

Configuration	1	2	3	4	5
1		.0067		.0030	.0000
2			.0012		.0001
3				.0005	.0000
4					.0001
5					

Table 10 shows the mean for all the total force readings for each configuration. This includes all the trials, not just the median. Also included is a percent reduction in force of a configuration over the rigid mode. As can be seen, Configurations 1 and 3 achieve roughly a 25% reduction in combined force over the rigid configuration.

Table 10: Combined Force Summary Comparison

Configuration	**Mean Total Force**	**Reduction in Force (from Rigid)**
1	197.49	24.994%
2	224.79	14.625%
3	193.37	26.558%
4	226.77	13.873%
5	263.3	-

3.5 Conclusion

The major design concept used in the advanced dynamic seating system was the variable stiffness concept. Two embodiments of this concept were used in the seat back and seat bottom. Each concept worked well, although both the seat back motor and the seat bottom actuator have weaknesses. The seat back motor is too weak to effectively drive the roller up the seat back with a teenager or young adult resting their weight against the seat back. As well, the complications due to the magnet holding system and

split washers indicate the motor should be changed to a power-off brake motor. The linear actuator for the seat bottom is strong enough to return the seat bottom to the upright position, but it is too slow for practical application. Its speed needs to be increased without decreasing the power output. Both of these changes will add to the overall cost of the system, but both are needed for the system to be effective.

Of the five configurations tested for reducing interaction forces, two were equally good. The first allows the seat back, seat bottom, and footrest to move dynamically during a thrust, with both the roller wheel and the flexure bar in their lowest positions. The other configuration allows the seat back to move dynamically, but locks out the seat bottom and footrest. The roller is also at its lowest position in this configuration. Both of these configurations give roughly a 25% reduction in total forces (seat back, seat bottom, and seatbelt) felt during a thrust as compared to the rigid configuration.

If the dynamic seat back alone is as effective as the seat back in combination with the dynamic seat bottom and footrest, then cost dictates that this is the only component that should be added to wheelchairs. This is a fair conclusion, and indicates that great benefit can be achieved with only a single dynamic component.

However, it may be that the particular type of dynamic seat bottom and footrest used in this investigation are not the best designs. Certainly, the current seat bottom moves too slowly. Therefore, different types of seat bottoms and foot rests should be designed and evaluated. Further investigation should be done into how these components can be improved to get an even better performance for the whole system. Having these extra components allows for a much greater amount of customization for the user needs, and has the potential to give better performance.

Certain other indicators might also show benefits from the fully dynamic system, such as the foot force. This was not investigated, but seems logical that the foot forces would be reduced when the footrest is dynamic, due to the decrease in "bridging", in which the feet are carrying a large amount of the weight of the body.

In summary, the dynamic seating system does effectively reduce interaction forces and pressures as compared to a rigid chair. This would lead to an improved user experience during the thrust, and less breakage of chairs and seating components.

CHAPTER 4

LOAD DISTRIBUTION IN STANDARD CONFIGURATIONS

Pressure relief is a major concern for those who experience extensor thrusts. Excessive pressure results from being belted into the wheelchair to help maintain posture and avoid the chance of sliding out of the chair during a thrust episode. While previous chapters have dealt with seating systems designed to improve comfort during the extensor thrust, they have not eliminated the need for restraints. As periodic pressure relief is needed to avoid the formation of pressure ulcers, intervention from caregivers is required throughout the day. While some users, such as those with paraplegia, might be able to reposition themselves and keep to a schedule for posture adjustments, many who experience extensor thrusts lack the muscle strength and control to reposition themselves.

One technological advance that has decreased the need for human intervention in pressure relief is powered wheelchairs. In addition to having motors and actuators that drive the wheels, power chairs can also contain motors and actuators that reposition the user by way of a joystick or other control interface. This adds to the freedom of the user and caregiver as those without the strength or muscle control to position themselves can now effectively accomplish that task with the aid of their powered positioning system on the wheelchair.

The standard configurations for pressure relief are tilt-in-space, recline, and standing, shown schematically in Figure 71. Each of these methods changes the load distribution by changing the angles of the seating components. The weight that is normally carried by the buttocks and the feet in a standard seated posture is shifted to other body parts. In the case of tilt, the weight is shifted onto the user's back, and the

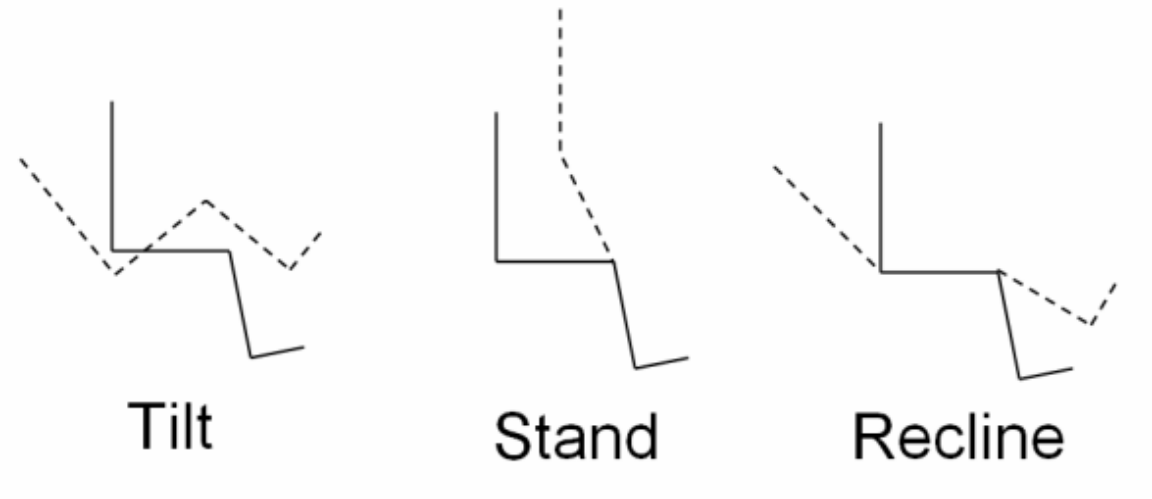

Figure 71: Schematic of Tilt, Recline, and Stand Positions

head carries its own weight. Recline has a similar shifting of the weight as the user is brought into a horizontal position. Standing unloads the buttocks, but increases the loading on the feet, while also loading the knees by means of a knee strap.

Many studies have been done on the effectiveness of these methods [26], [27], [28], [29]. While indicating that they are effective, no study has been done that compares the three methods against each other using a single seating platform. This is an important study because it can affect government policies regarding the distribution of healthcare funds based on the effectiveness of these methods to relieve pressure. Currently, tilt-in-space and recline are accepted by the government as effective means of pressure relief, but standing is not, thereby limiting the funding for wheelchairs with standing functionality. Many in the medical world, however, feel that standing is an effective form of pressure relief, and also see added benefits from a standing chair in the area of social interaction and functional activities in public facilities, where items are often situated to be within the reach of a standing individual.

This chapter seeks to perform a comparative study of the methods of tilt, recline, and standing. The forces at the head (tilt and recline), knee (standing), seat back, seat bottom, and footrest will be measured and compared for different angled positions of tilt, recline, and stand. The positions will range from an upright position to 55° of tilt, 180° of recline, and 75° of stand. These measurements will be taken using a Levo Combi wheelchair, which is shown in Figure 72.

The Levo wheelchair has recline and standing capabilities, but lacks tilting abilities. Therefore, to perform the comparative experiments with a single chair, a tilting mechanism was designed and built with the help of Lingua Kong and Jon Jowers at CATEA.

A computer model was also developed to add to the knowledge gained during these experiments. This was done as the first part of a larger study at CATEA that will eventually take experimental data from a much larger group of participants. They will use the same setup for the tilt, recline, and standing measurements that is developed in this chapter.

Figure 72: Levo Combi Wheelchair

4.1 Levo Wheelchair

The Levo Combi wheelchair was chosen because of its ability to recline and stand. Tilting can be accomplished by means of a mechanism that tilts the entire chair, but recline and standing are functions of the seating surfaces of the wheelchair itself, and so cannot be recreated externally to the wheelchair. Some items of note on the wheelchair include a seat depth adjustment. This is very important for standing as the user's knee joint is assumed to be in a specific location relative to the moving components. If not properly adjusted, this can lead to incorrect standing posture and improper loading of the knee.

Another important feature is the footrest, which unfortunately does not support the entire foot. An extended footplate was constructed from plywood to allow a more accurate force reading under the foot. Force measurements need to be taken behind the head, specifically during tilt and recline. To accommodate different subjects, a headrest was fabricated which allows both vertical and horizontal adjustments. This allows the headrest to be positioned directly behind the head during an upright, seated configuration. Finally, the knee block is a noteworthy feature. This must be attached during standing to allow the knee to help support the person's body. During standing, the force on the knee is determined by measuring the force at the knee block.

To see the versatility of the Levo Combi, Figure 73 demonstrates the available positions of the seating system. As can be seen, the two main functions are standing and reclining. Other options include lift, of use when working at desks of different heights, as well as a minor amount of tilt. The published amount of tilt capable of the Combi is 15°, which is not enough for this study. The tilt is also difficult to achieve, as the tilt

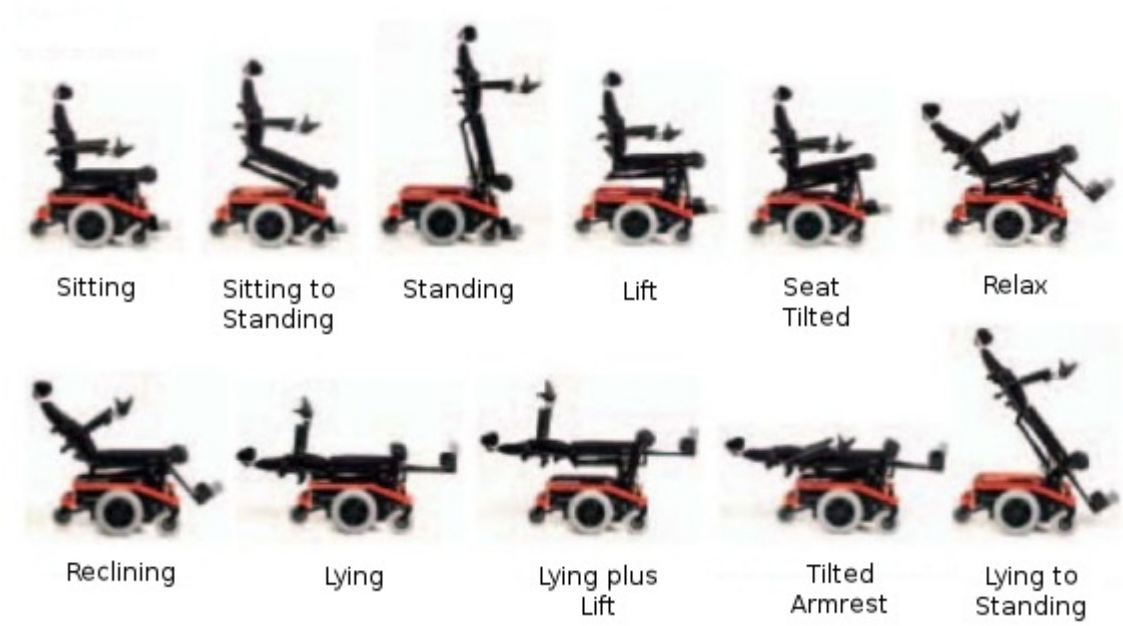

Figure 73: Levo Combi Wheelchair Positions

configuration must be maneuvered into by way of adjusting the relative amounts of stand, recline, and lift of the chair.

4.2 Tilt Mechanism

Given that the amount of tilt the Combi is capable of is inadequate for the study, a tilt mechanism was constructed. This was a significant challenge, as the system needs to tilt a 350 lb. chair (including the weight of the batteries) and a 200 lb. person to 55°. In addition to these requirements, the mechanism needs to be transportable, as future studies will take place at the Shepherd Center, and not in CATEA's laboratory. The system also must be operable by two technicians, both to tilt the subject and to record the data at various angles. Two mechanisms were designed and built, with the second replacing the first due to inadequacies in the operation of the first mechanism.

4.2.1 Tilting Ramp

The first design was accomplished by attaching two wooden platforms together with 120° of angle between them. A support brace helped to support the bending moment. The wheelchair was mounted to one of the platforms, and the whole system was tilted by hand to various angles. A schematic of this design is shown in Figure 74. This platform was successfully used to obtain experimental data from two test subjects for use in a preliminary study of tilt, recline, and standing, done in conjunction with this project [30].

Several problems exist with this design. First, it is not effectively operated by a team of two technicians. Even with a roughly 2-to-1 lifting ratio, it still leaves 138 lbs. for each to lift. Furthermore, it is difficult fix the ramp at a certain angle by placing blocks under it while simultaneously supporting the load. Due to these limitations, this mechanism was dismantled, and a new tilting mechanism was designed and constructed.

Figure 74: Schematic of Tilting Ramp Platform

4.2.2 Overhead Winch Design

The second tilt mechanism was designed using an overhead winch mounted to a frame. The platform is tilted using cables and pulleys. The finished mechanism is shown in Figure 75. This design was chosen because of its robust construction, along with the relatively inexpensive cost of an overhead winch. The overhead winch has the benefit of being able to lift the large load required and also hold it at various angles without consuming power. A 2-D schematic of the design is shown in Figure 76.

The largest component of the design is the support frame. Two identical frames are located on either side of the tilting platform. Each is constructed of 4x4's, bolted

Figure 75: Overhead Winch Tilt Mechanism

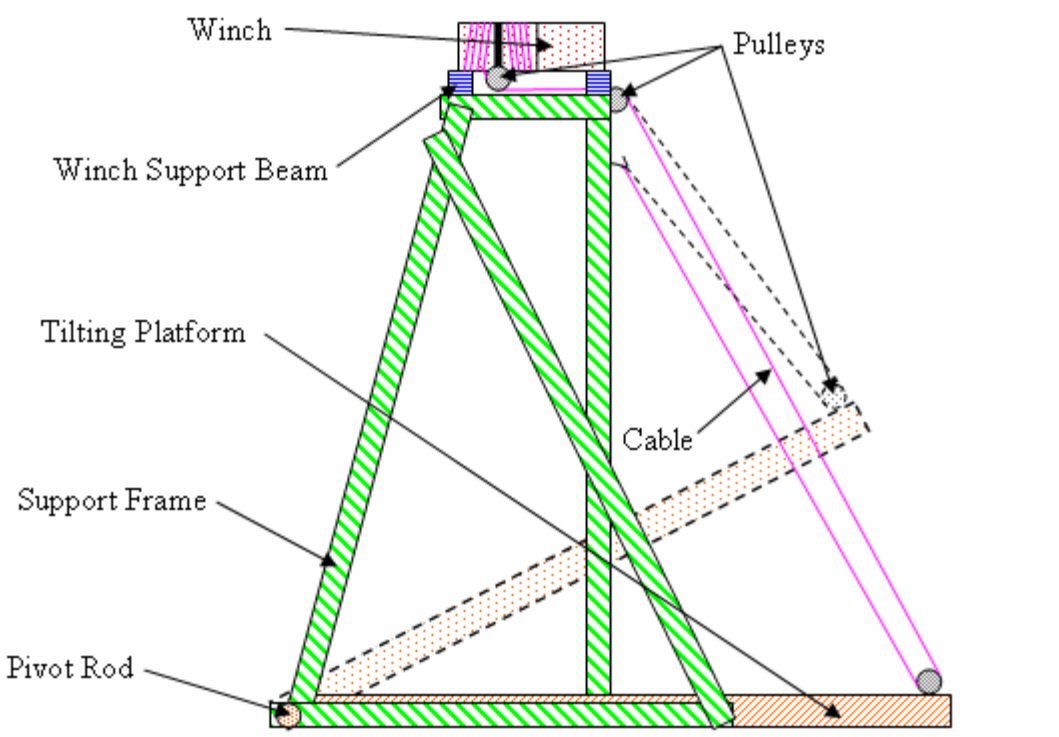

Figure 76: Schematic of Overhead Winch Mechanism

together with carriage colts. The base of the support frame is wider than the top to keep the system stable when tilting begins.

The tilting platform attaches to the support frame by way of a pivot rod, which is mounted into both support frames. The tilt platform is constructed of 2x4's overlaid with a sheet of plywood. This construction allows the platform to withstand the large bending loads during tilting.

The overhead winch, shown in Figure 77, is supported by two winch support beams, each of which spans the support frame. This allows the winch to stay roughly centered over the wide base supports, minimizing the potential for tipping caused by the top-heavy load of the winch location. The winch lifts the tilting platform using cables and pulleys. To keep the platform level during tilting, two cables are attached to the platform, one on each of the front edges. As the winch turns, both cables spool simultaneously, keeping

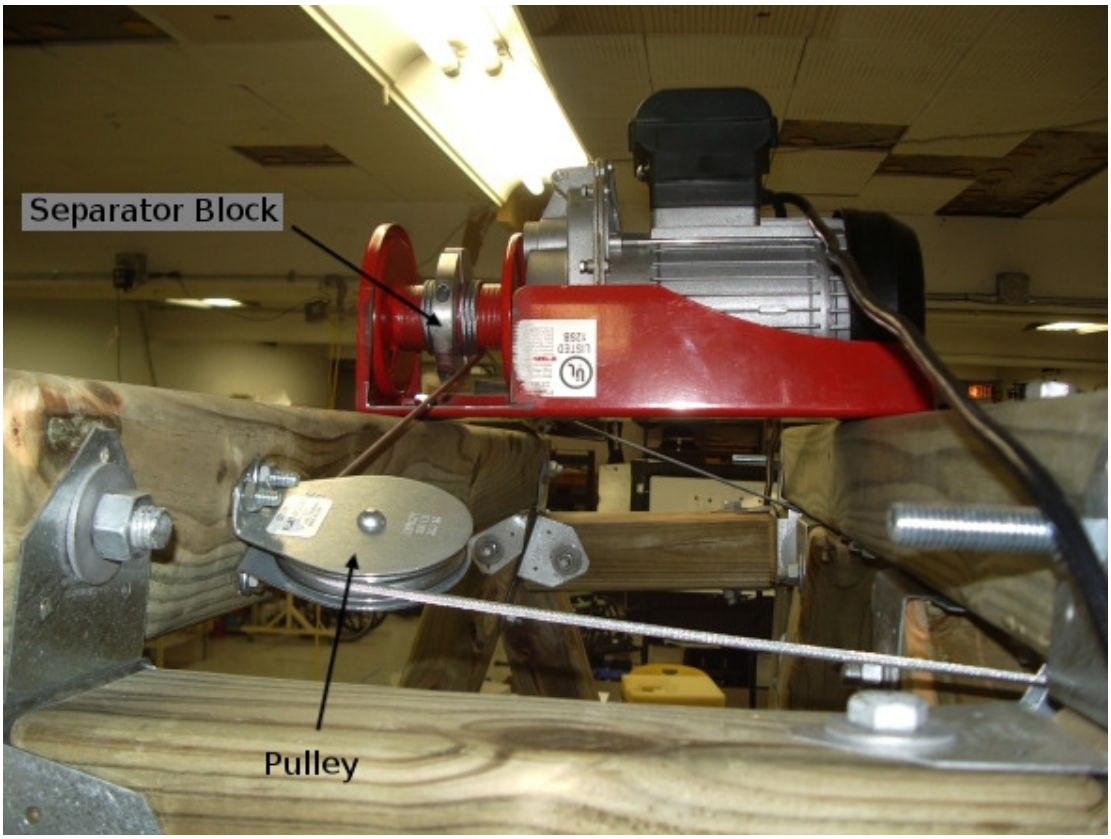

Figure 77: Overhead Winch with Separator Block

the front edge of the platform level. A separating block is fixed to the winch spool to keep the two cables from interfering with each other. This separating block also has two helical grooves cut in its interior surface, allowing it to clamp the ends of the cables. This lets the cables begin spooling from the separator block outwards, and helps maintain proper spooling.

The overhead winch is operated with a two-button pendant, hanging from the side of the support frame. When a button is not pressed, the auto-brake engages and stops the winch. The auto-brake functions without power as a safety feature.

A final component of the tilt mechanism is a removable ramp, shown in Figure 78. This allows the wheelchair to drive onto the tilt platform. This is not used during the experimental protocol, and so is designed as a detached component.

Besides the requirement to lift a 200 lb. person sitting in a 350 lb. chair, the tilt mechanism is also required to be transportable. As this tilt mechanism is quite large, it is designed to be easily dismantled into major components for transportation. The ramp is obviously easy to transport on its own, but the use of carriage bolts to assemble the system makes dismantling major components quite easy. First, the pulleys are removed from the front edge of the tilting platform (see Figure 78). The tilting platform is then pulled off the pivot rod. The flexibility of the support frame allows the base to the widened, and the pivot rod to be removed. Next, the four bolts holding the winch support beams are removed. The winch, pulleys, and cables are all attached together with the support beams, and are transported as one unit. This leaves the two support frames, which do not need to be further dismantled to transport.

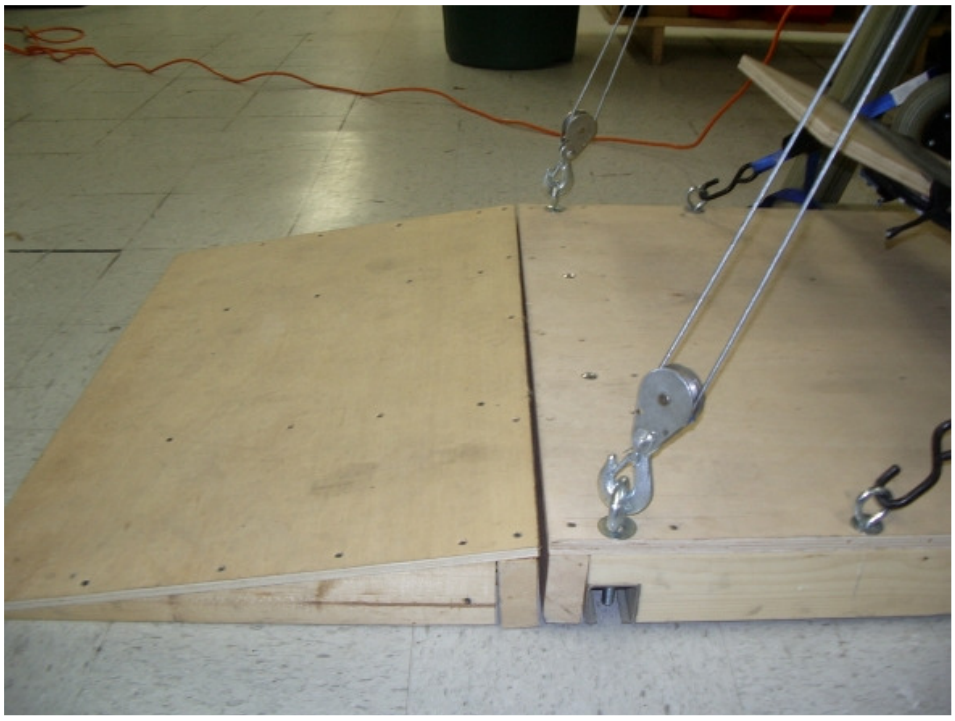

Figure 78: Removable Ramp for Tilt Platform

4.3 Wheelchair Mountings

The three methods of tilt, recline, and standing each require different mounting configurations. While recline and standing can be done separate from the tilt mechanism, it is desirable to allow all three to occur while the wheelchair is on the tilting platform to reduce the length of time needed to collect the data. As tilt is the hardest to accomplish, its requirements are the primary design objectives.

Tilt requires two main mounting components: a wheel block to stop the wheelchair from sliding down the platform as it tilts, and a tie-down on the front casters to keep the wheelchair from tipping backwards. These two components are shown in Figure 79. The wheel block is shaped to have two points of contact with the wheel. The tie-downs are

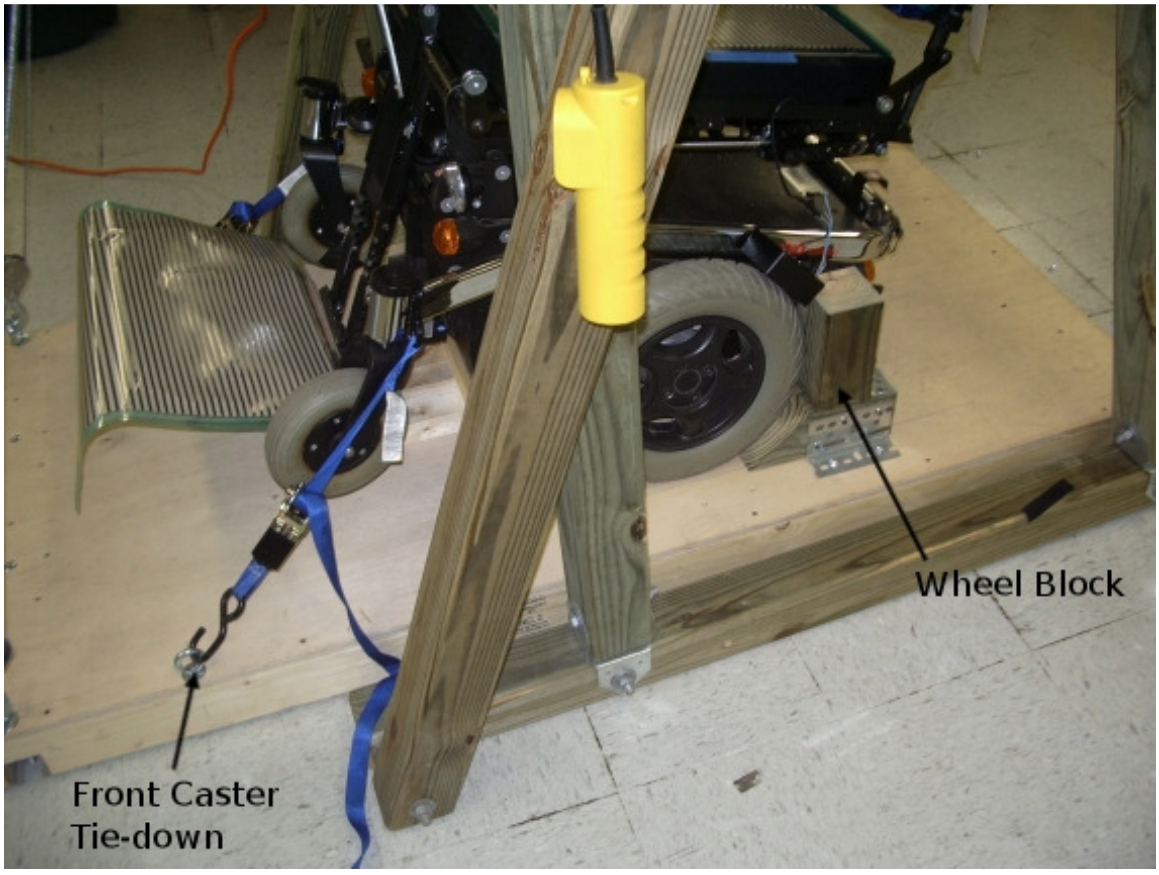

Figure 79: Wheel Block and Front Caster Tie-down

tightened separately for each caster and attached to eye-hooks on the platform.

The wheel blocks are placed a foot and a half from the pivot rod to help the center of mass of the wheelchair stay in front of the point of rotation. This is necessary because the cables would be unable to stop the platform from rotating backwards if the center of mass of the system moved behind the point of rotation.

To help keep the angle of the platform lower while still allowing large angles of tilt for the wheelchair, a 15 degree tilting block was incorporated into the design as seen in Figure 80. This block gives the wheelchair an initial 15 degrees of tilt. The tie-downs function to keep the tilt block sandwiched between the wheelchair and the tilting platform. This simple addition to the design helps to keep the angles of the platform lower, ensuring that the system remains stable at all times. It also adds to the comfort of the user as sitting in a wheelchair on a platform tilted beyond 45° is somewhat frightening. This position is shown in Figure 81, where a subject is sitting in the pre-

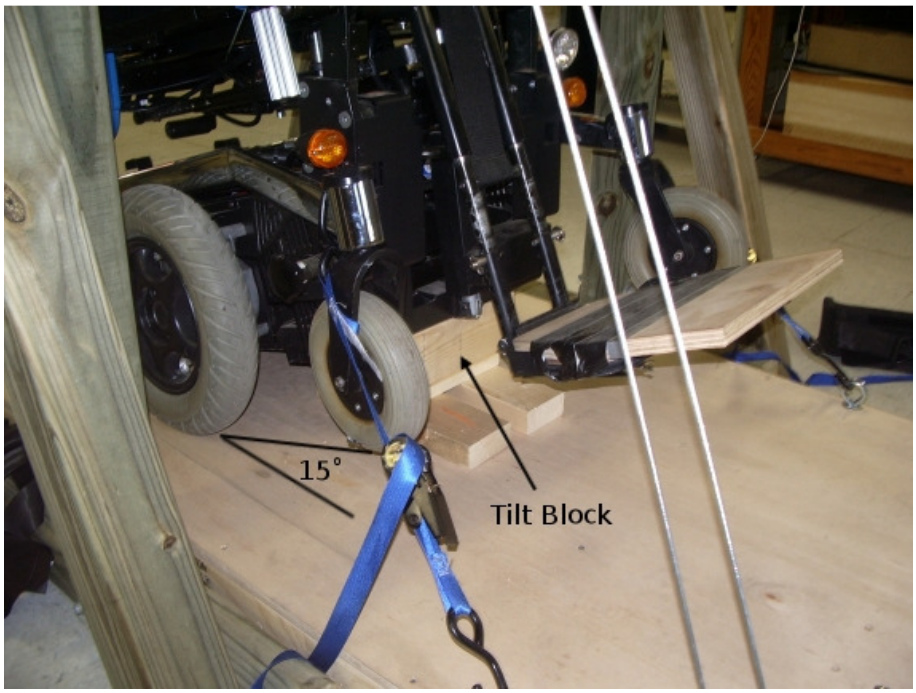

Figure 80: 15 degree Tilting Block

Figure 81: Subject in Chair with Platform tilted to 35 degrees

tilted chair with the platform tilted to 35°. This amounts to 50° of total tilt. Even at this angle, the user can easily feel dangerously close to tipping over.

The next configuration to consider is recline. Because this is a normal function of the wheelchair, the wheel blocks and caster tie-downs theoretically should not be needed. Unfortunately, to allow for the initial 15° of tilt, the rear caster was removed because it impeded the chair from tilting. This rear caster provided the support needed during large angles of recline to keep the wheelchair from tipping. Given that it was removed to accomplish tilt, a recline block is needed to keep the wheelchair from tipping. This is shown in Figure 82. The wheelchair in reclining position is shown in Figure 83.

The final wheelchair configuration is standing. The only potential issue in this configuration is the possibility of the headrest striking the winch support beams as the

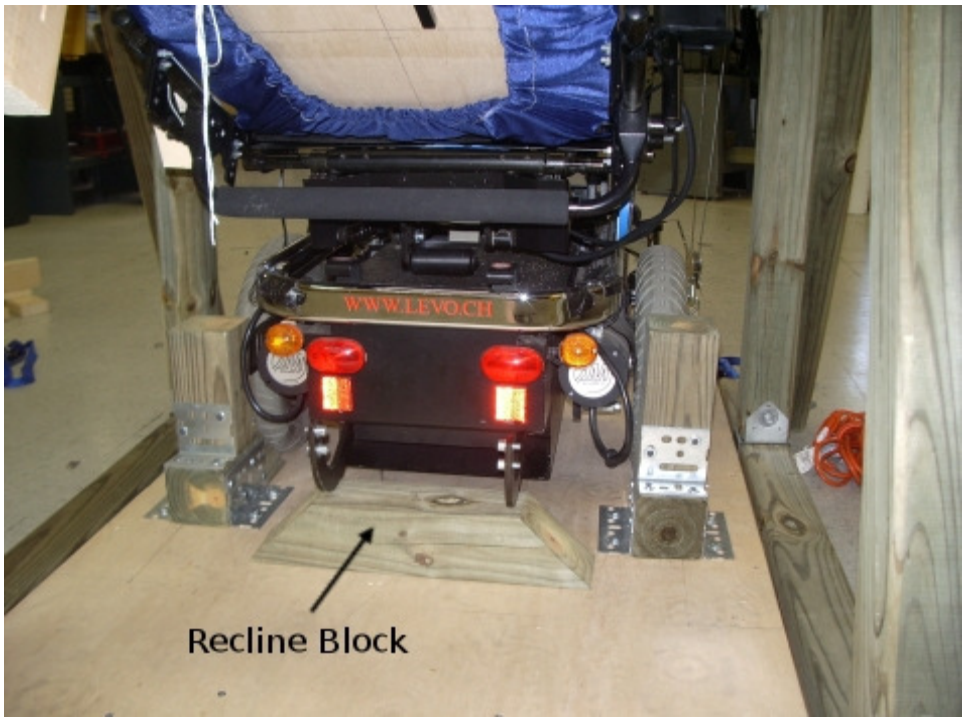

Figure 82: Anti-tip Block During Recline

Figure 83: Levo Wheelchair in Recline Position on Tilt Platform

height of the chair increases, as seen in Figure 84. To alleviate this, the wheelchair must be driven forward to the edge of the platform before attempting standing. No tipping issues are present for standing because the center of mass of the person and wheelchair remains between the drive wheels and the front casters.

4.4 Methodology

A specific protocol is used to ensure that the data collected during the study is accurate. First, the Levo Wheelchair is instrumented with four Tekscan pressure mats to collect data at various angles of tilt, recline, and standing. These pressure mats are calibrated each week, and the calibration is checked before each test subject to ensure

Figure 84: Levo Wheelchair in Standing Configuration

that the readings are accurate.

The configuration angles for data collection are listed in Table 11. The order in which data is taken is randomized for each subject. The configuration (tilt, recline, and standing) is first randomized, and then the necessary angles are randomized within each configuration. This randomization eliminates the possibility of erroneous trends due to sensor drift or other causes.

Along with randomizing the data points, the pressure mats are also checked to ensure a proper calibration. Additionally, the person is weighed and measured. The measurements are used to size the seat depth and adjust the headrest. The subject can then be positioned in the Levo wheelchair, with the pressure mats at the appropriate position for the first configuration. For tilt and recline, a pressure mat is placed behind the head. For standing, that pressure mat is removed and placed under the knee strap. A lap belt and chest belt are then secured around the person, and the subject's arms are positioned across his or her chest.

The wheelchair is then moved to the appropriate angle according to the predetermined order, and the subject relaxes in that position for one minute. After one minute, the pressure plots from the mats are recorded using Tekscan's BPMS software.

Two key issues in the use of pressure mats that had to be dealt with were the

Table 11: Angles for Data Collection

Tilt	Recline	Standing
0°	100°	0°
15°	120°	20°
25°	140°	40°
40°	160°	60°
55°	180°	75°

phenomena of creep and hysteresis. In the case of hysteresis, the pressure reading is dependent on whether the pressure reading started under the current pressure and built up to it, or whether the pressure started above the current pressure and dropped down to it. The best way to deal with this would be to unload the pressure mats after each reading, adjust the chair to the proper orientation, and transfer the subject into the chair. The challenge with this is that the wheelchair might be in any degree of tilt or recline. For the case of standing, it would be nearly impossible to properly strap someone into a standing position of the wheelchair.

Because unloading after each configuration angle is not practical, hysteresis will inevitably exist in the readings, especially in the readings of the seat bottom, which will have a larger amount of pressure in the upright sitting configuration, and hopefully a lower pressure at other positions. One way to help remove any trends in the data due to the hysteresis is to randomize the data, which was done. As well, the mats are calibrated with a routine that attempts to minimize both hysteresis and creep.

Creep is a phenomenon that causes the pressure reading to continue to increase at a slow, steady rate with a constant weight on the mat. The original protocol to be used in the experiments called for a full unloading of each mat after every data point.

While feasible to do, this adds a great deal of extra work and time to the experimental protocol. Several tests were performed to see the actual effect of creep in the mats and the effect of unloading the mats. These were performed to determine if an unloading procedure is necessary to counteract creep in the mats.

Two tests were done with an effort to mimic the actual situation in subject testing. Both tests placed a known weight on a flat mat, separated by a piece of 2” foam to help

distribute the weight. Readings were taken at one minute intervals. Each test used a different weight to see what effects different weights have on creep.

During a subject test without unloading, the mats would feel the load from the person for approximately six minutes total for a given configuration (tilt, recline, or standing). This allows for five different angles, with a one minute holding time at each angle, and time to move the wheelchair between angles. To see the effects of creep, we need to compare the reading at one minute with the reading at six minutes. To see the effect of taking longer than expected during the testing, the load was left on the mat for eleven minutes. The results are shown in Table 12.

Table 12: Mat Reading for Creep Study

	75 lbs Load		*145 lbs Load*	
Time (min)	**Load Reading**	**Percent Increase**	**Load Reading**	**Percent Increase**
1	74.44446	-	144.259	-
2	77.06088	3.5146	146.078	1.2609
3	77.71384	4.3917	146.9765	1.8837
4	78.36627	5.2681	147.8677	2.5016
5	79.82562	7.2284	148.7959	3.145
6	80.97003	8.7657	149.1299	3.3765
7	81.48951	9.4635	149.4367	3.5892
8	81.96961	10.1084	149.6378	3.7286
9	82.26785	10.509	150.1087	4.055
10	82.54002	10.8746	150.4995	4.3259
11	82.86384	11.3096	151.3632	4.9246

As can be seen, the reading does increase as time progresses, but it appears to level off after a few minutes. Even so, the difference between the reading at one minute and the reading at six minutes is less than 10% for the 75 lbs load. The readings for the 145 lbs load appear better, showing less than a 5% increase, even after eleven minutes.

While this will introduce slight errors in the readings, this is acceptable because randomization of the positions will reduce any trends that would be caused by the creep.

As well, this is a worst-case scenario. In reality, for different angles, the forces are less than the maximum reading, so the creep will affect the readings less. For these reasons, the protocol was modified to only unload the mats between configurations (i.e. between tilt and standing), and not between individual angles of data within each configuration.

4.5 Modeling

A model of a person in the tilt, recline, and stand configurations was developed in conjunction with the data collection on the actual wheelchair. A screen shot of the model in a tilt configuration is shown in Figure 85. The software used to create the simulated person and configurable seating platform was Working Model® 2D.

Working Model is a commercial package that allows for the creating of complex

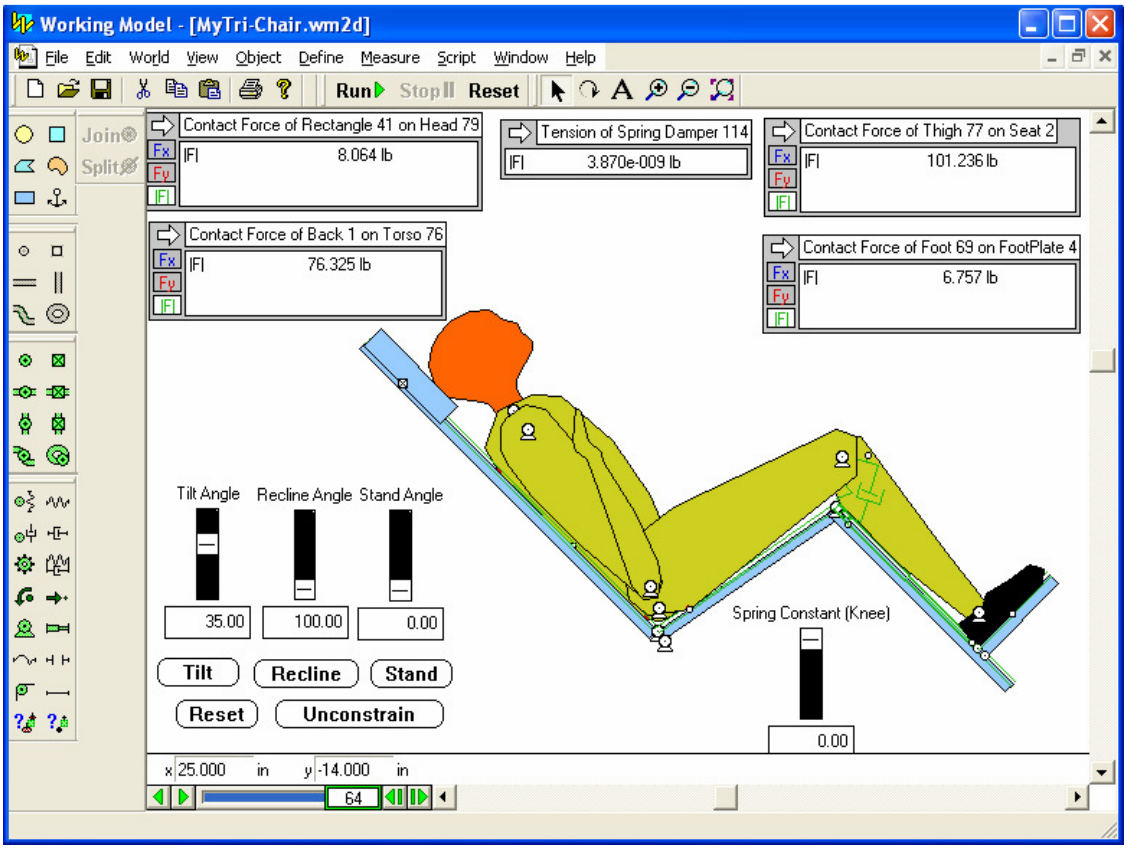

Figure 85: Simulated Tilt Configuration using Working Model 2D

shapes and dynamic interactions through the use of constraints such as pins, slots, and friction. The software uses fixed geometry of bodies and treats all bodies as rigid. However, the properties used to evaluate the dynamic interactions between bodies can be highly customized. The coefficient of friction between bodies, the mass, and the location of the center of mass can all be changed.

To construct a person for the model, polygons were created that approximate the shape of each body segment. In particular, segments were created for the head, trunk, upper arm, forearm and hand, thigh and pelvis, shank, and feet. As the software is only a two-dimensional representation of the body, the weight of both feet were included in the foot. The same is true for the shank, thigh, and arm. The body joints were modeled as frictionless pin joints, with connections at the neck, hip, knee, and ankle joints. The shoulder and elbow were kept fixed.

Geometry plays an important role in the model, as the fixed geometry and rigid body representation does not allow for the accurate modeling of the flexible spine or soft tissue deformation. As well, all interactions between the person and the seat were modeled using friction. Because of this, the location of edges on the bodies was critical. After several tries to find a suitable setup, the back was modeled as a flat surface to allow for full contact with the seat back in tilt. The feet were also modeled with a flat surface for full contact at the footrest. The thighs could only make point contact with the seat bottom due to kinematical relationships as the chair moves through positions of recline and stand. The best location for this point interaction was chosen to be the approximate location of the ischial tuberosities.

The software allows for the display of contact forces between bodies. This allows the extraction of normal forces at the head, back, seat, and feet. For the forces felt at the knee block in standing, a spring was used. The tension in this spring shows the forces supported by the knee block. The configuration of the simulated seat can be easily changed to different angles of tilt, recline, and stand by moving slider bars. The spring constant is also changed to remove its effects during tilt and recline.

The body parameters chosen for the simulated person are shown in Table 13. These numbers come from the average body segment masses for a male given by de Leva [24]. These are used to represent the subjects in the test, all of whom are able-bodied.

Table 13: Body Segment Parameters in Person Model

Body Segment	Percent Body Weight
Head&Neck	6.94
Trunk	43.46
Upper Arm	5.42
Forearm&Hand	4.46
Thigh	28.32
Shank	8.66
Feet	2.74

To predict the pressure relief that would be gained by someone with a spinal-cord injury, these parameters could be changed to reflect the changes in the body mass parameters. These parameters obviously depend on the type of injury sustained. For someone with the full use of his or her upper body, the upper body segments will become more developed through propulsion activities. For someone who cannot propel himself or herself, the distribution will be quite different. Fortunately, the model allows for the prediction of pressure relief for any type of body parameter distribution.

One last note about the model needs to be made. Because the interaction between the person and chair is modeled with friction, the issue of static indeterminacy is critical.

Even though the software runs a dynamic simulation, the wheelchair stays in a fixed position while any transient effects die out. This leaves a static response. For several interconnected rigid bodies all making friction contact with the chair, this leads to a statically indeterminate problem. Working Model handles this situation by ignoring enough of the interactions to regain static determinacy. Unfortunately, this is equivalent to treating some of the seating surfaces as frictionless. While this is needed for the mathematics, it does not accurately reflect the reality of the pressure relief configuration, due to the use of foam mats and other conditions where friction is very important to the interactions.

One way to overcome this limitation in the software would be to include deformation of the bodies. This eliminates the indeterminacy, but unfortunately, requires a finite-element analysis. Working Model is not setup to do this, and so the model will not fully reflect reality. Still, it provides a useful analysis of the experimental data, in which trends can be analyzed. Discrepancies will be explained in terms of why the software is predicting a certain outcome based on its assumptions.

4.6 Results

The ultimate goal of this study is to accumulate experimental data for many subjects in order reach a high confidence level in the results. Those with spinal-cord injuries, as well as able-bodied subjects, will be included in this study. For this thesis, however, only the first five tests have been completed, along with a preliminary model.

Data was collected from the four pressure mats and converted to a percentage of the total body weight of the test subject. The data for tilt, recline, and stand configurations

are tabulated in Appendix E. The results are also shown graphically in the following pages for each of the five test subjects, along with the simulated results from the model. The legend for which line on the graph corresponds to which test or simulated subject is given in Table 14.

Table 14: Legend for Pressure Relief Data

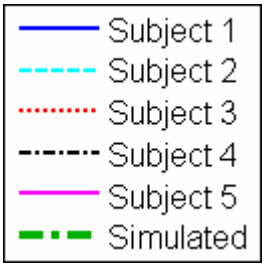

4.6.1 Tilt Results

The data for the tilt configuration is shown in Figure 86. This graph has four subplots within it, detailing the data for the head, back, seat, and feet. This allows for a better comparison of how each of the forces is changed as the tilt angle increases.

As can be seen, the head and feet readings are quite low compared to the seat and back forces, which is expected. As well, we see the trend that the seat is carrying the majority of the weight of the person in the upright position, and that weight transfers to the back as the tilt angle increases.

It is interesting to note that the experimental data is tightly bunched, even though the test subjects have varying heights and weights. This shows a consistency in how the body's weight is distributed in different seated postures, regardless of weight or height.

The simulation data, however, does not agree with the experimental data in two specific regards. First, the seat force is too high in the upright configuration. This is due to the rigid body approximation in the model. A test was done in which a person sat

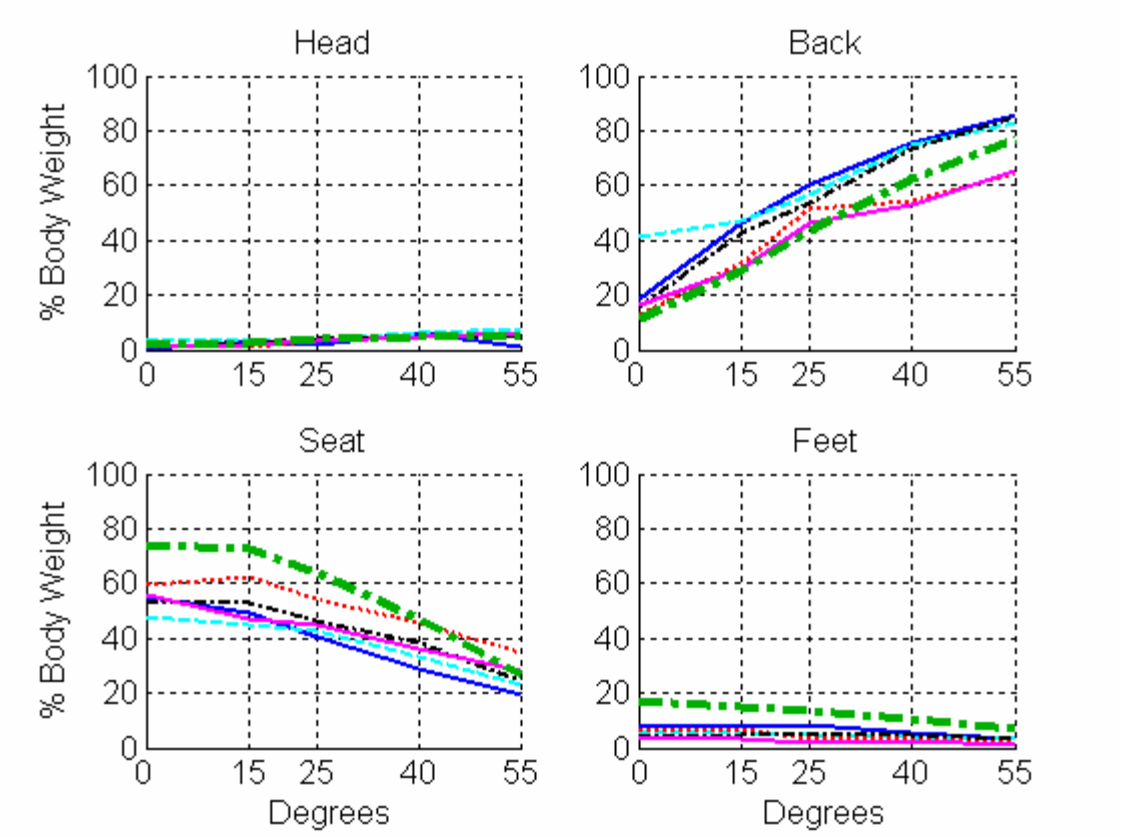

Figure 86: Experimental and Simulated Forces in Tilt

upright without leaning against the seat back of the chair. In this posture, the seat force was measured between 78 to 80 percent of the body weight (%BW).

The model assumes that the back is kept rigid, and does not allow for "slouching" in the seat. With the starting seat-to-back angle at 100° in the upright configuration, the model predicts that the majority of the weight of the upper body is carried by the seat bottom. The model accurately predicts the seat load in the situation when a person keeps his back rigid, giving a seat load of around 75%BW. The model is predicting the rigid spine situation correctly, but most people do not keep their back rigid when they sit in a chair and relax.

The second area in which the model does not agree with the experimental data is that it predicts a foot force which is too high throughout the tilting process. This problem

stems from the need to model the thighs and pelvis as a single body with a point contact on the seat bottom. Because the weight of the thighs is not distributed across the seat bottom through soft-tissue interaction, the model predicts that some of the weight of the thighs is transferred to the feet.

Two modifications could be made to the model to attempt to alleviate this discrepancy. First, the location of the center of mass could be adjusted. This would simply redistribute the weight from the front of the thighs closer to the point contact, allowing the seat bottom to absorb more of the weight. The other method would be to adjust the contact point on the seat. This would affect the configuration of the user in different angles of recline and stand, and would therefore need to be done with great care, as it could lead to unexpected consequences.

Even with the discrepancies, the model does follow similar trends with the experimental data, giving confidence that the data collected is an accurate representation of the true force distribution during tilt.

Another comparison was done by examining the sum of the four force readings and converting it to a percent of the total body weight. This is shown in Figure 87. As can be seen, the simulated forces have a larger sum in the upright configuration due to the problems mentioned earlier.

The fact that the sum of the forces exceeds the total body weight is not a cause for concern in the data. If one considers a block resting in the corner of a upright box, the total weight will be felt on the bottom panel of the box. If the box is tilted 45°, however, the two panels in contact with the block will each register a normal force equal to the weight of the block multiplied by the cosine of 45°. Summing these two readings gives

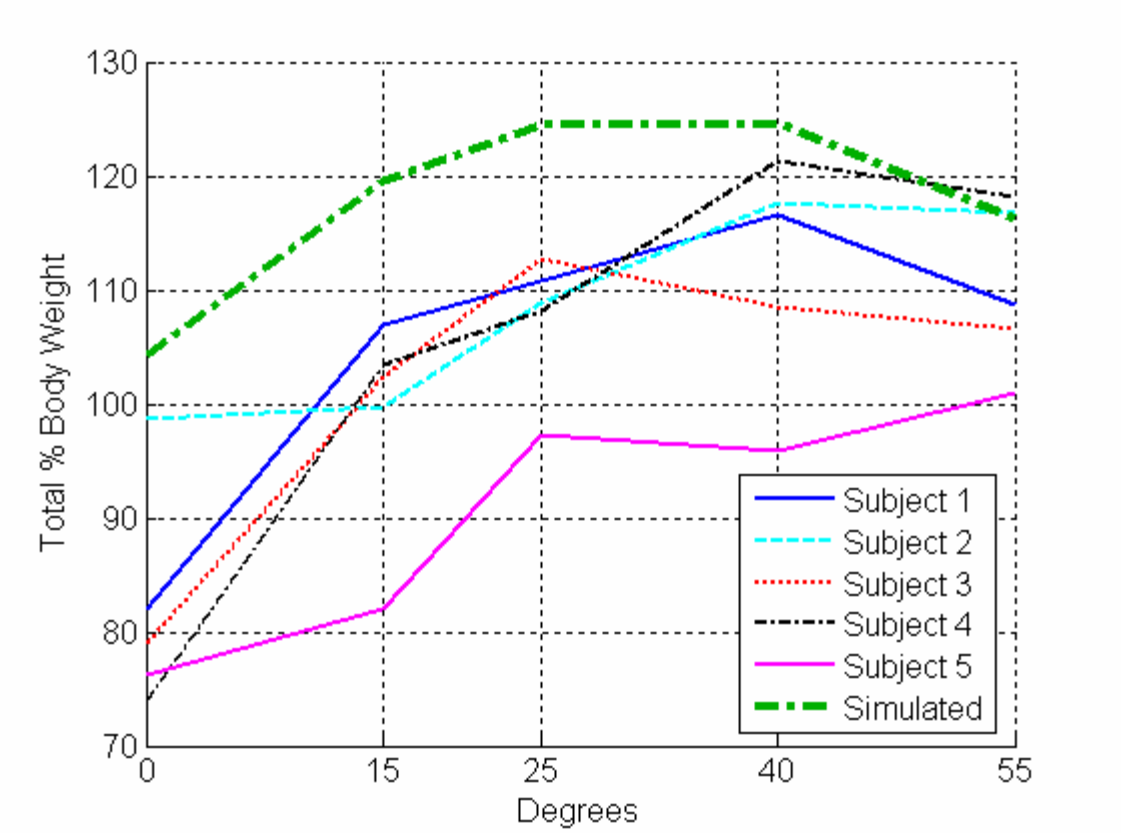

Figure 87: Sum of Forces in Tilt

141%BW reading because the normal force readings are not inline with gravity. Thus, having a combined force reading greater than the body weight is not an error, but is expected in the tilt configuration.

4.6.2 Recline Results

After analyzing the force in tilt, we looked at the experimental and simulated forces in recline. These are shown in Figure 88. The experimental data follow trends similar to those seen in tilt, with the head and feet forces remaining low. The seat force starts high, and then decreases, while the back force increases at large angles of recline.

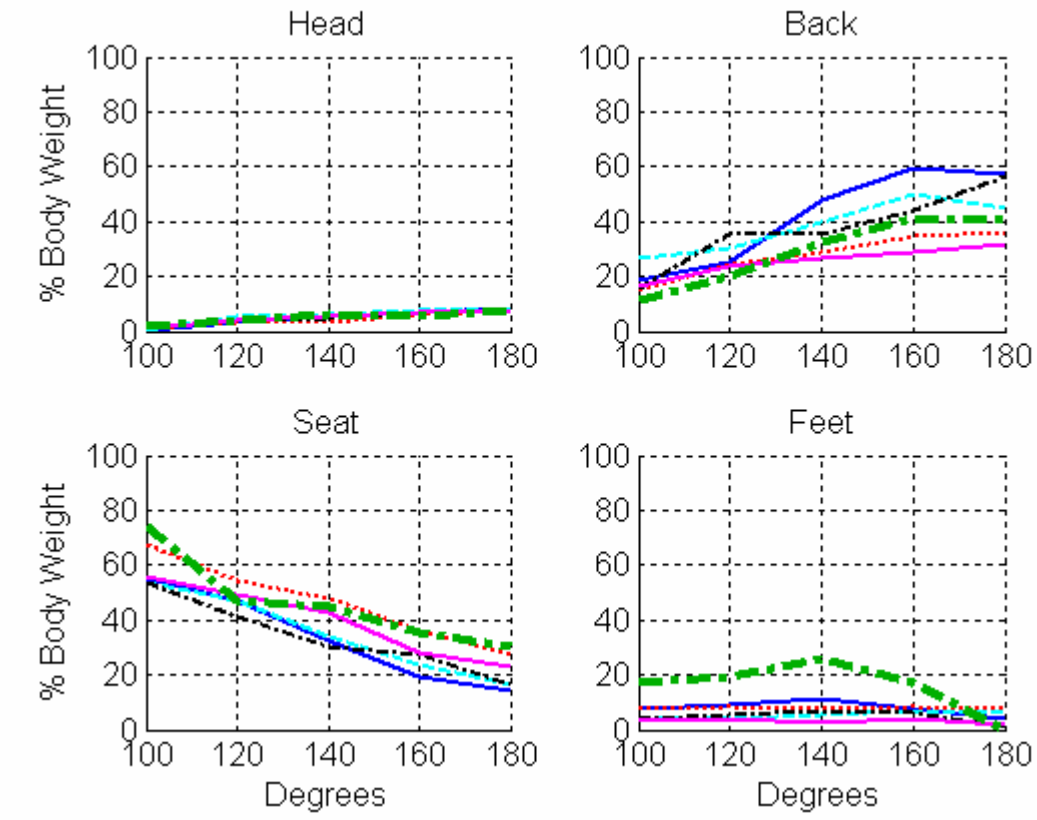

Figure 88: Experimental and Simulated Forces in Recline

The model for recline predicts the experimental data much better for the seat than it did in the tilt configuration. This is due in part to the fact that "slouching" is not possible as the seat-to-back angle opens up. The spine is brought into a straighter configuration, better matching what the rigid model predicts.

One serious discrepancy between the predicted and experimental data is seen in the foot force. While the initial error in the rigid configuration is due to the same problem in the upright tilt position, the model now predicts a rise in foot force at 140° of recline. This is not due to the point contact load, but is instead caused by the frictionless approximation that the software makes when dealing with static indeterminacy. In recline, the model allows the seat back to create a friction force that keeps the person from sliding out of the seat. This leaves no frictional forces on the seat bottom. As the

footrest comes more in line with the seat bottom, the shear forces that would normally exist at the seat bottom are instead transferred to the normal force at the footrest.

Beyond 140° of recline, the shear forces on the seat bottom should decrease, and finally be completely eliminated at 180° of recline. This explains why the predicted foot force reading agrees with the experimental data at high degrees of recline.

The sum of the four mat forces is shown in Figure 89. While the sum of the forces reaches above 120%BW for some users in tilt, the sums in recline never exceed 100%BW for the experimental data. The model predicts combined forces above 100%BW, but this is due to the over-prediction of the foot force at low to moderate angles of recline.

This flat trend with summed forces in recline is consistent with expectations. As the

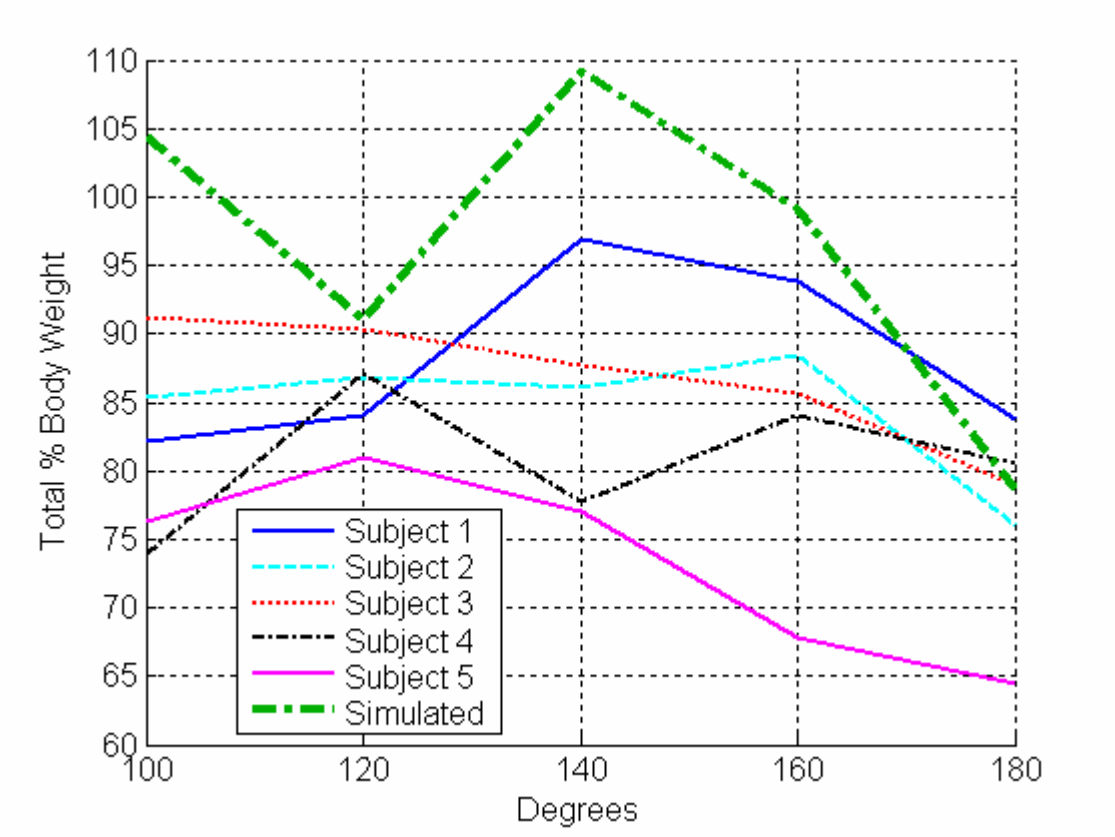

Figure 89: Sum of Forces in Recline

recline angle increases, the body is brought into a supine position. The weight of each body segment is only taken by a single chair component, rather than a combination of two normal forces. As a result, the sum of forces tends to stay quite level compared to tilt.

4.6.3 Stand Results

The final configuration we looked at is standing. The experimental and predicted results, with a knee force measurement instead of a head measurement, are shown in Figure 90. The knee forces have been adjusted to remove the preload bias at 0° of stand. In the upright configuration, the knee block is unnecessary to maintain a seated position. Including the preload would give a false sense that the knee block is holding some of the

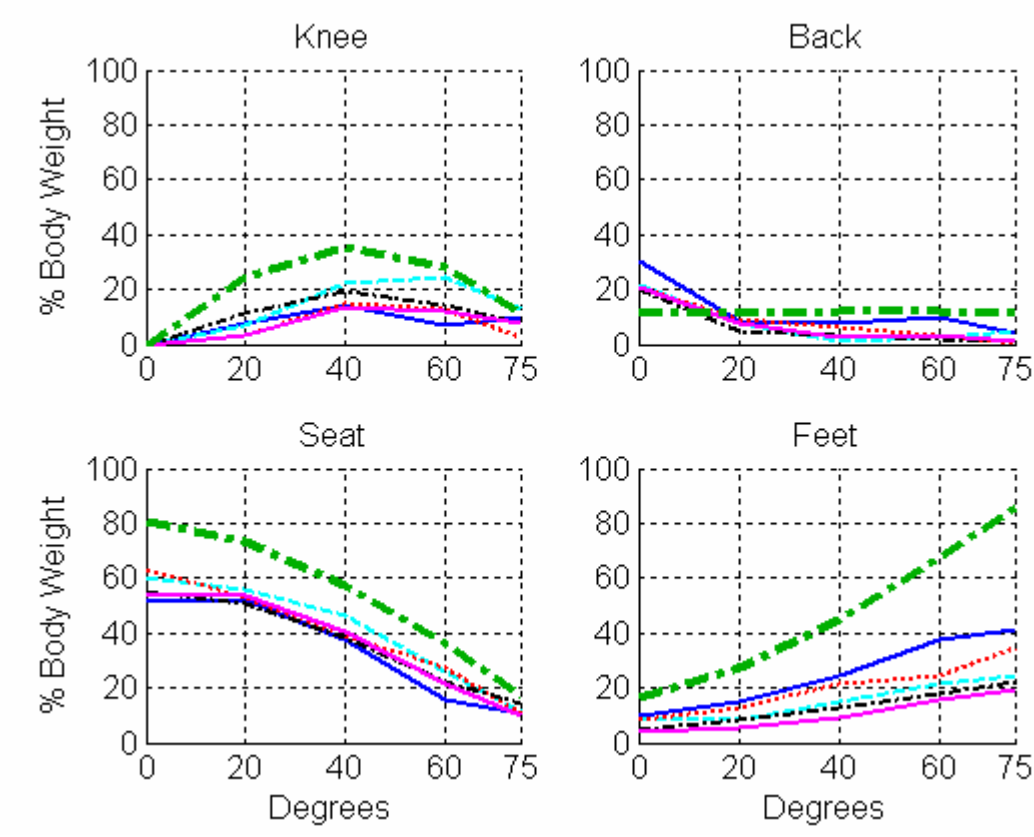

Figure 90: Experimental and Simulated Force in Stand

weight of the body. Instead, it is just a reading of the preload tension in the knee block. To account for this, the force reading at 0° of stand is subtracted from the readings at all stand angles. A chart of the preloads for each test subject, along with the simulated preload in the knee spring is given in Table 15. To calculate the total force at the knee for a given stand angle, the percent body weight preload reading should be added to the experimental readings in Figure 90.

Table 15: Knee Preload Forces

Subject	Knee Preload
1	11.53%BW
2	14.69%BW
3	11.52%BW
4	8.55%BW
5	15.4%BW
Simulation	4.59%BW

Looking at Figure 90, we see an obvious departure from the trends in tilt and recline. The seat forces still start high and are reduced as the stand angle increases. However, instead of the back forces taking the weight from the seat bottom, the feet and knees absorb the weight as stand progresses. The back forces drop off almost completely for large angles of stand.

This reduction in back forces further highlights the effects of a "slouched" position. In the upright configuration, the back forces are higher than at larger angles of stand, even though the angle of the back rest remains constant throughout the move. What changes is the seat-to-back angle, which opens up as the seat bottom angle increases. Opening up the seat-to-back angle causes the spine to straighten and reduces back forces. The model, keeping a rigid spine approximation throughout, predicts a nearly constant back force at every angle of stand.

Along with the back forces, other discrepancies exist between the simulated and experimental data for every mat reading in stand. The first is the forces at the seat bottom. The model consistently over-predicts the seat forces for every angle of stand. This is caused by a frictionless approximation in the model, this time at the seat back. With the addition of the knee spring in the model, the software effectively treats the seat back and seat bottom as frictionless. The frictionless seat back causes the shear forces that would otherwise be taken by the back to be transferred as normal forces on the seat bottom, causing an incorrect prediction.

Similarly, with the frictionless seat bottom assumption, the shear forces on the seat bottom are transferred to the knee block. This causes an incorrect prediction for the knee forces, especially at 40° of stand. At higher angles of stand, the shear forces on the seat are reduced, and this leads to the model more accurately predicting the knee forces at 75° of stand.

The final discrepancy between the model and experimental data is seen in the foot force data. In this case, however, it is the foot force which is most likely the erroneous reading. At 75° of stand, we expect the feet to hold more than 80% of the body weight. In fact, we would expect the feet to hold 100% of the body weight at 90° of stand. Because of this, we expect that the force reading from the mats is in error.

Upon inspection of data, we found that the pressure reading at the foot was dominated by localized pressure points corresponding to the tread pattern on the test subjects' shoes. While these pressures gave a force reading, it is known that the conversion from pressure to force is most accurate for moderate pressure reading that are distributed evenly across the mat. Creating a few points of very high pressure is likely to

cause an inaccurate force conversion. With the experimental data suggesting that the feet are only taking between 20 and 40 percent of the weight of body at 75° of stand, we conclude that the force is being significantly under-read.

For future experimental data, a hard foam sheet should be used to help distribute the weight more uniformly. This should correct the force readings at the foot. For our data, the error exists, and we will trust the simulated prediction as a more accurate representation of the actual forces at the footrest.

We also looked at the combined forces from the four mats for the standing configuration. The results are presented in Figure 91. In this graph, the simulated forces are much higher than the experimental. Both are believed to be in error. As with recline, opening up the seat-to-back angle should cause the total force reading to remain

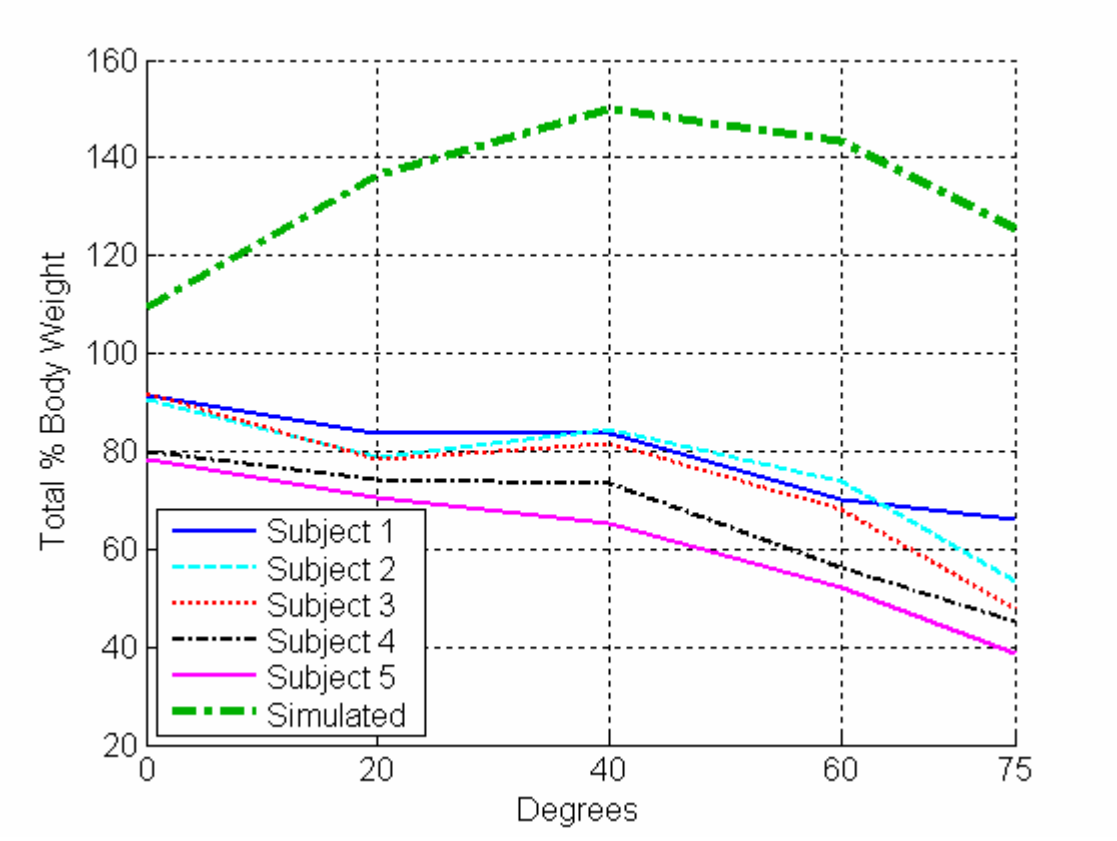

Figure 91: Sum of Forces in Stand

relatively constant. Instead, the experimental total force declines with larger angles of stand. This is caused by the inaccurate force reading at the footrest. The simulated forces are much too high, with errors caused by the frictionless seat back and seat bottom approximations in the software.

4.6.4 Comparison of Methods

After examining the individual experimental data, together with the simulated data, conclusions about how the weight of the person is actually being distributed during tilt, recline, and stand can be drawn. The end goal of these methods is to achieve pressure relief at the seat bottom, but we also need to investigate how the other seating forces are affected by each configuration.

Looking first at tilt, we assume that the experimental data is the best predictor of the actual distribution of forces at the seating elements. To get a best fit, we take the average of the five test subjects and fit a 2^{nd} order polynomial to the data averages. This "best fit" summary is shown in Figure 92 The polynomial trendlines used, along with their R^2 values, are given in Table 16.

We see that pressure relief at the seat bottom comes with a price in tilt, namely very high back forces. While the seat bottom starts with around 55% of the body weight in the upright position, the back force takes more than 75% of the body weight at 55° of tilt. For even further angles of tilt beyond 55°, we expect that the seat bottom forces will continue to decline, eventually reaching near zero, while the seat back forces will continue to climb and support the full weight of the upper body and thighs.

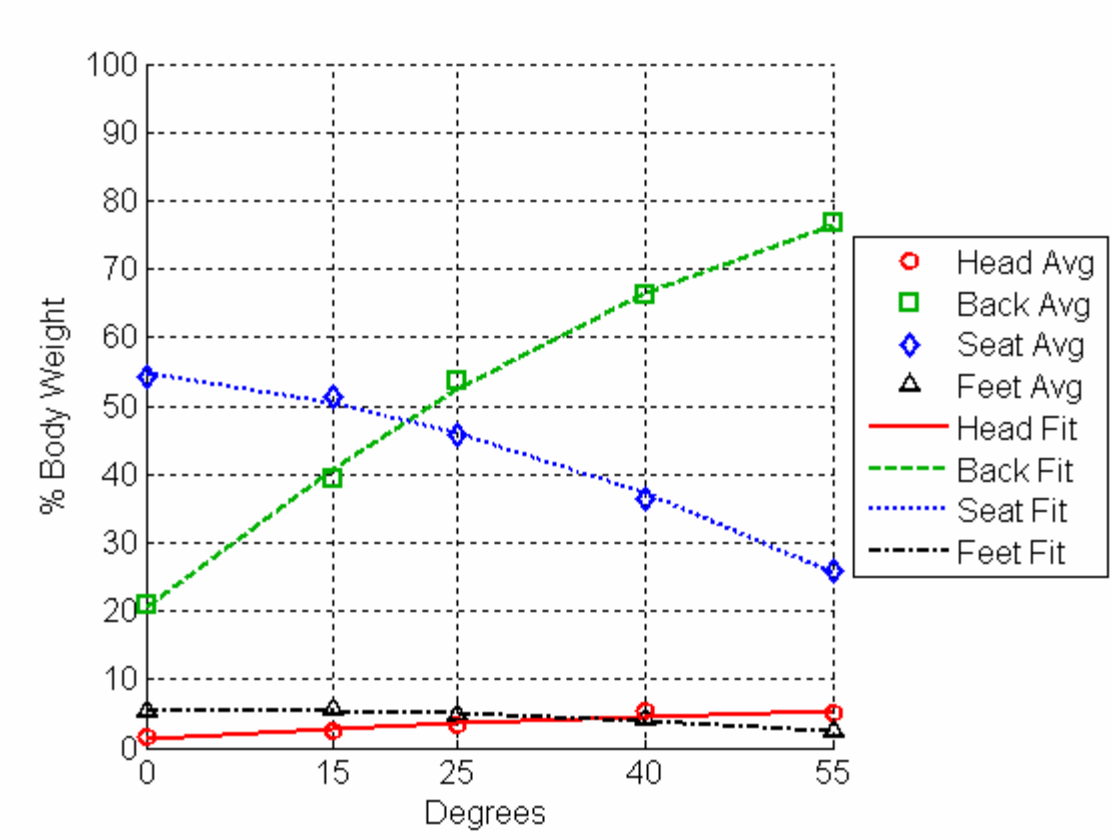

Figure 92: Best Fit for Tilt Results

Table 16: Polynomial Fit Lines for Tilt

	2nd Order Polynomial Fit	R^2 Value
Head	$-0.0006x^2 + .1059x + 1.2842$	0.9304
Back	$-0.0085x^2 + 1.4867x + 20.52$	0.9979
Seat	$-0.0060x^2 - 0.2005x + 54.756$	0.9965
Feet	$-0.0012x^2 + 0.0154x + 5.3514$	0.9709

Looking next at recline, we performed a similar analysis, trusting the experimental averages to be the best indicator of the actual forces felt during recline. The "best fit" summary is shown in Figure 93. The polynomial trendlines used, along with their R^2 values, are given in Table 17.

We immediately see a benefit of using recline rather than tilt. While the back forces increase at large angles of recline, they do not rise as high as in tilt. In fact, the back force in full recline is less than the force at the seat bottom in the upright position. As

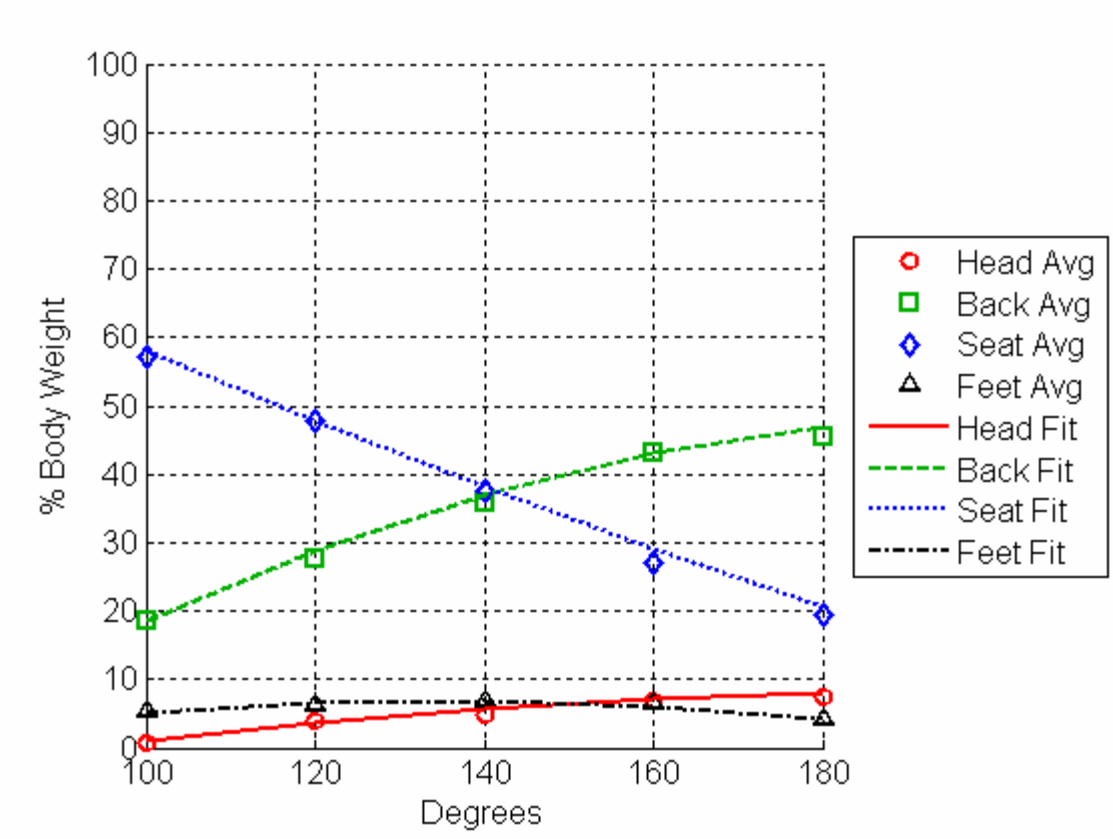

Figure 93: Best Fit for Recline Results

Table 17: Polynomial Fit Lines for Recline

	2nd Order Polynomial Fit	R^2 Value
Head	$-0.0007x^2 + 0.2807x - 19.937$	0.9811
Back	$-0.0026x^2 + 1.085x - 64.009$	0.9960
Seat	$+0.0006x^2 - 0.6353x + 115.44$	0.9982
Feet	$-0.0013x^2 + 0.3536 - 17.245$	0.9108

with tilt, the head and feet forces remain low, with the headrest taking the weight of the head in full tilt and recline. The foot force, instead, drops off in full tilt and recline.

For a best approximation of the forces during stand, we use the experimental averages for the seat, back, and knee forces. As mentioned previously, the experimental foot forces are believed to be too low, so the predicted foot forces from the model are used for an analysis of the overall effectiveness of standing. The "best fit" graph is

presented in Figure 94. The polynomial trendlines used, along with their R^2 values, are given in Table 18.

As can be seen in the figure, the seat bottom force drops off significantly in full stand, while the foot force rises significantly. For those needing pressure relief at the heels, this would be problematic. However, for those who only need pressure relief at the seat bottom, and can support their weight with their feet and ankles, stand is a good

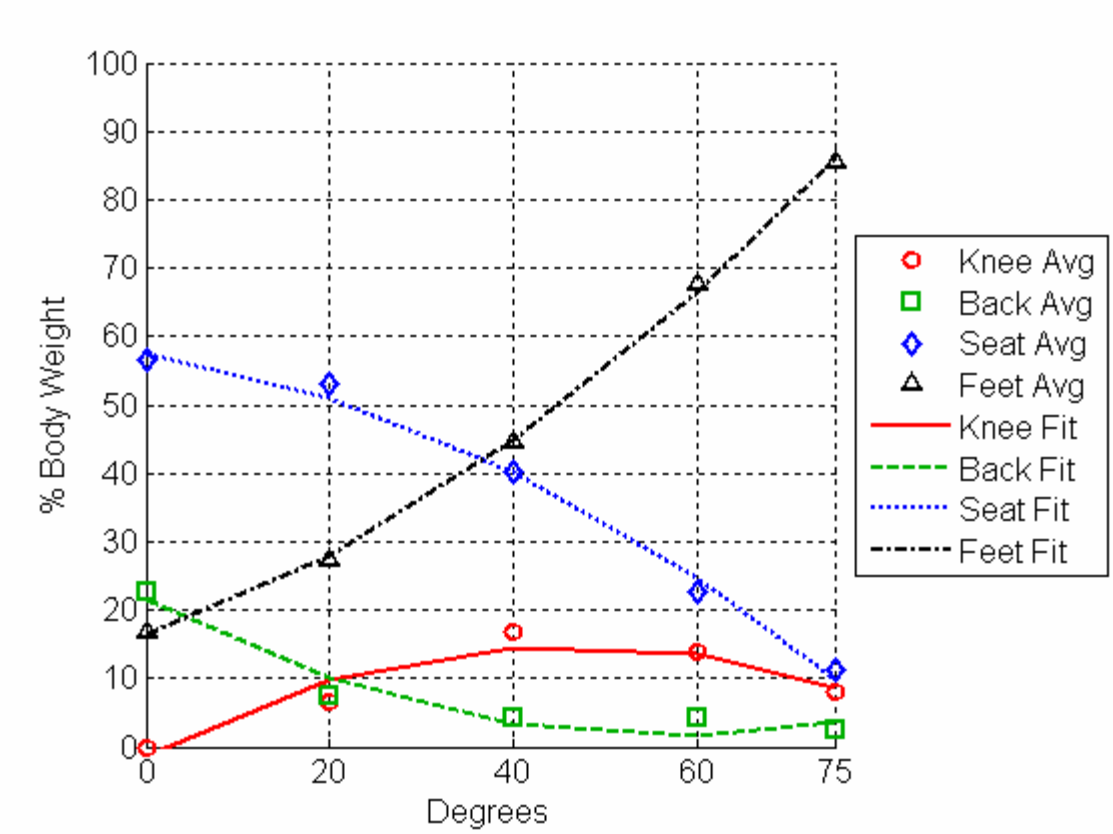

Figure 94: Best Fit for Stand Results

Table 18: Polynomial Fit Lines for Stand

	2nd Order Polynomial Fit	R^2 Value
Knee	$-0.0075x^2 + 0.6949x - 1.1921$	0.9045
Back	$+0.0061x^2 - 0.6962x + 21.551$	0.9432
Seat	$-0.0058x^2 - 0.1988 + 57.438$	0.9933
Feet	$+0.0063x^2 + 0.456x + 16.42$	0.9994

option.

For those who need pressure relief at the seat back, stand is the only option to consider, as both tilt and recline increase the back forces, with tilt causing very large forces.

Along with the foot force, another issue that does need to be considered is the force at the knee block. Stand loads the knee with force, while neither tilt nor recline puts and load on the knee at all. Thus, the condition of a person's knees is critical to prescribing stand. In truth, however, the knee load is not excessively large, so it should not cause any problem for someone with healthy knees.

As a final evaluation of effective pressure relief, we looked at a comparison of just the seat bottom forces in tilt, recline, and stand. The best estimation for the seat forces were used. The results are shown in Figure 95, with the recline angles being adjusted by 100° to line up with the tilt and stand angles.

From this graph, we see that at low angles (0-40°), tilt and recline are more effective at giving pressure relief for the seat bottom. However, at 50°, stand overtakes recline in its effectiveness, and the two trendlines continue to diverge beyond this point, allowing for much more pressure relief at the seat bottom in full stand than in full recline. Tilt seems to follow a similar trend as stand at larger angles, but without data for those points, extrapolation is inaccurate.

Another comparison can be drawn by looking at the specific percent body weight carried by the seat bottom in the upright position as well as in the full range of each configuration. The graph shows that approximately 55% of the body weight is taken by the seat in the upright position. At a full tilt of 55°, the seat load drops to about 26% of

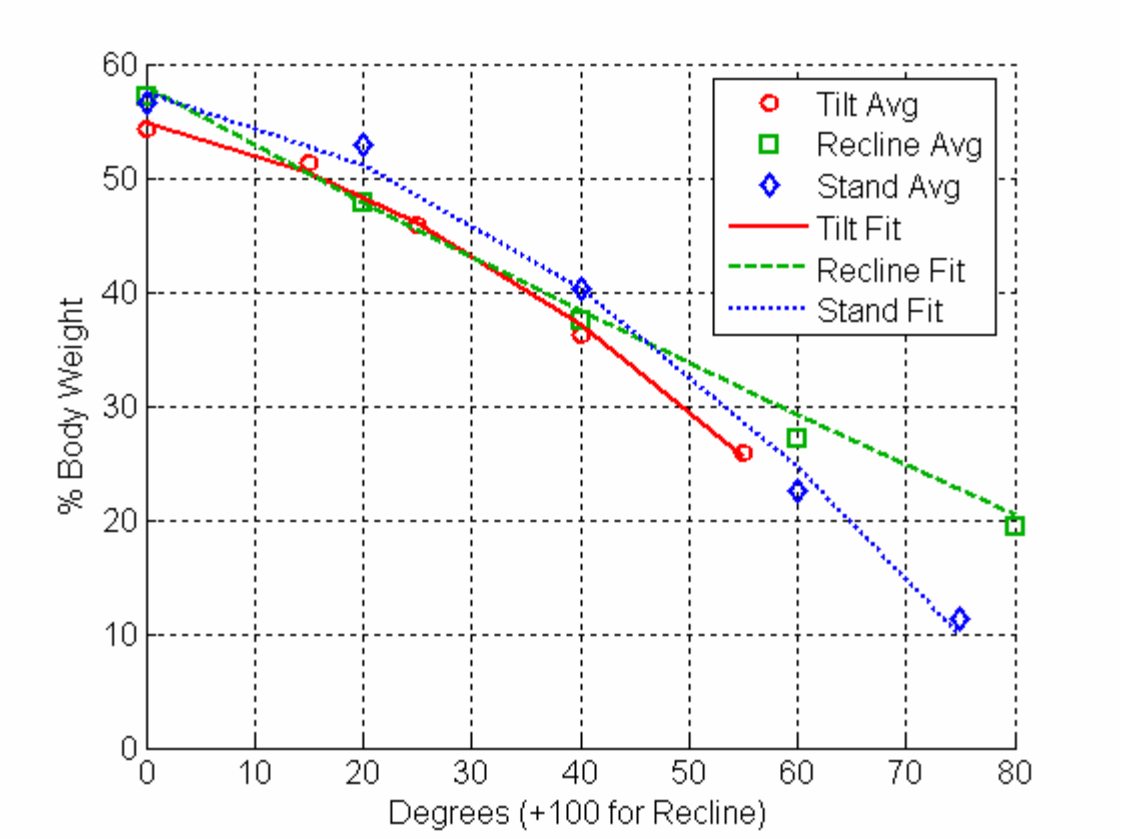

Figure 95: Comparison of Pressure Relief at Seat Bottom

the body weight. At full recline, the seat load is approximately 19.5 %BW. At full stand, with the seat in 75° of forward tilt, the seat load drops to about 11.3%BW.

4.7 Conclusion

From the data, we conclude that stand is an effective form of pressure relief, along with tilt and recline. Each has strengths and weaknesses which must be considered by a clinician in order to choose the best method for a given user.

For those able to handle their full weight on their feet, and who have healthy knees, stand is an excellent option as it provides the largest reduction in seat bottom forces at its full range. As well, it provides for improved social interaction, with the user being at the

same height as able-bodied individuals. It also allows for greater accessibility for the user.

For those who cannot use stand due to a limitation, recline is a good method of pressure relief at the seat bottom. In addition, it does not create very large back forces during the motion. There is a limitation in how much pressure relief can be achieved at the seat bottom in full recline, with the weight of the thighs never being removed from the seat bottom in full recline.

Tilt is also an effective means of pressure relief for those who can handle the large back forces. It is perhaps the simplest mechanical solution for achieving pressure relief as the seat-to-back angle does not change, and the footrest length remains the same. A large reduction in seat bottom forces is possible, limited only by how far the seat can tilt.

For the full angles of tilt, recline, and stand tested in this setup, tilt is the least effective means of pressure relief at the seat bottom, reducing the seating forces from roughly 55%BW in the upright position to 26%BW. Recline achieves 19.5%BW, and stand achieves 11.3%BW.

CHAPTER 5

CONCLUSION

This thesis provides insight into the design and development of a dynamic seating system for individuals who experience high-tone extensor thrusts. It also shows a comparison of pressure relief methods in the tilt, recline, and stand position. Contributions of this thesis include:

- Development and analysis of a hinged-back dynamic seating system with integration of sensors and active components
- Design and evaluation of control algorithms for active breakaway
- Fabrication and testing of passive breakaway using a dynamic footrest
- Design, fabrication, and evaluation of an advanced dynamic seating system using the variable stiffness concept
    - Flexible seat back with motor-driven roller wheel
    - Flexible seat bottom with actuator-driven, tilt-away rigidizer
    - 2-DOF footrest with magnetic breakaway
- Development of alternative seating concept based on seat lifting concept
- Design and fabrication of tilting mechanism for pressure relief study
- Development of computer model for pressure relief study
- Collection of data for comparison of tilt, recline, and stand for effectiveness of pressure relief on seat bottom

5.1 Hinged-Back Dynamic Seat

The thesis presented a single hinged-back seating system that was used to experimentally verify that dynamic components reduce forces during high-tone extensor thrusts. Both forces on the seat back and on the foot rest were shown to decrease as the

seat back angle increased during an unconstrained extensor thrust. While the amount of data was small for this test, it was sufficient to motivate further study with the advanced dynamic seating system.

Additionally, two control algorithms were developed, based on a force threshold and a force gradient threshold criteria. These methods were shown to be effective based on the chosen criteria, but both possess serious flaws. To correct for these weakness, a modified algorithm is needed. It would use the force gradient threshold with the addition of a minimum force threshold. This minimum force threshold would need to be exceeded for a few seconds before the force gradient algorithm begins testing for its threshold. This would eliminate false readings due to transient vibrations in a no-load condition, and also for the case in which the user leans forward and then falls back against the seat back. Additionally, a check needs to be made once the force gradient is exceeded to ensure that it doesn't drop below the threshold for a certain amount of time. This guards against a stray noise spike in the signal. While adding time delays, these measures are needed to create a robust sensing algorithm.

5.2 Development of Advanced Dynamic Seating System

The design of an advanced dynamic seating system was discussed in Chapter 3. The strengths and weaknesses of two variable stiffness implementations were discussed. Specifically, the seat back motor and seat bottom actuator need to have more power to be effective for teenagers and young adults. The seat back motor needs to be replaced with a power-off brake motor with enough torque to effectively drive the roller back up the seat back when the person is leaning his or her weight against the seat back. The seat

bottom actuator has enough power to return the seat bottom to its starting position, but needs to do so at least three times as fast as the current setup. This must be done with an increase in power, rather than by changing the gear ratio of the existing the actuator.

The dynamic seating system was shown to be effective in reducing interaction forces during extensor thrusts. In particular, two of the tested configurations proved the most effective. The first is the flexible seat back with the roller in its lowest position, with the seat bottom and footrest locked out. The other configuration allows the seat back, seat bottom, and footrest to move dynamically, with the roller and flexure bar in their lowest settings. These two configurations reduce the combined seat back, seat bottom, and seatbelt forces by roughly 25% as compared to the rigid configuration. They also reduce the peak pressure on the seat back as compared to the rigid configuration. The other dynamic configurations were not as effective as these two configuration, but they all were more effective that the rigid configuration. This is an important result, indicating that any combination of dynamic components effectively reduces interaction forces as compared to a rigid seating system.

5.3 Pressure Relief Comparison

A tilt mechanism was designed and built for use in a comparison of pressure relief using tilt, recline, and stand in a Levo wheelchair. A computer model was also developed to provide reliability of the experimental data. The model was shown to have significant weaknesses at predicting the specific force profiles for each configuration. However, it did verify trends in the data. As well, it highlighted a source of error in the foot force data in standing.

Using the best estimate for the actual force distribution in the three methods, it was shown that the seat bottom forces were reduced from 55% body weight to the percent body weight shown in Table 19.

Table 19: Seat Bottom Reduction Comparison

55° of Tilt	26% body weight
180° of Recline	19.5% body weight
75° of Stand	11.3% body weight

5.4 Future Work

5.4.1 Dynamic Seating Systems

Looking first at the methods of sensing and differentiating extensor thrusts, future work includes a study that looks specifically at quantifying the forces felt during an extensor thrust. The criteria used in this thesis were based on the perceptions of a focus group who have significant interaction with those affected by extensor thrusts. However, these perceptions are not guaranteed to be accurate. This study could include a highly instrumented chair that records all interaction forces on the chair during voluntary and involuntary extensor thrusts for many different users. This would give useful data for testing algorithms against, and would allow the algorithm to be refined. It would also broaden the knowledge about extensor thrust forces in general. This test setup could also be transportable, to allow for the measurement of forces that occur during transportation or other activities where vibrations could lead to false positives in the algorithm.

Needed improvements for the dynamic seating system include instrumenting the system with sensors to allow integration with the control algorithms developed with the hinged-back chair. This could also lead to interesting work in determining where the best location is to sense a thrust.

Further study needs to be done testing the effectiveness of the advanced dynamic seating system with those affected by extensor tone. While the able-bodied mock extensor thrusts are a good measure, verification is needed showing that similar results occur for those who experience actual extensor thrusts.

Additional investigation also needs to be done into how the fully dynamic system can be modified to further reduce interaction forces. It was shown that the dynamic seat back alone is as effective at reducing interaction forces. However, the foot force needs to be investigated, as the foot force is likely higher when the footrest is locked out.

As well, the footrest system needs to be modified to allow for a better motion. The coupler bar was introduced into the footrest design to simplify the breakaway system. However, it complicated the force measurement by imposing a prescribed footrest extension profile. Because the rotation of the footrest does not line up with the anatomical knee joint, the leg extension will not follow this prescribed motion. This caused the user to push back off the footrest and increase the back forces in an unknown manner. This effect was further complicated when the seat bottom was allowed to bend because of the change in the knee location.

The net result is that in simplifying the breakaway system, unknown forces were been created. To correct this, the original Miller's Adaptive sliding coupler should be used to allow for three degrees of freedom in the footrest. This would allow the footrest

to elongate as needed, rather than causing the user to push off the footrest. This could show an improvement in the fully dynamic configuration over the seat back alone. If the fully dynamic configuration is shown to be more effective, the footrest breakaway could be redesigned to capitalize on this improved dynamic motion.

Other future work for the dynamic seating system includes a long-term study on the effects of a dynamic seating system on muscle control problems. If a wheelchair responds to the user appropriately, remaining rigid when needed and becoming dynamic as needed, will the user begin to develop increased muscle control? Will the user learn where the breakaway point is and fine-tune his or her voluntary thrust forces around it?

The study could include the effects of a dynamic system on the emotions of the user. Does a more comfortable user experience results in improved moods?

Finally, the study could include an investigation into environmental challenges that are faced with a dynamic seat system. For instance, what are the consequences of forgetting to lockout the dynamic components in a crowded area? This study would lead to a much greater understanding of how to improve future dynamic seating systems around the needs of the user.

Additional future work involves developing an optimization scheme that attempts to calculate the optimal dynamic parameters for a user based on his or her specific thrust profiles. For this, the setup mentioned earlier to quantify the forces during a thrust could be used. After measuring the forces, they could be used as inputs to an advanced model that would calculate the optimal dynamic components and stiffnesses based on thrust profiles and user body segment parameters. This optimization would likely attempt to

minimize interaction forces. A highly adjustable prototype could be built to test the predicted configuration for effectiveness with each specific user.

5.4.2 Pressure Relief Study

The pressure relief study was done using able-bodied test subjects. Further tests need to be done using those with spinal-cord injuries to see if the same trends hold. Based on the tight band of data from the five subjects, varying significantly in weight and height, it is expected that the same trend will hold for those with spinal-cord injuries. Even so, the testing needs to be done to verify this assumption.

To improve the model, a finite-element package is likely needed. This should eliminate the inaccuracies due to static indeterminacy, as the body elements are allowed to deform. This deformation allows for a solution to an otherwise indeterminate problem. As well, the use of a finite-element package allows for the modeling of a flexible spine to capture the "slouching" effect. It also allows for a more accurate modeling of the soft-tissue interactions that occur at the seat bottom. While this finite-element model would be much more complex to create initially, it should allow for a much better representation of the reality of interactions that occur for different pressure relief methods.

APPENDIX A

DSS SURVERY REPORT

Note: This survey was prepared, administered, and summarized by RL Grubbs of the Center for Assistive Technology & Environmental Access (CATEA) at Georgia Tech. The entire summary of results follows.

DSS Survey Report

For

Dynamic Seating System Design Team

(Intended audience—DSS Design team)

*This study and subsequent analysis has not generated ALL design criteria for a dynamic seating system. It has generated MOST of the customer requirements and design criteria that are important to the stakeholders involved. Focus group participants generated many customer requirements that cannot be addressed in the first iteration of a prototype dynamic seating system.

*The follow-up survey and subsequent analysis was done to identify the importance and priorities of customer requirements. Table 1-Design Criteria for DSS (pages 12-14) was derived from analysis of customer requirements from focus group data and from survey data from the follow-up survey.

RL Grubbs, Principle Investigator/Study Moderator
Rehabilitation Engineering Research Center on Wheeled Mobility
Center for Assistive Technology & Environmental Access
Georgia Institute of Technology
December 2004

1.1 Who participated in the study?
1.2 What experience do they have with specialized seating?

		QBK1-Respondents' Demographics					QBK2-Experience with Specialized W/C Seating				
Respondent ID	Count n=	Parent Caregiver	YA w/c user	Therapist	Vendor	Other	Great Deal	Above Average	Average	Not Much	Very Little
1009	1				1			1			
1041	1				1			1			
1042	1				1		1				
103	1	1						1			
1038	1			1				1			
109	1	1					1				
106	1	1					1				
107	1		1				1				
1011	1			1							1
1003	1				1			1			
1010	1			1					1		
1039	1			1						1	
1004	1				1				1		
1043	1			1					1		
1040	1			1				1			
1007	1			1				1			
1006	1			1					1		
105	1	1						1			
1044	1			1						1	
1045	1			1						1	
1002	1			1					1		
108	1	1							1		
102	1	1					1				
Raw Score	23	6	1	11	5	0	5	8	6	3	1
%		26	4	48	22	0	22	35	26	13	4

A group of 23 stakeholders participated in the one of three focus groups and follow-up mail survey (n=23) conducted between April and November 2004. Six families (i.e. parent/caregiver and child/user), one adult user, 11 therapists (i.e. 7 physical therapists, 4 occupational therapists) and 5 vendors participated (see **Figure 1**) in the study.

Most participants considered themselves to have at least average or better experience with wheelchair seating systems for users with thrust/high extensor tone. **Figure 2** contains demographic information about study participants.

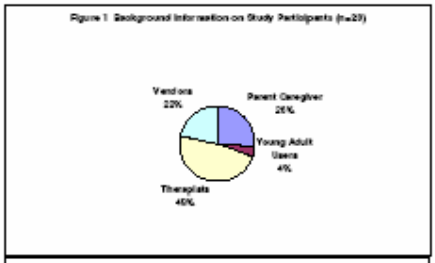

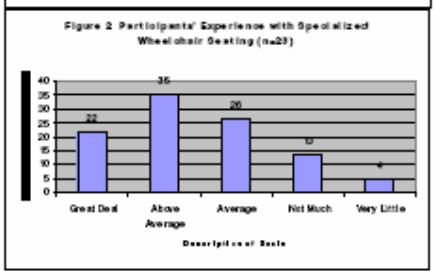

2.1 How do thrusts travel through the body?
2.2 How are purposeful thrusts used?

		QT1-Involuntary thrusts travel from...				QT2-Purposeful thrusts are used to...								
Respondent ID	Count n=	Pelvis out to extremities	Head down to trunk, extremities	Legs up to trunk, arms, head	Initiate in different parts of body	Assist with Transfers	Change Position in W/C	Reach for Objects	Access Switches	Raise Head	Communicate	Drive w/c	Other	Not witnessed
1009	1	1					1	1	1	1	1	1		
1041	1	1						1	1		1			
1042	1				1	1	1	1	1	1	1	1		
103	1				1	1	1		1	1	1			
1038	1			1		1	1	1	1	1	1			
109	1		1			1	1	1	1	1	1	1		
106	1				1	1	1	1	1	1	1	1		
107	1				1	1	1	1	1	1	1	1		
1011	1		1			1			1	1		1		
1003	1			1		1	1		1		1			
1010	1				1	1	1	1	1	1	1	1		
1039	1				1	1		1	1	1	1	1		
1004	1			1					1		1	1		
1043	1				1	1		1	1	1		1		
1040	1				1	1		1	1	1				
100	1				1	1	1	1	1	1	1	1		
1006	1				1	1	1	1	1	1	1			
105	1	1						1			1			
1044	1		1			1		1	1		1			
1045	1				1	1	1	1	1					
1002	1				1	1	1	1	1	1	1	1		
108	1		1			1	1	1	1	1	1			
102	1	1				1		1	1			1		
Raw Score	23	4	4	3	12	19	14	19	22	16	18	13	0	0
% or Rank		17	17	13	52	Rank 2	Rank 5	Rank 2	Rank 1	Rank 4	Rank 3	Rank 6		

Participants were asked to discuss their experience with and knowledge about thrusts. During focus groups, participants identified emotional, physical and environmental triggers for involuntary thrusts and symmetrical and asymmetrical patterns of body movement during involuntary thrusts. When asked where involuntary thrusts (spasms) initiate and how they travel through the body, survey results appear to indicate that a majority of participants (52%) believe that thrusts initiate in different parts of the body (see **Figure 3**).

Figure 3 Where do thrusts initiate and how do they travel through the body? (QT1)

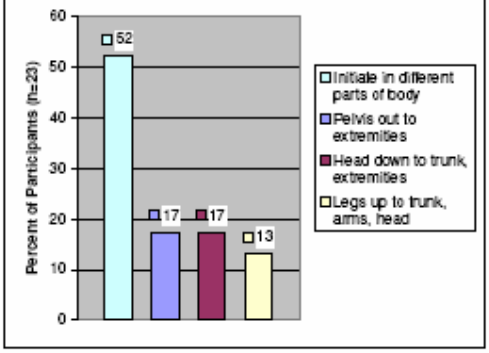

Participants appear to agree that purposeful thrusts are used to accomplish certain tasks. Whereas an involuntary thrust may last a few seconds, purposeful thrusts may last longer depending on the activity or task the person is doing. On the survey, participants were asked to mark a list of activities that children and young adults do using purposeful thrusts. These activities are ranked in **Figure 4**.

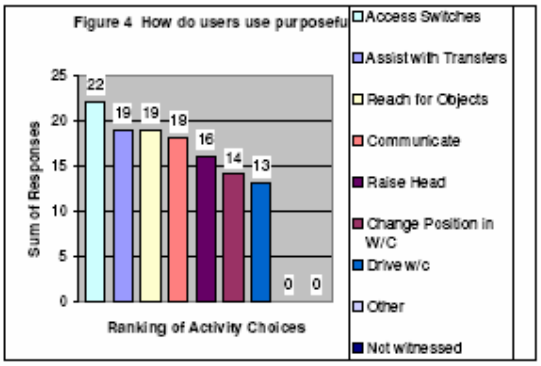

2.3 How do purposeful and involuntary thrusts differ?
2.4 How does the seating system react to user thrust?

		QT3-QT10--About thrusts--How strongly do you agree that...							
Respondent ID	Count n=	Use purposeful thrusts	Involuntary is fast	Purposeful lasts longer	Involuntary stronger	Thrust in upper body	Thrust in lower body	Want static SS	DSS react differently
1009	1	3	1	2	1	0	0	3	1
1041	1	3	2	1	0	0	0	1	3
1042	1	2	2	1	1	1	2	1	2
103	1	3	2	3	0	0	0	0	1
1038	1	3	3	2	1	1	2	0	2
109	1	3	3	3	3	3	1	3	3
106	1	3	3	2	1	1	1	1	2
107	1	3	3	2	1	0	0	1	2
1011	1	3	2	1	1	1	2	2	3
1003	1	2	1	2	2	1	2	1	2
1010	1	3	2	2	1	0	2	1	2
1039	1	2	2	3	2	1	2	1	2
1004	1	3	2	2	2	0	3	2	1
1043	1	3	2	3	1	1	2	1	3
1040	1	2	2	2	1	1	1	1	1
1007	1	3	2	1	3	1	2	2	3
1006	1	3	2	2	0	0	0	0	3
105	1	3	2	3	1	1	2	0	3
1044	1	3	2	3	0	2	2	1	0
1045	1	3	1	1	1	1	2	1	2
1002	1	3	2	2	2	0	0	0	3
108	1	3	3	3	3	3	1	0	3
102	1	3	2	2	2	1	1	2	3
Raw Score	23	65	48	49	30	20	30	25	50

Figure 5 How do purposeful and involuntary thrusts differ and how does the seating system react?

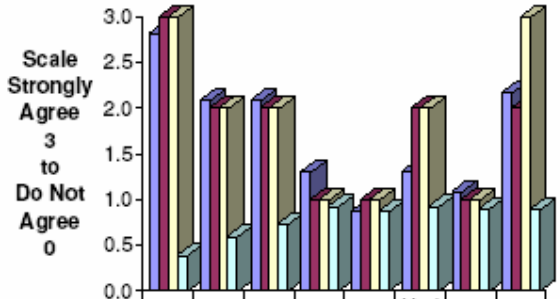

	QT3	QT4	QT5	QT6	QT7	QT8	QT9	QT10
	Yes	Yes	Yes	No	No	Undecid	No	Yes
Mean	2.8	2.1	2.1	1.3	0.9	1.3	1.1	2.2
Median	3	2	2	1	1	2	1	2
Mode	3	2	2	1	1	2	1	3
Standard Deviation	0.4	0.6	0.7	0.9	0.9	0.9	0.9	0.9

As illustrated in **Figure 5**, survey results indicate participants believe that-

- **(QT3)** purposeful thrusts are useful for accomplishing various tasks,
- **(QT4)** involuntary thrusts are faster than purposeful thrusts,
- **(QT5)** purposeful thrusts tend to last longer depending on the task, and
- **(QT10)** a dynamic seating system should react differently to purposeful versus involuntary thrusts.

Participants **do not agree** that-

- **(QT6)** involuntary thrusts are more intense than purposeful thrusts,
- **(QT7)** thrusts occur more frequently in the upper body, and
- **(QT9)** a static seating system is preferred to a dynamic one for accommodating the use of purposeful thrusts.

Participants appear to be **divided** on **(QT8)** whether or not thrusts occur more frequently in the lower body.

There are several important implications for the seating system that can be drawn from this data. First, differences appear to exist between purposeful and involuntary thrusts. Purposeful thrusts tend to be slower than involuntary thrusts, but both types of thrusts are similar in intensity or forces that must be accommodated. This finding supports the idea that the seating system must react differently to purposeful versus involuntary thrusts.

Based on content analysis of focus group data, it appears that when thrusts are used in a purposeful manner, the user depends on a stable or static area, a "stable center of control," to push against to accomplish a desired function. For example, when reaching for an object, the person uses her torso and upper extremity to thrust her arm outward. This is a slower more controlled movement and may last longer. The user appears to benefit from a stable center of control that allows her to push against, while she thrusts her upper extremity outward to accomplish the reaching function. It appears that the seating system needs to offer some rigidity for the user to push against during purposeful thrusts, but at the same time support (or at least not inhibit) the movement of the extremities in accomplishing the intended task. The seating system needs to be designed so a fixed lower back section and velocity sensitive securements maintain pelvic positioning.

In a second example, the user changes position by arching her back and pushing her head against the headrest to shift her torso in the seat. If the headrest gives too quickly during this purposeful thrusting movement, the difficulty may be increased. It appears that, to accommodate purposeful thrusts, the dynamic seating system must provide for a stable center while supporting the desired movement of the extremities in a slow, controlled manner. The seating system "dampens" purposeful thrusts by providing adjustable resistance to the thrust and providing adjustable pressure in the rate-of-return to a neutral position. Participants compared this feature to a car's anti-lock brakes or to the adjustable resistance of exercise machines.

According to survey results, participants believe that involuntary thrusts are explosive and "lightening fast." They indicate that, to be effective, the seating system must react differently to purposeful and involuntary thrusts (see **Figure 5**). The basic difference is that during involuntary thrusts, the system provides less dampening resistance, whereas, during purposeful thrusts, the system provides more dampening resistance. Both types of thrust require adjustable force in the rate-of-return.

Thrusts occur in both upper and lower body. When asked on the survey where thrusts occur more frequently, participants appear to indicate that thrusts occur with about the same frequency in upper and lower body (see **Figure 5**).

Focus group discussions indicated that involuntary thrusts (spasms) are likely to be almost constant in young children with traumatic brain injury. On average, participants indicated that involuntary thrusts occur about 6 to 10 times an hour. In users who are taking Rx Baclofen, the frequency of involuntary thrusts drops to about 3 times an hour. Participants indicated that a child's thrusts are less powerful than teen and young adult thrusts due in part to muscle development and "more rehearsal of the movement."

This has implications for the durability of the seating system and components. For example, this finding appears to indicate that headrest assemblies must be just as durable as footrest and armrest assemblies. Taking the average of 10 thrusts an hour multiplied by 10 hours of seating system use daily, components must withstand approximately 100 thrusts each day or 36,500 thrusts per year for approximately three to five years.

3.1 What assembly and adjustability features are desired?

		QA1-QA10--About Adjustability--How acceptable is it that...									
Respondent	Count	Remove SS from base	SS Folds	Doesn't remove or fold	2" in width depth, no kit	2" depth only, no kit	2" depth kit	2" in depth and or width kit	Adjusts w/o tools	Universal tool Adjust	Adjusts w special tool
1009	1	3	1	0	3	3	2	2	3	3	1
1041	1	3	3	1	3	2	1	2	2	3	0
1042	1	3	0	0	3	2	0	1	2	3	1
103	1	3	2	3	3	1	1	3	2	2	0
1038	1	3	2	0	3	2	2	2	1	3	1
109	1	1	3	3	3	3	3	3	3	3	0
106	1	1	2	3	3	3	2	2	3	3	2
107	1	1	2	3	3	3	2	2	3	3	2
1011	1	3	2	0	2	1	1	2	3	2	0
1003	1	3	2	1	3	2	1	1	3	2	0
1010	1	3	3	1	2	2	2	2	1	3	3
1039	1	3	3	0	3	1	0	0	1	3	2
1004	1				3	3	3	3	0	3	0
1043	1	3	1	0	3	1	1	3	2	2	
1040	1	2	2	0	3	2	1	1	2	3	0
1007	1				3	2	2	2	0	1	3
1006	1	3	3	0	3	3	3	3	3	3	0
105	1	3	2	0	3	2	1	0	3	2	0
1044	1	3	2	0	3	0	0	2	1	2	2
1045	1	3	3	0	3	0	0	3	3	2	0
1002	1	2	1	1	2	1	1	2	3	2	1
108	1	3	3	0	0	0	0	3	3	2	0
102	1	3	3	3	3	2	1	0	3	3	0
Raw Score	23	55	45	19	63	41	30	44	50	58	19

Content analysis of focus group data indicates that participants want a seating system assembly (frame) that is compatible with manual and power bases and components (e.g. backs, seat cushions, securement belts and postural supports) from different manufactures. Participants experience difficulty removing the seating system for transport.

Based on survey results-

- **(QA1)** participants want to remove the seating system from the base, or
- **(QA2)** if the seating system doesn't remove, participants expect it to fold.
- **(QA3)** Stated in a negative manner, they **do not find it acceptable** for the seating system **not** to remove from the base **or** fold for transport (see **Figure 6**).

Figure 6 What are the portability features of the seating system? (QA1-QA3)

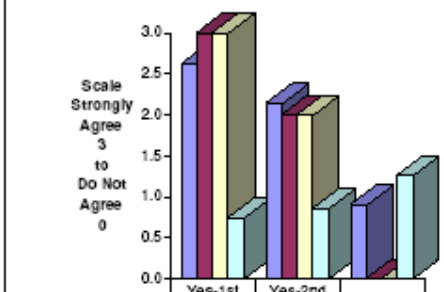

	Yes-1st Choice	Yes-2nd Choice	No
Mean	2.6	2.1	0.9
Median	3	2	0
Mode	3	2	0
Standard Deviation	0.7	0.9	1.3

Removevs Foldsvs Doesn't Remove or Fold

During focus groups, participants were asked about the range of sizes and how much adjustment an ideal seating system should have. Content analysis of focus group data indicates that seating system width ranges are 10″ to 22″ and seat depth ranges are 5″ to 14″. Participants expect the seating system to integrate with current back components for funding purposes.

How will the dynamic seating system address growth? On the survey, participants were asked to choose between two options for addressing growth—**growth adjustments or** the use of **growth kits**.

Figure 7 summarizes survey responses to growth adjustment questions-

- **(QA4)** participants 1st choice is the 2″ growth adjustment option in seat width and depth, without requiring a growth kit,
- **(QA7)** participants 2nd choice appears to be a growth kit that adds 2″ to the seat width and/or seat depth as a one-time increase,
- **(QA5)** participants 3rd choice is a growth adjustment of 2″ in seat depth only with no growth kit required, and
- **(QA6)** participants appeared to dislike the growth kit option that would add 2″ to the seat depth (see Figure 7).

Figure 7 How does the seating system address growth needs of users? (QA4-QA7)

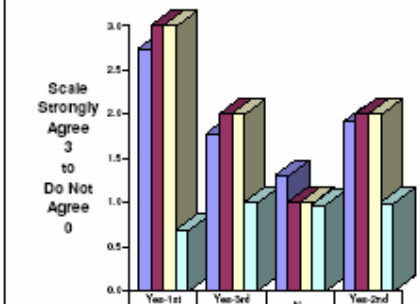

During focus groups, participants described the difficulty they have making seating system adjustments, often several times a day, to accommodate the changing positioning needs of the user. Participants appear to want the seating system to have variable positioning and adjustments that are non-incremental and that telescope for infinite adjustment with a locking mechanism.

On the follow-up survey (see **Figure 8**);

- **(QA9)** participants 1st choice is to make adjustments using a universal tool,
- **(QA8)** participants 2nd choice is to make adjustments without the use of tools.
- **(QA10)** Participants find it unacceptable to require a special tool for making

Figure 8 How are adjustments made to the seating system? QA8-QA10)

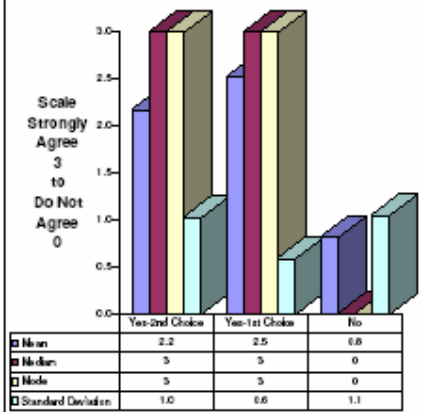

adjustment and that only therapists and vendors could use.

During focus groups, participants identified several mounting issues and solutions. They recommended that the seating system support multiple mounting locations for securements because one mounting location doesn't fit all users needs. They recommended that the seating system use the same (generic) fastener throughout (e.g. 10/32nd or 25/20) to make assembly and adjustment more convenient.

4.1 What are the dynamic features of the seating system?
4.2 What advanced design methods are employed?
4.3 What features do stakeholders want in "rate-of-return"?

		QDM1-QDM7–Dynamic movement of SS--How strongly do you agree that...						
Respondent ID	Count n=	Use electronic sensor, motors	ONLY mechanical devices	Senses amount of force needed	Parent/CG adjust return rate	ONLY Therapists Vendors adjust return rate	Disable w/single action	Features work independently
1009	1	1	1	2	1	3	3	3
1041	1	3	1	3	3	2	3	3
1042*	1	3	3	3	3	0	3	2
103	1	1	2	2	2	0	3	3
1038	1	3	1	3	1	2	3	3
109	1	3	0	3	3	0	3	3
106	1	2	2	3	3	2	3	3
107	1	3	2	3	3	2	3	3
1011	1	2	1	2	1	2	3	1
1003	1	1	2	2	0	3	2	2
1010	1	2	2	2	0	3	1	3
1039	1	1	2	2	3	1	2	1
1004*	1	0	2	2	2	2		3
1043	1	2	1	2	0	2	2	1
1040*	1	2	2		1	2	1	3
1007*	1	3	0	2	1	1	2	0
1006	1	3	1	3	3	1	3	3
105	1	3	1	3	3	0	2	2
1044	1	2	0	2	0	2	3	2
1045	1	3	1	2	1	0	3	3
1002	1	1	1	2	1	2	3	3
108*	1	3	0	3	3	0	3	3
102*	1	1	2	3	3	0	3	2
Raw Score	23	48	30	54	41	32	57	55

Focus group participants discussed several issues surrounding the changing needs of the user throughout the day. At certain times during each day, the user needs variable positions to assist with activities. For example, participants discussed the problems associated with transfers from bed to wheelchair. According to participants, this transfer is best accomplished by getting the user into a "tucked" position to reduce involuntary thrusts. Participants want the seating system to match this "tucked" position, so that the seat-to-back angle is < 90°, in a tilt-in-space configuration. Closing the seat-to-back angle and tilting the user back, makes the transfer easier and helps to work the person's hips back into the seat.

During sit-to-stand transfers, the seat-to-back angle opens up > 90°, thereby putting the person into extension so that she/he can use a purposeful thrust to stand up. Based on content analysis of focus group data, it appears that the ideal seating system permits manual manipulation of seat-to-back angle, seat tilt and back recline so they can be separately and individually configured. It also seems that participants want to be able to set the amount of angle and lock it at "tucked" and "open" and "functional" positions to reduce or facilitate thrusts (e.g. at 70°, 85°, 90°, 110°, 120° and 145°).

It's important to note that participants don't expect the seating system to be dynamic all the time, but rather they expect "dynamic," flexible joints (e.g. at neck, shoulders, lumbar spine, wrists, knees and ankles) that can be set and changed to create the best position for the user at different times, based on changing needs throughout the day.

Participants discussed the need for the seating system to have both tilt-in-space and recline functionality. As stated earlier, tilt-in-space assists with positioning, re-positioning after thrusts and changing positions during the day as task demands change and the need for pressure relief becomes apparent. Recline opens the user's chest up in order to help them breath without putting them into extension. Participants expect the seating system to function in a manner that will support (or at least not inhibit) this development.

Figure 9 What advanced design methods does the seating system use? (QDM1-QDM2)

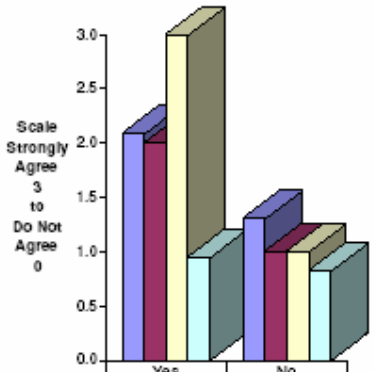

	Yes	No
Mean	2.1	1.3
Median	2	1
Mode	3	1
Standard Deviation	0.9	0.8

Electronic Sensors/Motors vs ONLY Mechanical Devices

Survey data indicates that respondents want electronic sensors and motors to provide advanced sensing and control of the system (see **Figure 9**). During involuntary thrusts, sensors decrease dampening resistance and during purposeful thrusts, sensors increase the amount of dampening resistance. Variable dampening features in the system improve user's switch access, transfers, ability to reach for objects, communication and breathing. Because the system accommodates different types of thrusts, the user will be encouraged to be more active and muscle use will be developed as the user learns to control and use thrust patterns necessary to accomplish self-selected tasks.

Electronic sensors and motors adjust the force necessary in rate-of-return after thrusts, but the rate-of-return can also be adjusted by parents and caregivers (see **Figure 10**).

For added safety, survey respondents indicate that the dynamic features such as variable dampening and adjustable rate-of-return must be enabled and disabled using a single action. They want the dynamic features to work independently and be able to be turned ON or OFF independently (see **Figure 11**). For example, participants want to be able to turn OFF and/or lock out the dynamic functions of footrests in order to reduce self-stimulatory movements in which the user uses the system to do continuous movement or "play" with the dynamic features.

During focus groups, participants identified problems with current headrest assemblies and expectations for features in an ideal headrest. The headrest component assembly and cushioning materials must be durable enough to withstand a minimum of 36,500 thrusts per year for a period of 3 to 5 years. Headrests incorporate dynamic features (i.e. dampening resistance and adjustable rate-of-return), flex from 90° to 120° and protect the user from injury during thrusts while maintaining effective positioning.

Participants identified problems with current footrest assemblies and expectations for features in an ideal footrest assembly. The component assembly and materials must be durable enough to withstand a minimum of 36,500 thrusts per year for a period of 3 to 5 years. Footrests incorporate dynamic features (i.e. dampening resistance

Figure 10 How does "rate-of-return" operate in the seating system? (QDM3-QDM5)

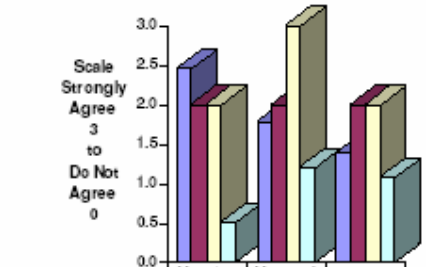

	Yes-1st Choice	Yes-2nd Choice	No
Mean	2.5	1.8	1.4
Median	2	2	2
Mode	2	3	2
Standard Deviation	0.5	1.2	1.1

Senses force needed / Parent/CG adjust rate vs ONLY Therapists/Vendor adjust

Figure 11 How do dynamic features of the seating system work? (QDM6-QDM7)

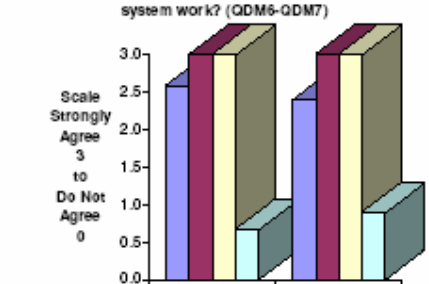

	Yes	Yes
Mean	2.6	2.4
Median	3	3
Mode	3	3
Standard Deviation	0.7	0.9

Disable w/ single action & Features work independently

and adjustable rate-of-return) and flex 90° at the knee. Footplates incorporate dynamic features (i.e. dampening resistance and adjustable rate-of-return) and flexes 15° plantar to 15° dorsi-flexion. Footrest assemblies protect the user from injury during thrusts while maintaining effective positioning.

Participants identified problems with current armrest assemblies and expectations for features in an ideal armrest. The component assembly and materials must be durable enough to withstand a minimum of 36,500 thrusts per year for a period of 3 to 5 years. Armrests incorporate dynamic features (i.e. dampening resistance and adjustable rate-of-return) and allow for some degree of abduction/adduction and flexion/extension. Armrests prevent user's arms from falling off during thrusts while maintaining effective positioning.

Desirable securements are made from wide, soft yet durable materials (i.e. withstand a minimum of 36,500 thrusts per year) and are available in various sizes to secure the head, pelvis, arms, ankles, etc. Seatbelts are velocity sensitive—in higher velocity (during involuntary thrusts) they minimize user movement, and in lower-velocity (during purposeful thrusts) they permit some movement.

Table 1 lists the design criteria for the dynamic seating system based on content analysis of focus group data and results of the analysis of the follow-up survey.

Table 1: Design Criteria for Dynamic Seating System (DSS)

Category	DSS Design Criteria
Legend/Key	***-Indicates statement from content analysis of focus data +-Indicates statement from survey analysis**
Assembly	• Is compatible with manual and power bases* • Is removable and/or foldable for transport+ • Is a carrier for components (e.g. backs, seat cushions, seat belts, postural supports) from various manufacturers* • Base attachment hardware lasts for 3 years (is durable enough to withstand multiple, daily seat removals/folds and forces that are applied when someone pushes the user in the wheelchair)*
Adjustability	• Seat widths range from 10" to 22" and seat depths from 5" to 14"* • Growth-at least 2 inches in seat width and depth without a growth kit+ • Uses non-incrementally, variable adjustments (e.g. with telescoping tubes and locking mechanism)* • Uses a single, universal tool to make adjustments+
Mounting	• Is integrated into current back components (for funding purposes)* • Is compatible with components (e.g. backs, seat cushions, seat belts, postural supports) from various manufacturers* • Supports multiple mounting locations for securements* • Uses the same (generic) fastener throughout (e.g. 10/32nd or 25/20)* • Mounting hardware withstands approximately 36,500 thrusting movement per year for a minimum of 3 years (10 thrusts per hour on average X 10 hours per day w/c use X 365 days each year = 36,500 thrusts annually)*

Category	DSS Design Criteria
Legend/Key	***-Indicates statement from content analysis of focus data +-Indicates statement from survey analysis**
Variable Positioning	• Permits manual configuration (e.g. can be configured differently based on the needs of the user—amount of seat tilt, back recline, seat height)* • Includes locking pre-sets at specific angles (e.g. 70°, 85°, 90°, 110°, 120°) are used to assist with tasks, for example the seat-to-back angle can be locked at 70° or a "tucked position" during transfers--a "tucked position" minimizes thrusting and assists in bed to w/c transfers* • Includes tilt-in-space and recline functionality*
Dynamic Movement	• Pelvic positioning is maintained by a fixed lower back section • Flexible joints match the joints of the user (e.g. at neck, shoulders, wrists, lumbar spine, knees and ankles)* • System reacts differently to involuntary versus purposeful thrusts+ • System has adjustable dampening capability* • Electronic sensors and/or motors provide advanced sensing and control+ • Sensors adjust the rate-of-return to return user to upright+ • Rate-of-return is adjustable by parents/caregivers+ • Dynamic features are enabled and disabled using a single action+ • Dynamic features work independently from each other and are turned ON and OFF independently (e.g. dynamic footrest function can be turned OFF to reduce self-stimulatory movements of the user)+
Headrests	• Headrest component assemblies and cushioning materials are durable enough to withstand a minimum of 36,500 thrusts per year for 3 years* • Headrests are dynamic (e.g. flexes from 90° to 120°)* • Headrest dampening is adjustable (e.g. based on the force applied by user during thrusting movements)* • Headrest rate-of-return is slow, controlled and can be adjusted* • Headrests protect the user from injury during thrusts while maintaining effective head positioning*
Footrests	• Footrests are durable enough to withstand a minimum of 36,500 thrusts per year for at least 3 years* • Footrest assembly is dynamic (e.g. allows for 90° extension at knee)* • Footrest dampening is adjustable (e.g. based on the force applied by user during thrusting movements)* • Footrest rate-of-return is slow, controlled and can be adjusted* • Footplate is dynamic (e.g. 15° plantar to 15° dorsi-flexion)*
Armrests	• Armrest are durable enough to withstand a minimum of 36,500 thrusts per year for at least 3 years* • Armrests are dynamic (e.g. they allow for some degree of abduction/adduction and flexion/extension)* • Armrests prevent user's arms from falling off during thrusts*

Category	DSS Design Criteria
Legend/Key	***-Indicates statement from content analysis of focus data** **+-Indicates statement from survey analysis**
	• Armrests dampening is adjustable (e.g. based on the force applied by user during thrusting movements)* • Armrests rate-of-return is slow, controlled and can be adjusted*
Securements	• Wide, soft and durable securements are available (e.g. to secure head, pelvis, arms, ankles)* • Seatbelts are velocity sensitive--in higher velocity (e.g. during involuntary thrusts), the seatbelt minimizes user movement, and in lower velocity (e.g. during purposeful thrusts), it permits movement* • Securements are durable enough to withstand a minimum of 36,500 thrusts*

APPENDIX B

UNDERGRAD DESIGN CALCULATION

Note: This comes from an appendix of [31], and is included here for reference.

Detent Hole Calculation

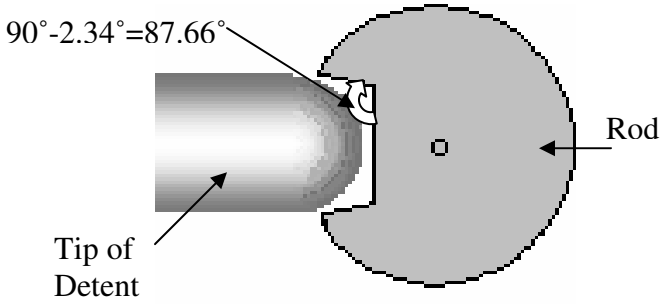

Figure: Detent Groove Geometry

$$Torque = 4.9" \times 40 lbs = 196 in - lbs$$

The 4.9" is the length from the resultant force, F_{total}, to the center of the shaft or rod. The 40lbs is the amount of force desired to break away the detent.

$$Force_{\text{detent}} = \frac{4.9" \times 40 lbs}{0.5"} = 392 lbs$$

The 0.5" is the distance from the center of the rod to the center of the detent.

$$Angle_{grove} = \arctan\left(\frac{force_{\text{start breakaway}}}{force_{\text{detent}}}\right) = \arctan\left(\frac{16}{392}\right) = 2.34^{o}$$

APPENDIX C

THRUST INTERACTION FORCE DATA

Seat Back Normal Forces

Subject	Configuration	Trial 1	Trial 2	Trial 3	Range
A	1	140.65	135.84	138.42	4.8121
	2	131.77	130.2	137.3	7.0976
	3	141.12	151.55	158.54	17.4151
	4	199.98	192.09	192.78	7.8874
	5	199.8	202.51	210.04	10.239
B	1	137.52	130.64	137.22	6.8805
	2	120.12	126.96	132.09	11.9651
	3	125.87	137.36	134.9	11.4825
	4	169.74	157.86	173.23	15.368
	5	177.48	182.39	188.53	11.0584
C	1	62.477	58.711	54.241	8.2361
	2	57.623	56.989	45.305	12.3178
	3	35.871	45.431	44.442	9.5604
	4	72.356	74.281	76.167	3.8117
	5	91.204	94.322	94.477	3.2728
D	1	74.032	53.844	74.112	20.2677
	2	79.722	76.312	77.397	3.4098
	3	96.109	98.346	91.512	6.8341
	4	85.383	100.91	122.71	37.3303
	5	163.98	164.15	164.8	0.8273
E	1	59.085	57.196	64.338	7.1415
	2	60.158	46.654	53.708	13.5041
	3	78.957	80.634	89.096	10.1395
	4	101.94	101.81	117.39	15.5778
	5	142.19	132.12	125.18	17.0069

Seat Back Contact Area

Subject	Configuration	Trial 1	Trial 2	Trial 3	Range
A	1	166.24	167.25	166.37	1.0124
	2	173.23	170.26	168.47	4.7636
	3	190.63	188.75	193.19	4.4416
	4	205.29	202.95	202.81	2.4737
	5	138.11	130.64	135.65	7.4706
B	1	168.85	166.48	162.82	6.0327
	2	160.32	158.52	160.49	1.9775
	3	174.43	168.96	174.08	5.4692
	4	191.36	194.97	202.9	11.544
	5	156.21	150.01	148.98	7.232
C	1	119.49	116.49	114.76	4.7354
	2	115.25	115.77	108.58	7.1845
	3	104.33	109.59	107.5	5.2602
	4	117.11	118.6	117.47	1.4916
	5	98.282	98.44	97.965	0.4746
D	1	154.9	144.12	152.13	10.775
	2	134.41	131.94	131.46	2.9425
	3	187.39	189.38	174.69	14.695
	4	155.99	181.57	187.5	31.518
	5	116.34	109.58	108.64	7.7009
E	1	125.45	126.29	129.72	4.2714
	2	117.91	117.07	119.63	2.5628
	3	123.32	119.96	125.97	6.0116
	4	143.33	146.39	152	8.6694
	5	108.37	113.67	114.76	6.3913

Seat Back Center of Pressure

Subject	Configuration	Trial 1	Trial 2	Trial 3	Range
A	1	19.309	19.072	18.926	0.3832
	2	18.547	18.836	19.201	0.6542
	3	18.035	18.069	18.094	0.0598
	4	18.033	17.908	17.647	0.3856
	5	20.976	21.238	20.737	0.5019
B	1	20.121	20.188	20.642	0.5203
	2	20.543	20.741	20.564	0.1986
	3	20.301	20.944	20.549	0.6431
	4	17.154	17.781	17.978	0.8241
	5	20.271	20.515	20.71	0.439
C	1	20.149	20.398	20.304	0.2487
	2	20.138	20.184	20.148	0.0467
	3	19.665	19.432	19.129	0.5362
	4	19.903	19.85	19.706	0.1966
	5	21.88	21.959	22.006	0.1257
D	1	19.039	19.144	19.031	0.1129
	2	20.35	20.451	20.352	0.1009
	3	17.558	17.596	18.487	0.9292
	4	18.802	17.444	17.853	1.3579
	5	21.968	22.286	22.186	0.3177
E	1	19.388	19.761	19.525	0.3731
	2	19.96	19.716	20.012	0.2959
	3	20.344	20.3	20.061	0.2831
	4	18.884	18.905	18.689	0.2169
	5	21.511	21.509	20.607	0.904

Seat Back Peak Pressure Index (PPI)

Subject	Configuration	Trial 1	Trial 2	Trial 3	Range
A	1	141.88	128.53	135.48	13.35
	2	128.75	130.78	143.69	14.944
	3	123.44	143.5	145.38	21.938
	4	166.89	193.22	209.91	43.02
	5	279	279	279	0
B	1	104.75	96	105.65	9.65
	2	98.464	108.5	100.66	10.036
	3	91.714	131.72	108.85	40.008
	4	135.2	94.889	126.5	40.311
	5	148.25	188.44	193.68	45.429
C	1	64.556	61.023	57.75	6.8056
	2	68.344	64.472	55.705	12.639
	3	45.875	55.625	55.469	9.75
	4	61.321	65.429	67.714	6.3929
	5	65.844	72.313	79.313	13.469
D	1	64.389	56.7	64.725	8.025
	2	83.325	79.75	82.475	3.575
	3	46.563	46.472	62.361	15.889
	4	49.417	42.813	52.462	9.649
	5	207.79	279	279	71.214
E	1	60.781	54.808	59.675	5.9736
	2	68.611	48.841	56.175	19.77
	3	78.938	88.219	95.938	17
	4	73.583	66.333	81.925	15.592
	5	172.28	128.25	125.7	46.581

Seat Bottom Normal Forces

Subject	Configuration	Trial 1	Trial 2	Trial 3	Range
A	1	69.3156	66.442	67.644	2.8735
	2	127.7518	132.55	127.47	5.0773
	3	81.1262	50.687	39.476	41.6502
	4	51.2084	42.379	34.254	16.9544
	5	84.3666	77.525	92.603	15.0787
B	1	55.3054	59.916	59.071	4.6104
	2	102.991	82.975	79.907	23.0836
	3	46.8616	48.827	39.257	9.5702
	4	44.5716	44.915	50.508	5.9367
	5	52.3615	51.002	51.724	1.36
C	1	40.8249	42.287	47.735	6.91
	2	63.9486	60.702	69.895	9.1932
	3	46.6591	53.229	47.516	6.5697
	4	49.3739	50.15	50.866	1.4924
	5	75.3513	73.111	74.538	2.2405
D	1	67.5391	89.603	61.892	27.7106
	2	64.8374	76.226	68.824	11.3887
	3	26.3351	22.803	20.13	6.2053
	4	41.7052	33.286	24.545	17.1607
	5	19.6046	21.014	21.936	2.3312
E	1	34.3064	34.124	31.51	2.7963
	2	24.1587	25.057	22.45	2.6072
	3	12.7273	14.191	14.679	1.9515
	4	17.2926	15.516	14.486	2.8069
	5	15.1832	14.85	15.567	0.7166

Seat Bottom Contact Area

Subject	Configuration	Trial 1	Trial 2	Trial 3	Range
A	1	70.051	70.367	73.405	3.3538
	2	92.072	95.197	84.795	10.402
	3	65.89	55.543	49.939	15.952
	4	57.038	54.104	50.98	6.0583
	5	71.612	71.19	76.207	5.0172
B	1	55.686	58.534	57.395	2.8476
	2	81.224	70.979	67.67	13.554
	3	54.918	53.577	48.504	6.4139
	4	50.624	52.769	55.641	5.0172
	5	57.223	56.636	57.54	0.904
C	1	59.448	62.446	66.349	6.9011
	2	79.614	77.659	85.888	8.2296
	3	56.201	55.647	54.025	2.1753
	4	60.613	59.935	62.06	2.1244
	5	72.812	71.19	72.139	1.6216
D	1	62.928	79.416	63.723	16.488
	2	58.154	62.19	58.407	4.0359
	3	39.866	37.089	34.663	5.203
	4	55.159	49.042	36.021	19.138
	5	30.646	33.749	35.911	5.2658
E	1	48.686	50.186	47.365	2.8208
	2	37.406	37.853	35.12	2.7325
	3	20.25	20.289	22.108	1.8588
	4	27.457	25.312	23.793	3.6632
	5	24.126	25.628	27.305	3.1798

Seat Bottom Center of Pressure

Subject	Configuration	Trial 1	Trial 2	Trial 3	Range
A	1	11.423	11.46	11.441	0.0374
	2	11.356	11.341	11.497	0.1558
	3	12.098	12.056	11.773	0.3252
	4	12.181	12.003	11.788	0.3927
	5	11.801	11.926	11.884	0.1254
B	1	12.136	12.066	12.1	0.0701
	2	11.738	11.826	11.921	0.1832
	3	12.275	12.38	12.301	0.1052
	4	12.294	12.192	12.269	0.1025
	5	12.4	12.409	12.419	0.0193
C	1	11.938	11.915	11.906	0.0314
	2	11.882	11.882	11.763	0.1196
	3	12.277	12.425	12.439	0.1619
	4	12.184	12.214	12.159	0.0545
	5	12.271	12.241	12.235	0.0367
D	1	11.509	11.355	11.478	0.1534
	2	12.206	12.225	12.369	0.1636
	3	11.771	11.755	11.725	0.0458
	4	11.612	11.612	11.801	0.1897
	5	12.44	12.291	12.325	0.1484
E	1	12.545	12.449	12.47	0.0957
	2	12.234	12.355	12.267	0.1208
	3	11.896	12.217	12.339	0.4423
	4	12.608	12.291	12.37	0.3171
	5	12.624	12.562	12.651	0.0899

Seat Bottom Peak Pressure Index (PPI)

Subject	Configuration	Trial 1	Trial 2	Trial 3	Range
A	1	112.88	125.13	137.79	24.9167
	2	214.25	227.34	227	13.0938
	3	158.72	156.66	106.65	52.073
	4	125.39	142.78	100	42.7778
	5	135.5	168.42	153.64	32.9167
B	1	110.79	154.96	159.9	49.1083
	2	154	137.53	170.66	33.1285
	3	124.82	137.33	154.55	29.7286
	4	149.1	125.92	156.29	30.369
	5	181.96	173.94	180.18	8.0268
C	1	88.417	96.591	103.9	15.4833
	2	183.53	149.03	175.14	34.5035
	3	160.47	166.97	167.88	7.4062
	4	126.75	119.39	121.36	7.3571
	5	190.47	179.41	187.38	11.0625
D	1	137.39	145.38	137.93	7.9861
	2	162.7	153.86	158.93	8.8389
	3	67.906	83.333	86.556	18.6493
	4	67.056	90.125	71.269	23.0694
	5	72.107	65.958	62.844	9.2633
E	1	110.63	125.65	124.8	15.0288
	2	77	90.341	90.9	13.9
	3	56.938	78.281	82.094	25.1563
	4	96.861	76.278	71.8	25.0611
	5	89.625	84.469	86.625	5.1562

Seatbelt Preload

Subject	Configuration	Trial 1	Trial 2	Trial 3	Range
A	1	2.6224	3.603	3.1999	0.9806
	2	6.8823	5.1427	5.1362	1.7461
	3	3.6545	3.7554	4.353	0.6985
	4	2.84	0	3.2575	3.2575
	5	5.4246	2.0574	3.7278	3.3672
B	1	1.3899	0.8126	0.8992	0.5773
	2	0.9172	0.9154	0.808	0.1092
	3	2.3365	1.7802	1.8663	0.5563
	4	3.049	2.5917	2.5713	0.4777
	5	2.7827	3.1321	2.8446	0.3494
C	1	0.7055	0.8199	0.9024	0.1969
	2	0.9847	0.7042	0.7103	0.2805
	3	1.3634	0.7984	0.7651	0.5983
	4	0.7989	0.7172	1	0.2828
	5	0.7033	0.8024	0.803	0.0997
D	1	2.987	1.6448	1.593	1.394
	2	2.5624	2.9031	1.7697	1.1334
	3	0.7084	0.6096	0.7021	0.0988
	4	1.1602	0.7065	0.7031	0.4571
	5	0.4135	0.3991	0.4977	0.0986
E	1	0.3957	0.2979	0.1374	0.2583
	2	0.1683	0.1056	0	0.1683
	3	1.3165	1.0351	0.7492	0.5673
	4	0.6363	0.5485	0.3036	0.3327
	5	0.4	0.3905	0.3963	0.0095

Seatbelt Tension

Subject	Configuration	Trial 1	Trial 2	Trial 3	Range
A	1	90.232	82.147	87.186	8.0849
	2	114.82	98.885	121.32	22.4353
	3	98.874	97.7	101.32	3.6223
	4	130.25	124.47	114.94	15.3157
	5	105.39	90.653	94.342	14.7412
B	1	88.243	105.94	95.987	17.6932
	2	87.363	93.29	99.842	12.479
	3	105.42	102.01	114.15	12.1461
	4	106.89	109.87	109.22	2.9851
	5	86.359	89.749	86.874	3.3907
C	1	28.144	25.063	21.424	6.7201
	2	30.314	27.83	24.432	5.8817
	3	26.683	28.099	24.84	3.2585
	4	31.937	33.626	34.302	2.3654
	5	29.546	32.949	35.081	5.5344
D	1	22.681	12.663	19.252	10.018
	2	42.916	42.363	37.467	5.4486
	3	13.252	14.348	19.633	6.3804
	4	12.26	9.8175	14.584	4.7662
	5	32.652	40.144	43.738	11.0858
E	1	28.293	22.11	27.178	6.1831
	2	39.636	26.456	22.89	16.7463
	3	26.96	27.941	25.124	2.8171
	4	26.206	14.691	24.826	11.515
	5	35.13	39.463	33.531	5.9316

Total Force (Sum of Back, Bottom, & Belt Forces)

Subject	Configuration	Trial 1	Trial 2	Trial 3	Range
A	1	300.19	284.42	293.25	15.771
	2	374.35	361.64	386.09	24.456
	3	321.12	299.94	299.33	21.787
	4	381.44	358.94	341.97	39.473
	5	389.56	370.69	396.98	26.296
B	1	281.07	296.49	292.27	15.423
	2	310.48	303.23	311.84	8.6125
	3	278.16	288.19	288.3	10.146
	4	321.2	312.65	332.96	20.307
	5	316.2	323.14	327.13	10.935
C	1	131.45	126.06	123.4	8.0462
	2	151.89	145.52	139.63	12.253
	3	109.21	126.76	116.8	17.546
	4	153.67	158.06	161.34	7.6695
	5	196.1	200.38	204.1	7.994
D	1	164.25	156.11	155.26	8.9958
	2	187.48	194.9	183.69	11.213
	3	135.7	135.5	131.27	4.4213
	4	139.35	144.02	161.84	22.493
	5	216.23	225.31	230.48	14.244
E	1	121.68	113.43	123.03	9.5964
	2	123.95	98.166	99.048	25.787
	3	118.64	122.77	128.9	10.255
	4	145.44	132.02	156.7	24.682
	5	192.5	186.43	174.28	18.222

APPENDIX D

THRUST INTERACTION FORCE METHODOLOGY

GAUGE SETUP

The thrust interaction forces were collected using two Conformat pressure mats and an E-DFE-200 Chatillon digital force gauge.

The setup of the pressure mats is shown in Figure 96. Attaching the mats involves taping the back mat to the flexible seat back, and then taping a 2" foam mat over the pressure mat. This setup will eventually slide over time, so it may need to be retaped every day, but not between every person. A USB handle is attached to the Conformat, and the handle should be stuck to the Velcro attachment on the side of the wheelchair

Figure 96: Mat Placement for Dynamic Seat Data Collection

frame. Allowing the handle to freely hang from the mat can damage the mat, so attachment is necessary.

The seat bottom mat should be placed with the front sensor edge just over the front edge of the seat bottom. A smaller 2" foam mat is then placed on the pressure mat. The mat will need to be folded carefully around the edge of the foam mat and taped in place. The folding of the mat is done to minimize the possibility that the mat is pinched between the seat bottom and the wheelchair frame. The Conformat sensors can be folded, but the wires leading to the sensors around the edge of the pressure mat cannot be folded. They can be curved, but not fully bent, or they will be damaged. Some creativity is needed to find a way to not bend the pressure mat on the seat bottom. A second USB handle is attached to the seat bottom mat, and also attached via Velcro to the wheelchair frame.

The Chatillon gauge is attached to the left side of the wheelchair frame by way of a freely pivoting plate. The plate has four screws that are used to mount the force gauge. Be sure to only finger tighten the screws, as excess tightening can damage the force gauge. The hook attachment is used on the gauge, and this connects to the loose end of the seat belt. The serial cable in the force gauge container is used to connect the gauge to the computer.

SUBJECT SETUP

For each configuration, have the subject sit in the chair carefully. The foam mats want to slide around. Zero out the force gauge (press the zero button) before attaching the seat belt. Otherwise, there will be a preload bias in the results. Adjust the foot height as appropriate.

The motors need power, which is supplied by an AC adapter for the seat bottom actuator and a 24V DC power supply for the seat back motor (located in the electronics room). The button controls, together with the power setup, are shown in Figure 97. The three-toggle switch operates the seat bottom actuator, and the two-toggle switch and red push button work the seat back motor.

The footrest height can be adjusted using hex wrenches. The footrest is locked in place using a clamp. The magnets are not used because they will break away during the testing. The adjustments of the roller height is done using the split washers. Once the height is chosen, the washers need to be taped in place. Otherwise, the force from some users will pop them out. The seat bottom flexure bar is adjusted by loosing the screws in the two clamps and moving the bar. The person needs to be out of the chair to adjust the

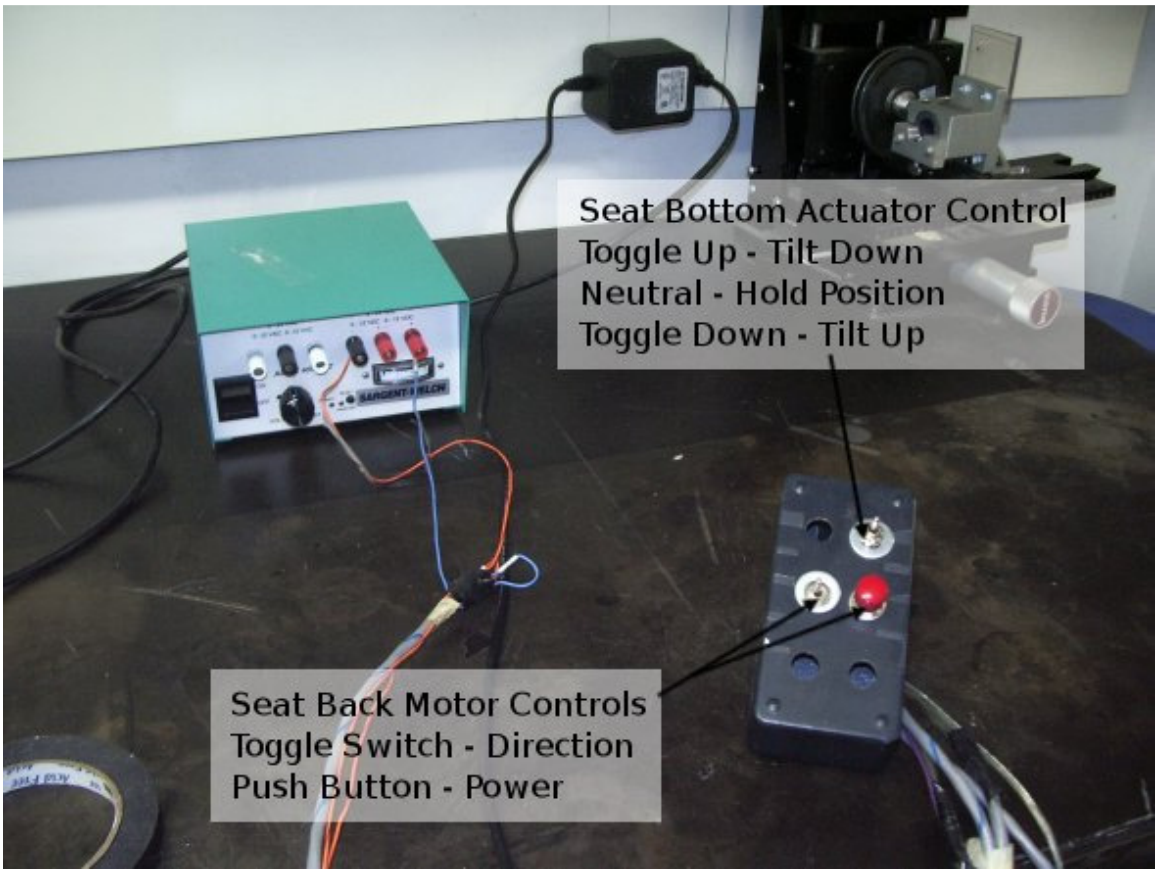

Figure 97: Dynamic Seat Motor Power and Control

flexure bar. The other adjustments can be done with the person still in the chair.

For each configuration, set the components as they need to be. Then, go to the computer, start recording, and tell the person to thrust. Once they are fully extended (give them 2 or 3 seconds), stop recording. Only then should you tell the person to relax. This allows the end forces to be an average of the fully-extended position.

SOFTWARE SETUP

Before collecting data with the pressure mats, be sure to have them calibrated. This calibration should be done before each session of data collection, but does not need to be done between every test subject. Instructions are located in a white binder near the calibration station.

The pressure data is captured using the Tekscan BPMS software. Ask for help from a local expert before using this the first time. It is a little tricky to select the correct sensor and setup. You also need to setup the movie capture parameters. The tests in this thesis used a 5 Hz sampling rate with 200 frames of data. Experiments will not use the full 200 frames. Manually stop the recording once the person was fully extended.

The force gauge software is called Nexygen. The interface is relatively straightforward, although the navigation is somewhat awkward. There is a users manual on the CD to help with any questions.

The standard procedure for recording is to start recording using Nexygen. Then, switch to the Tekscan and start recording. Next, tell the person to thrust. After they are fully extended, stop the Tekscan. Switch to the Nexygen and stop that. Then, tell the

person to relax. You then need to save the Tekscan file. The Nexygen will keep all the tests separate, and save everything as one big file later.

POSTPROCESSING

Once all the data has been collected, convert the Tekscan files into ASCII format by choosing Save As ASCII, and selecting Whole Movie. The Nexygen runs should be saved separately as well. They can be exported into Excel files or CSV.

At this point, the data can be extracted using MatLab. The files readasf_DSS.m and readDFE.m are used to read the ASCII movies and the CSV files, respectively. These are found in the Closeout DSS project folder on CATEA's network. These files work by reading in the data, showing a graph of the data, and asking the user to select the point at which the person is in the fully extended position. There is not synchronized motion data, so look for the spike in force and choose that point manually. The forces and pressures come from an average of all the frames of data from this selected point to the end.

ExtractDSS.m and ProcessDSS.m can be analyzed to show how the data can be extracted. They are quite a roundabout way of doing things, as the process was being changed while analyzing the data. The data extraction could be done another way, but these show how to use the readasf_DSS and readDFE m-files.

APPENDIX E

DATA FROM PRESSURE RELIEF STUDY

Test Subject Parameters

	Gender	Height	Weight (lbs)
Subject 1	Male	5' 11"	168
Subject 2	Male	5' 8"	135
Subject 3	Female	5' 3½"	140
Subject 4	Female	5' 5½"	149
Subject 5	Female	5' 2"	118

Note: all percentages are listed as percent body weight of the test subject.

Tilt Head Percentages

Subject	0°	15°	25°	40°	55°
1	0.6356	3.2848	1.6065	5.9285	0.78851
2	3.952	2.968	4.2456	6.4039	7.6265
3	0.74885	1.3652	3.1589	4.5903	5.4938
4	0.91262	2.715	3.6567	4.5943	5.1743
5	1.1298	2.0394	3.5519	4.9963	6.514
Simulation	1.9187	2.9007	3.7273	4.7493	5.4467

Tilt Back Percentages

Subject	0°	15°	25°	40°	55°
1	18.694	46.531	59.969	75.735	85.544
2	41.326	46.74	56.775	74.546	83.031
3	12.56	31.644	51.621	54.407	64.363
4	15.868	42.687	53.643	73.707	84.871
5	16.124	29.634	46.656	52.844	65.331
Simulation	11.572	28.971	43.339	62.297	77.01

Tilt Seat Percentages

Subject	0°	15°	25°	40°	55°
1	55.135	49.488	40.769	29.043	19.149
2	47.465	44.55	42.783	32.912	23.024
3	59.733	62.758	54.48	45.313	34.88
4	53.305	52.996	46.209	38.406	24.533
5	56.075	47.009	45.061	35.836	28.001
Simulation	73.753	72.883	63.889	46.861	26.639

Tilt Feet Percentages

Subject	0°	15°	25°	40°	55°
1	7.6253	7.6253	8.4046	5.7867	3.2185
2	5.9658	5.4842	5.0507	3.8006	3.1515
3	5.9334	6.5894	3.4129	4.2612	1.8158
4	3.9394	4.9394	4.7107	4.5984	3.6359
5	2.9543	3.3055	1.9686	2.2045	1.0826
Simulation	17.101	14.816	13.457	10.666	7.1493

Tilt Total Reading Percentages

Subject	0°	15°	25°	40°	55°
1	82.09	106.93	110.75	116.49	108.7
2	98.709	99.743	108.85	117.66	116.83
3	78.975	102.36	112.67	108.57	106.55
4	74.025	103.34	108.22	121.31	118.21
5	76.283	81.988	97.237	95.881	100.93
Simulation	104.35	119.57	124.41	124.57	116.25

Recline Head Percentages

Subject	100°	120°	140°	160°	180°
1	0.6356	3.6183	5.3703	7.2311	8.4488
2	0.62388	5.1424	6.2877	7.568	7.6333
3	1.0802	3.1699	3.1014	6.3553	7.9921
4	0.91262	4.2138	4.5964	6.7085	6.7584
5	1.1298	3.8507	5.358	7.0881	7.0357
Simulation	1.9187	4.0287	6.238	5.5133	7.9047

Recline Back Percentages

Subject	100°	120°	140°	160°	180°
1	18.694	24.847	47.832	59.173	57.327
2	26.396	30.141	39.734	49.753	45.206
3	15.224	24.094	29.115	34.403	36.245
4	15.868	35.703	35.508	44.347	56.362
5	16.124	23.977	26.677	28.494	31.986
Simulation	11.572	20.133	32.223	41.067	40.345

Recline Seat Percentages

Subject	100°	120°	140°	160°	180°
1	55.135	46.744	32.722	19.61	14.049
2	53.537	47.357	34.277	23.957	16.654
3	67.353	54.657	47.908	36.443	27.137
4	53.305	41.563	30.335	27.016	16.219
5	56.075	48.963	42.424	28.307	23.272
Simulation	73.753	47.256	45.152	35.586	30.444

Recline Feet Percentages

Subject	100°	120°	140°	160°	180°
1	7.6253	8.7878	11.056	7.7764	3.9554
2	4.7663	4.1171	5.7839	7.1471	6.5622
3	7.5503	8.3655	7.5128	8.4516	7.5459
4	3.9394	5.7065	7.2822	6.0432	1.2681
5	2.9543	4.1496	2.5715	3.9451	2.1862
Simulation	17.101	19.684	25.631	16.929	0

Recline Total Reading Percentages

Subject	100°	120°	140°	160°	180°
1	82.09	83.998	96.98	93.791	83.78
2	85.322	86.757	86.082	88.426	76.056
3	91.208	90.286	87.636	85.653	78.92
4	74.025	87.186	77.721	84.115	80.608
5	76.283	80.941	77.031	67.835	64.479
Simulation	104.35	91.102	109.24	99.095	78.693

Stand Knee Percentages

Subject	0°	20°	40°	60°	75°
1	0	7.8059	14.048	6.7981	9.65
2	0	6.9705	22.352	24.48	12.753
3	0	3.5609	14.838	12.719	2.4674
4	0	11.037	19.098	14.263	7.8706
5	0	3.5519	13.636	11.827	7.9977
Simulation	0	24.377	35.407	28.152	11.127

Stand Back Percentages

Subject	0°	20°	40°	60°	75°
1	30.289	8.5022	7.8777	9.9153	4.2115
2	21.673	7.5691	0.75691	2.39	5.0759
3	20.466	9.2115	6.0946	3.1412	0.26508
4	20.396	4.4591	3.48	2.1558	1.187
5	20.853	7.6176	2.2753	3.122	1.2373
Simulation	11.539	11.222	12.15	11.823	11.37

Stand Seat Percentages

Subject	0°	20°	40°	60°	75°
1	51.29	52.515	37.267	15.483	10.881
2	59.926	55.56	46.131	25.728	10.973
3	62.992	52.632	38.791	27.694	10.457
4	55.288	50.43	38.43	22.179	14.018
5	53.342	53.538	40.525	21.692	10.145
Simulation	80.953	73.432	57.535	35.875	17.315

Stand Feet Percentages

Subject	0°	20°	40°	60°	75°
1	9.954	14.797	24.61	37.762	41.205
2	8.9155	8.5967	15.251	21.214	24.446
3	8.2727	12.781	21.798	24.741	34.308
4	4.3843	8.2094	12.606	17.753	22.063
5	3.9635	5.649	8.8942	15.364	19.238
Simulation	16.787	27.34	44.728	67.555	85.662

Stand Total Reading Percentages

Subject	0°	20°	40°	60°	75°
1	91.534	83.62	83.802	69.958	65.947
2	90.515	78.696	84.49	73.813	53.248
3	91.731	78.185	81.522	68.295	47.498
4	80.068	74.135	73.615	56.352	45.138
5	78.158	70.356	65.331	52.005	38.618
Simulation	109.28	136.37	149.82	143.41	125.47

REFERENCES

[1] R. A. Cooper, "Advances in wheelchair and related technologies," *Medical Engineering & Physics*, vol. 23, pp. iii-iv, 2001.

[2] Miller's Adaptive Technologies, *Product Catalog*, 2004.

[3] "Maddak Corner Seat," Accessed Jan 2006, http://www.americandiscountmed.com/02_closeouts.php?a=view&recid=6

[4] "Therapedic Child Car Seat," Accessed Jan 2006, http://www.adaptivemall.com/colcarseat1.html

[5] "Diagnosis of Cerebral Palsy: A Research Status Report," UCP Research and Educational Foundation, Washington, D.C. September 2002 2002.

[6] "Cerebral Palsy," Accessed Jan 2006, http://www.marchofdimes.com/professionals/681_1208.asp

[7] "Cerebral Palsy Diagnosis," Accessed Jan 2006, http://www.about-cerebral-palsy.org/diagnosis

[8] "Paralysis," Accessed Jan 2006, http://www.healthatoz.com/healthatoz/Atoz/ency/paralysis.jsp

[9] A. P. Zeltwanger, D. Brown, and G. Bertocci, "Utilizing computer modeling in the development of a dynamic seating system.," presented at the 24th RESNA Conference, Reno, NV, USA, June 2001.

[10] "Dynamic Care System," Accessed Jan 2006, http://www.interco-gmbh.de/front_content.php?idcat=51

[11] M. Markwald (2002). Traveling Seat. US Patent **6,488,332 B1**

[12] S. Farricielli (1999). Ergonomically Designed Seat Assembly for a Portable Wheelchair. US Patent **5,904,398**

[13] D. L. Helman (1998). Headrest Assembly with User Actuated Pivotal Support Assembly. US Patent **5,791,735**

[14] G. Roth and H. Guenther (1994). Wheel Chair Electric Brake and Pedal Safety Kit. US Patent **5,358,266**

[15] J. L. B. Castillo (2002). Dynamic Footrest. US Patent **2002/0096930 A1**

[16] R. J. Jensen (1999). Dynamic Continuous Passive Motion Chair. US Patent **5,976,097**

[17] D. R. Thomas, MD, "Prevention and Treatment of Pressure Ulcers: What works? What doesn't?," *Cleveland Clinic Journal of Medicine*, vol. 68.

[18] "Staying Healthy After a Spinal Cord Injury," Northwest Regional Spinal Cord Injury System 1998.

[19] "Bedsores (Pressure sores)," Accessed Jan 2006, http://www.mayoclinic.com/health/bedsores/DS00570

[20] "Pressure ulcer," Accessed Jan 2006, http://www.nlm.nih.gov/medlineplus/ency/article/007071.htm

[21] "Guideline for prevention and management of pressure ulcers," Accessed Jan 2006, http://www.guideline.gov/summary/summary.aspx?ss=15&doc_id=3860&nbr=3071

[22] S.-W. Hong, H. Seomoon, V. Patrangenaru, W. Singhose, and S. Sprigle, "An Efficient Method for Identification of Human-Generated Forces during Extensor Thrust," presented at IASTED Internation Conference, Innsbruck, Austria, 2005.

[23] V. P. Patrangenaru, "Development of Dynamic Seating System for High-Tone Extensor Thrust," Georgia Tech, 2006.

[24] P. de Leva, "Adjustments to Zatsiorsky-Seluyanov's segment inertia parameters," *Journal of Biomechanics*, vol. 29, pp. 1223-1230, 1996.

[25] "Tukey's HSD Post Hoc Test Steps," Accessed May 2006, http://web.umr.edu/~psyworld/tukeyssteps.htm

[26] R. K. Shileds and T. M. Cook, "Effect of seat angle and lumbar support on seated buttock pressure," *Physical Therapy*, vol. 68, pp. 1682-1686, 1998.

[27] D. A. Hobson, "Comparative effects of posture on pressure and shear at the body-seat interface," *Journal of Rehabilitation Research and Development*, vol. 29, pp. 21-31, 1992.

[28] J. L. Henderson, S. H. Price, M. E. Brandstater, and B. R. Mandac, "Efficacy of three measures to relieve pressure in seated persons with spinal cord injury," *Archives of Physical Medicine and Rehabilitation*, vol. 75, pp. 535-539, 1994.

[29] R. Aissaoui, M. Lacoste, and J. Dansereau, "Analysis of sliding and pressure distribution during a repositioning of persons in a simulator chair," *IEEE Transactions on Neural Systems and Rehabilitation Engineering*, vol. 9, pp. 215-223, 2001.

[30] V. Agrawal, "Characterizing Load Transfer in Variable Positioning Wheelchairs," Georgia Tech 2005.

[31] R. Duncan, J. Fernandez, C. Howard, and J. Li, "Dynamic Footrest," Georgia Tech 2005.